Pergamon

Int. Comm. Heat Mass Transfer, Vol. 28, No. 6, pp. 751–762, 2001

0735-1933/01/$–see front matter

PII: S0735-1933(01)00279-2

A NUMERICAL AND EXPERIMENTAL INVESTIGATION OF THE MODELLING OF MICROWAVE MELTING OF FROZEN PACKED BEDS USING A RECTANGULAR WAVE GUIDE

Phadungsak Ratanadecho, K. Aoki and M. Akahori
Nagaoka University of Technology
1603-1, Kamitomioka, Nagaoka
Niigata, Japan , 940-2188

(Communicated by C.L. Tien and A. Majumdar)

ABSTRACT

The melting of frozen packed beds by microwave with rectangular wave guide has been investigated numerically and experimentally. It was performed for the two different layers, which consists of frozen and unfrozen layers. Based on the model combined the Maxwell and heat transport equations, the results show that the direction of melting against the incident microwave strongly depends on the structure of layered packed beds because the difference in the dielectric properties between water and ice. © 2001 Elsevier Science Ltd

Introduction

A study of melting process in material expose to microwave was studied by Pangrle et al. [1] and [2], which the one-dimensional model was developed for microwave melting of cylinders. Later, Zeng et al. [3] carried out two-dimensional microwave thawing in cylinders and their model predictions were compared with experimental data. In a recent work, Basak et al. [4] carried out microwave thawing studies with fixed grid based effective heat capacity method coupled with Maxwell's equations.

A number of other analyses of the microwave melting process have appeared in the recent literature (Coleman [5], Bialod et al. [6] and Cleland et al. [7]). However, most previous work the microwave energy absorbed was assumed to decay exponentially into the sample following the aid of Lambert's law. This assumption is valid for the large dimensions of sample used in study. For the small sample, the spatial variations of the electromagnetic field and microwave power absorbed within sample must be obtained by a complete solution of the unsteady Maxwell's equations.

Due to the limited amount of theoretical and experimental work on microwave melting process, the various effects are not fully understood and a number of critical issues remain unresolved. These effects of reflection rate of microwave and degree of incident wave penetration into the sample during microwave melting process have not been studied systematically.

Although previous investigation is replete with one-dimensional melting process, a little effort has been reported on study of two-dimensional heating process by microwave fields, especially, full comparison of prediction from mathematical model with experimental melting data. This study reports a comparison of simulations based on a two-dimensional model with experimental measurement in which the microwave of TE_{10} mode operating at a frequency of 2.45GHz is employed.

Experimental Apparatus

Figure 1 shows the experimental apparatus used. The microwave system was a monochromatic wave of TE_{10} mode operating at a frequency of 2.45GHz. MW energy is transmitted along the z-direction of the rectangular wave guide with inside dimensions of 109.22 mm × 54.61 mm toward a water load that is situated at the end of the wave guide. The water load (lower absorbing boundary) ensures that only a minimal amount of microwave is reflected back to the sample, while an upper absorbing boundary, which is located at the end of wave guide, is used to trap any microwave reflected from the sample to prevent it from damaging the magnetron. The sample studied is a multi-layered packed beds, which is consisted of a frozen layer (glass beads and ice) with thickness of 50 mm and the unfrozen layer (glass beads and water) with thickness of 50 mm. It is inserted in the rectangular wave guide. Output of magnetron is adjusted as 1000W. Dielectric properties of the sample at various conditions were measured [8]. During the experiment, the microwave field was generated using a magnetron (Micro Denshi Co., Model UM-1500). The powers of incident, reflected and transmitted waves were measured by wattmeter using a directional coupler (Micro Denshi Co., model DR-5000).

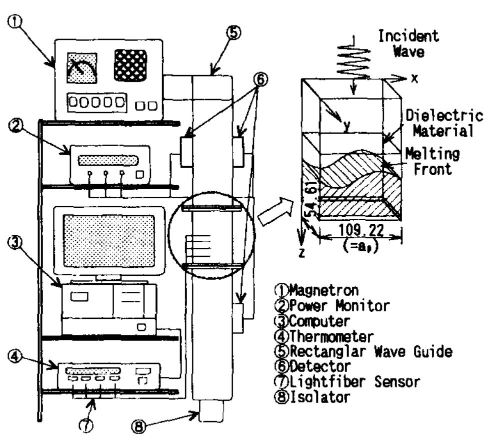

FIG. 1
Experimental apparatus.

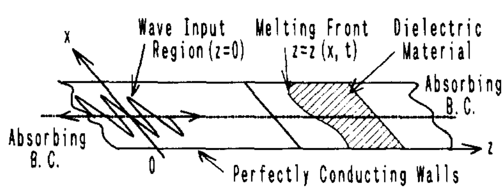

FIG. 2
Analytical model.

Mathematical Model Analysis

Assumptions and Analysis of Electromagnetic Field

Figure 2 shows the analytical model for microwave melting of multi-layered packed beds using a rectangular wave guide.

Assumptions The proposed model is based on the following assumptions:

(1) Since the microwave field is operated in TE10 mode, it propagates in a rectangular wave guide independently of the y-direction. Hence the electromagnetic field can be assumed to be two-dimensional plane (x-z plane), (2) the absorption of microwave energy by the cavity (including air) in the rectangular wave guide is negligible, (3) the walls of a rectangular wave guide are perfect conductors,
(4) the effect of the sample container on the electromagnetic field can be neglected.

Basic equations

The basic equations for the electromagnetic field are based on the well-known Maxwell relations. When a microwave field propagates though an isotropic medium, the governing equations are as follows:

$$\nabla \times \boldsymbol{E} = -\mu \frac{\partial \boldsymbol{H}}{\partial t} \tag{1}$$

$$\nabla \times \boldsymbol{H} = \sigma \boldsymbol{E} + \varepsilon \frac{\partial \boldsymbol{E}}{\partial t} \tag{2}$$

$$\nabla \cdot \boldsymbol{E} = \frac{q}{\varepsilon} \tag{3}$$

$$\nabla \cdot \boldsymbol{H} = 0 \tag{4}$$

For the microwave of TE_{10} mode, the components of electric and magnetic field intensities are given by:

$$\begin{aligned} E_x = E_z = H_y = 0 \\ E_y, H_x, H_z \neq 0 \end{aligned} \tag{5}$$

Using the relation of Eq.5, the governing equations (Eqs.1-4) can be written in term of the component notations of electric and magnetic field intensities:

$$\frac{\partial E_y}{\partial z} = \mu \frac{\partial H_x}{\partial t} \tag{6}$$

$$\frac{\partial E_y}{\partial x} = -\mu \frac{\partial H_z}{\partial t} \tag{7}$$

$$-\left(\frac{\partial H_z}{\partial x} - \frac{\partial H_x}{\partial z}\right) = \sigma E_y + \varepsilon \frac{\partial E_y}{\partial t} \tag{8}$$

where, permittivity (ε), magnetic permeability (μ) and electric conductivity (σ) are given by:

$$\varepsilon = \varepsilon_0 \varepsilon_r \tag{9}$$

$$\mu = \mu_0 \mu_r \tag{10}$$

$$\sigma = 2\pi f \varepsilon \tan\delta \tag{11}$$

Further, because the dielectric properties of each material are assumed to vary with temperature, the effective dielectric properties in multi-layered packed beds utilized throughout this study are obtained by using a mixing formula [9].

Boundary conditions

Corresponding to the analytical model shown in Fig. 2, boundary conditions can be given as follows;

(a) Perfectly conducting boundaries; boundary conditions on the inner wall surface of a rectangular wave guide are given by using Faraday's law and Gauss' theorem:

$$E_h = 0, \quad H_n = 0 \tag{12}$$

where subscripts h and n denote the components of tangential and normal directions, respectively.

(b) Continuity boundary condition; boundary conditions along the interface between different materials, for example between air and dielectric material surface, are given by using Ampere's law and Gauss theorem:

$$\begin{aligned} E_h &= E'_h, \quad H_h = H'_h \\ D_n &= D'_n, \quad B_n = B'_n \end{aligned} \tag{13}$$

where $'$ denotes one of the different materials.

(c) Absorbing boundary condition; at the both ends of the rectangular wave guide, the first order absorbing conditions proposed by Mur [10] are applied:

$$\frac{\partial E_y}{\partial t} = \pm \upsilon \frac{\partial E_y}{\partial z} \tag{14}$$

Here, the symbol ± represents forward or backward waves and υ is phase velocity of the microwave.

(d) Oscillation of the electric and magnetic flied intensities by magnetron; the incident wave due to magnetron is given by the following equations:

$$E_y = E_{yin} \sin\left(\frac{\pi x}{L_x}\right) \sin(2\pi f t) \tag{15}$$

$$H_x = \frac{E_{yin}}{Z_H} \sin\left(\frac{\pi x}{L_x}\right) \sin(2\pi f t) \tag{16}$$

E_{yin} is the input value of electric field intensity, L_x is the length of rectangular wave guide in x-direction, Z_H is the wave impedance

Assumptions and Analysis of Heat Transport

The temperature of the sample exposed to incident wave is obtained by solving the conventional heat transport equation with the microwave energy absorbed included as a local electromagnetic heat generation term.

Assumptions In order to analyze the process of heat transport due to microwave melting of multi-layered packed beds, we introduce the following assumptions:
(1) Corresponding to electromagnetic field, temperature field also can be assumed to be two-dimensional plane (x-z plane), (2) the surroundings of multi-layered packed beds are insulated, (3) the effect of the container on temperature field can be neglected, (4) the effect of the natural convection can be neglected, (5) local thermodynamics equilibrium is assumed, (6) in this study, in a macroscopic sense, the pore structure within the material is assumed to be homogeneous and isotropic. Therefore, a heating model for a homogeneous and isotropic material is used in the current analysis.

Basic equations The governing energy equation describing the temperature rise in the multi-layered packed beds are the time dependent heat diffusion equation:

$$\frac{\partial T}{\partial t}=a\left(\frac{\partial^2 T}{\partial x^2}+\frac{\partial^2 T}{\partial z^2}\right)+\frac{Q}{\rho\cdot C_p}\left(\frac{\partial T}{\partial z}\right)\frac{dz}{dt} \tag{17}$$

$$Q=2\pi f\varepsilon_0\varepsilon_r\tan\delta E_y^2 \tag{18}$$

where a is the thermal diffusivity and Q is the microwave energy absorbed term [16].

Boundary conditions

(a) Adiabatic condition; assuming that the surroundings of multi-layered materials are insulated:

$$\frac{\partial T}{\partial n}=0 \tag{19}$$

(b) Moving front boundary condition; the moving boundary between the unfrozen layer and frozen layer is described by the Stefan equation:

$$\left(\lambda_s\frac{\partial T_s}{\partial z}-q_{Bou}\Delta z_{Bou}-\lambda_l\frac{\partial T_l}{\partial z}\right)\left[1+\left(\frac{\partial z_{Bou}}{\partial x}\right)^2\right]=\rho_s L_s S_s\frac{\partial z_{Bou}}{\partial t} \tag{20}$$

where subscript Bou denotes solid-liquid fronts.

Mesh construction and Coordinate Transformation

For the construction itself of a coordinate mesh around even a sample multi-layered packed beds, the method of constructing a two-dimensional boundary-conforming grid for a microwave melting configuration is a direct algebraic approach based on the concept of transfinite or multivariate interpolation [17]. Furthermore, when the boundaries of the physical domain move with time, it is convenient to introduce a general curvilinear coordinate system:

$$x = x(\xi,\eta), z = z(\xi,\eta) \quad \text{or} \quad \xi = \xi(x,z), \eta = \eta(x,z) \tag{21}$$

The moving boundaries are immobilized in the dimensionless (ξ,η) coordinate for all times. With the details omitted, then the transformation of Eqs.(6)-(8) and Eqs.(17)-(20) are defined as:

$$\frac{1}{J}\left(x_\xi \frac{\partial E_y}{\partial \eta}\right) = \mu \frac{\partial H_x}{\partial t} \tag{22}$$

$$-\frac{1}{J}\left(z_\eta \frac{\partial E_y}{\partial \xi}\right) - z_\xi \frac{\partial E_y}{\partial \eta} = -\mu \frac{\partial H_z}{\partial t} \tag{23}$$

$$-\frac{1}{J}\left\{\left(z_\eta \frac{\partial H_z}{\partial \xi} - z_\xi \frac{\partial H_z}{\partial \eta}\right) - \left(x_\xi \frac{\partial H_x}{\partial \eta}\right)\right\} = \sigma E_y + \varepsilon \frac{\partial E_y}{\partial t} \tag{24}$$

$$\frac{\partial E_y}{\partial t} = \upsilon \frac{1}{J}\left(x_\xi \frac{\partial E_y}{\partial \eta}\right) \tag{25}$$

$$\begin{aligned} \frac{\partial T_j}{\partial t} &= \frac{a}{J^2}\left(\alpha \frac{\partial^2 T_j}{\partial \xi^2} - 2\beta \frac{\partial^2 T_j}{\partial \xi \partial \eta} + \gamma \frac{\partial^2 T_j}{\partial \eta^2}\right) + \\ &\frac{a}{J^3}\left[\left(\alpha \frac{\partial^2 x}{\partial \xi^2}\right)\left(z_\xi \frac{\partial T_j}{\partial \eta} - z_\eta \frac{\partial T_j}{\partial \xi}\right) + \alpha \frac{\partial^2 z}{\partial \xi^2} - 2\beta \frac{\partial^2 z}{\partial \xi \partial \eta} + \gamma \frac{\partial^2 z}{\partial \eta^2}\left(-x_\xi \frac{\partial T_j}{\partial \eta}\right)\right] \\ &+ \frac{Q_j}{\rho \cdot C_p} + \frac{1}{J}\left(x_\xi \frac{\partial T_j}{\partial \eta}\right)\frac{dz}{dt} \end{aligned} \tag{26}$$

$$\begin{aligned} &\left\{\lambda_s \frac{1}{J}\left(x_\xi \frac{\partial T_s}{\partial \eta}\right) - q_{Bou}\Delta z_{Bou} - \lambda_l \frac{1}{J}\left(x_\xi \frac{\partial T_l}{\partial \eta}\right)\right\}\left\{1 + \left(\frac{1}{J}\left[z_\eta \frac{\partial z_{Bou}}{\partial \xi} - z_\xi \frac{\partial z_{Bou}}{\partial \eta}\right]\right)^2\right\} \\ &= \rho_s L_s S_s \frac{\partial z_{Bou}}{\partial t} \end{aligned} \tag{27}$$

$$\text{where } J = x_\xi \cdot z_\eta - x_\eta \cdot z_\xi,\ \alpha = x_\eta^{\ 2} + z_\eta^{\ 2}, \beta = x_\xi \cdot x_\eta + z_\xi \cdot z_\eta, \gamma = x_\xi^{\ 2} + z_\xi^{\ 2} \tag{28}$$

Here, x_ξ, x_η, z_ξ and z_η denote partial derivatives, J is the Jacobien, β,α,γ are the geometric factors and η,ξ are the transformed coordinates.

Numerical Solution Method

In order to predict the electromagnetic field, a finite difference time domain (FDTD) method is applied [11]. The heat transport equation must be solved by the method of finite differences based on the notion of control volumes as described by Patankar [12]. Therefore, the calculation conditions are as follows: (1) Because the propagating velocity of microwave is very fast compared with the rate of heat transfer, different time steps of 1×10^{-12} [s] and 1 [s] are used for calculations of the electromagnetic field and temperature field, respectively, (2) number of grid; N = 112 (width) × 605 (length), (3) relative errors in the iteration procedure of 10^{-8} were chosen.

Results and Discussions

The Temperature Distributions and Melting Front

Figures 3 and 4 show the simulations of temperature distributions within the multi layered packed beds in the vertical plane (x-z) for the cases setting the frozen layer on and under the unfrozen layer, respectively, which correspond to that of initial temperature with 0°C and microwave power input of 1000W. Some of electromagnetic and thermo-physical properties used in the computation are given in Table 1.

TABLE 1

The electromagnetic and thermo-physical properties used in the computations

$\varepsilon_0 = 8.85419\times10^{-12}$[F/m],	$\mu_0 = 4.0\pi\times10^{-7}$[H/m]
$\varepsilon_{ra} = 1.0$	$\varepsilon_{rp} = 5.1$
$\mu_{ra} = 1.0$	$\mu_{rp} = 1.0$
$\tan\delta_a = 0.0$	$\tan\delta_s = 0.0124$
$\mu_l = 1.0$	$\rho_s = 1910.9$[kg/m^3]
$\rho_l = 1000.0$[kg/m^3]	$c_{ps} = 1.280$[kJ/(kg·K)]
$c_{pl} = 2.099$[kJ/(kg·K)]	$\lambda_s = 1.48$[W/(m·K)]
$\lambda_l = 0.610$[W/(m·K)]	

Figure 3, for the case setting a frozen layer on the unfrozen layer, since an ice in a frozen layer is highly transparent material, so that the incident microwave is easily irradiated to the unfrozen layer is highly absorptive material. In Fig. 3, it is seen that the maximum temperature was located at the leading edge of a unfrozen layer leads to heat transfer from the hotter region of higher microwave energy absorption (unfrozen layer) to the cooler, low microwave energy deposition region (frozen layer). As the thickness of unfrozen layer is increased due to the melting of frozen layer is progressed, where the strength of the microwave energy absorbed increases (Fig. 5). Consequently, the movement of melting front occurs at the interface between frozen layer and unfrozen layer. The temperature distribution within the unfrozen layer has a wavy shape and decays slowly along the propagation direction because a stronger standing waves form in the unfrozen layer. Furthermore, setting of a frozen layer on the unfrozen layer protects the reflection of wave from the surface leads to increase the penetration depth of the microwave inside the unfrozen layer. With increasing time, the temperature distribution within the unfrozen layer rapidly rises, causing the melting process to rise up. Nevertheless, the temperature distribution within the frozen layer stays colder due to the difference between the dielectric properties of water and ice. This is because the water is a highly absorptive material, while ice is highly transparent (which corresponds to

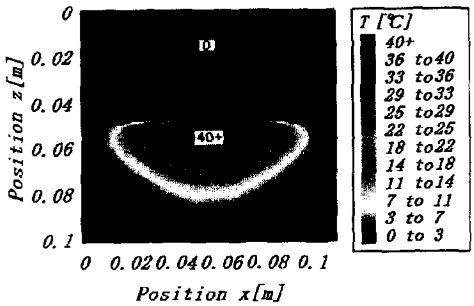

(a) 30s

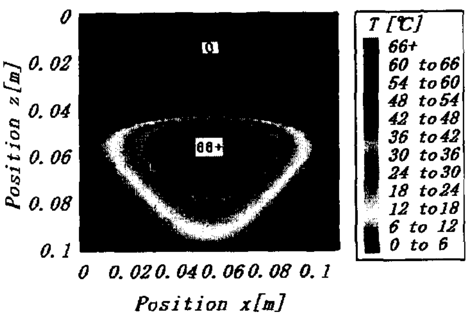

(b) 60 s

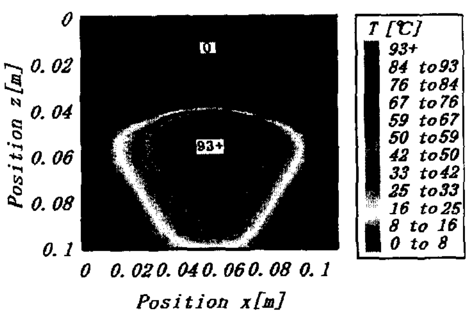

(c) 90s

FIG. 3
Simulation of T at various times (Setting the frozen layer on the unfrozen layer)

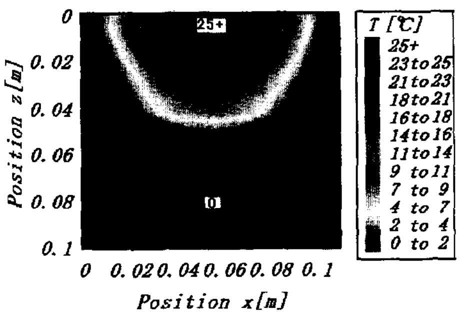

(a) 30s

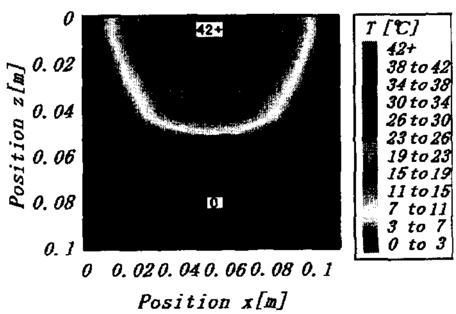

(b) 60 s

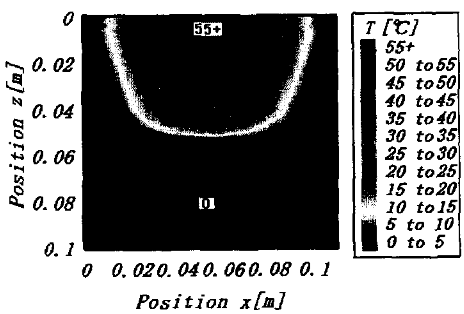

(c) 90s

FIG. 4
Simulation of T at various times (Setting the frozen layer under the unfrozen layer)

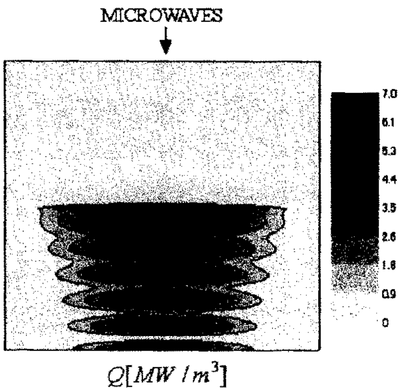

(a) 30s

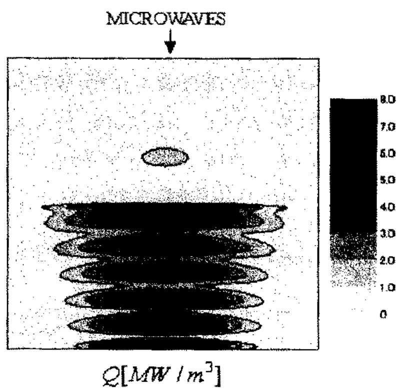

(b) 60s

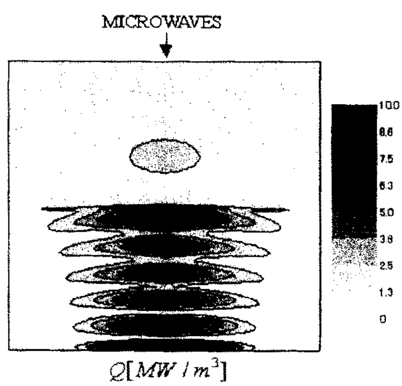

(c) 90s

FIG. 5

Simulation of Q at various times (Setting the frozen layer on the unfrozen layer)

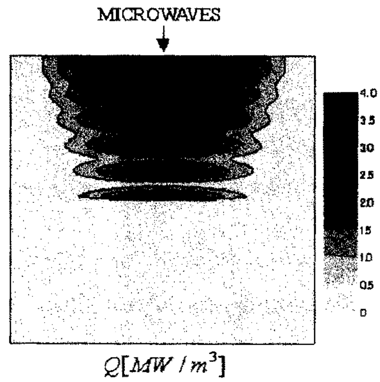

(a) 30s

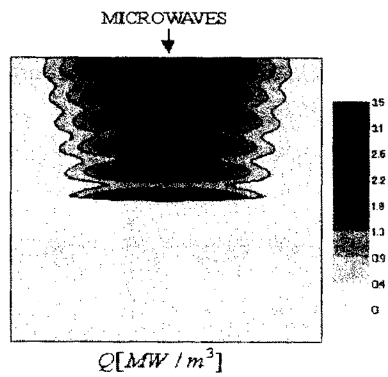

(b) 60s

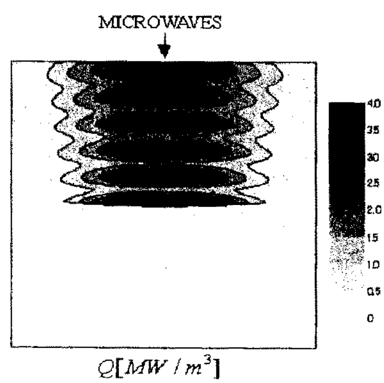

(c) 90s

FIG. 6

Simulation of Q at various times (Setting the frozen layer under the unfrozen layer) the lower microwave energy absorbed within frozen layer). At time 90s, there is a difference of about 92 degrees between the maximum and minimum temperatures.

On the other hand, in the latter case is shown in Fig.4, since the incident wave passing through cavity having low permittivity is directly irradiated to the unfrozen layer having high permittivity, the major part of microwave is reflected from the surface of unfrozen layer and having of the frozen layer under the unfrozen layer protects the reflection of microwave from the interface between the unfrozen layer and frozen layer, void the formation of standing waves leads to the strength of the microwave energy absorbed decreases (Fig. 6). Additionally, it is seen that the microwave energy absorbed within the unfrozen layer situated closet to the incoming microwave and slowly rises with the elapsed time. However, the microwave energy absorbed within the frozen layer is almost the same to former case indicating the dielectric properties dominated melting process. At 90s, there is a difference of about 55 degrees between the maximum and minimum temperatures. In contrast to that in the former case, the melting rate slowly rises with the elapsed time for this case. The following discussion refers to the effect of dielectric properties on the melting front during microwave melting process. Figures 7(a) and (b) show the measured and predicted results of the melting front for the cases of setting a frozen layer on and under the unfrozen layer, respectively.

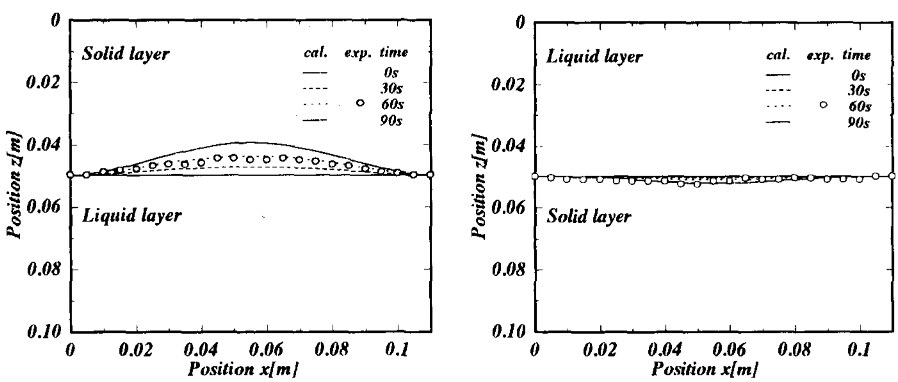

(a) (b)

FIG. 7

Measured and predicted interface position, (a) Setting a frozen layer (solid) on the unfrozen layer (liquid), (b) setting a frozen layer (solid) under the unfrozen layer (liquid)

In the former case, the shape of the melting front at various times is shown in Fig. 7(a), it can be seen that for the early stage of melting process, the melting front is almost parallel to the interface between frozen layer and unfrozen layer. Later, the melting front gradually exhibits a shape typical for microwave dominated melting. Since the most of the heating takes place at the middle region of rectangular wave guide, so that the interface moves faster in this location where the liquid water at the melting front strongly absorbs the microwave energy (as referred to Fig.5). However, the melting rate decreases toward the sidewalls, since the microwave energy absorbed in this location has a weak distribution.

On the other hand, in the latter case is shown in Fig.7 (b), Due to the high value of permittivity, the skin-depth heating effect causes a major part of the incident wave to be reflected from the surface of unfrozen layer (liquid) during the microwave melting process. This phenomenon explains why the microwave energy absorbed within the unfrozen layer in the this case (as referred to Fig. 6) is slightly lower than that observed in the former case and why the heating (Fig. 4) and microwave energy absorbed (Fig. 6) are more intense close to the leading edge of the unfrozen layer. In contrast to that in former case, the melting front is slowly moves with the elapsed time, and the melting front moves slowly along the propagation direction due to the characteristics of dielectric properties as explained in above paragraph.

During the experiment of microwave melting process, the impact on the uncertainty of our data may cause by variations in humidity, room temperature and another effects. The uncertainty in melting kinetics was assumed to result from errors in the measured melting front of the sample. The calculated melting kinetic uncertainties in all tests were less than 3.5 percent. The uncertainly in microwave energy absorbed was assumed to result from errors in measured input power and reflected power. The calculated uncertainty associated with temperature was less than 2 percent.

Conclusions

The following results concerning the microwave melting phenomena were obtained:
(1) A generalized mathematical model of melting process by microwave is proposed. It has been successfully used to describe the melting phenomena of several conditions. (2) The melting of frozen packed beds was performed for the two different layer packed beds which consists of frozen and unfrozen layers. The direction of melting against the incident microwave strongly depends on the structure of layered packed beds because of the difference in the dielectric properties between water and ice. (3) Based on a model combined the electromagnetic and temperature fields, the predicted results were in good agreement with the experimental results for the melting of frozen packed beds.

Nomenclature

a	thermal diffusivity [m^2/s]	L	latent heat [J/kg]
C_p	specific heat capacity [J/kgK]	Q	microwave energy absorbed term [W/m^3]
		q	electric charge density [C/m^3]
E	electric field intensity [V/m]	T	temperature [C]
f	frequency of incident wave [Hz]	t	time [s]
H	magnetic field intensity [A/m]	$\tan\delta$	loss tangent coefficient [-]

x, y, z Cartesian coordinates [-]

Greek letters

ε	permittivity [F/m]	σ	electric conductivity [S/m]
μ	magnetic permeability [H/m]	ω	angular frequency [rad/s]
υ	velocity of microwave [m/s]	λ	effective thermal conductivity [W/mK]

Subscripts

0	free space	l	liquid
a	air	r	relative
j	layer number	s	solid

References

1. B.P. Pangrle, K.G. Ayappa, H.T. Davis, E.A Davis and J. Gordon, *AIChE J.*, 37, 1789 (1991).

2. B.P. Pangrle, K.G. Ayappa, E. Sutano, H.T. Davis, E.A Davis and J. Gordon, Chem. *Engg. Comm.,* 112, 39 (1992).

2. X. Zeng and A. Faghri, *ASME J. Heat Transfer*, 116, 446 (1994).

4. T. Basak and K.G. Ayappa, *AIChE J.*, 43, 1662 (1997).

5. C.J. Coleman, Appl. *Math. Modelling*, 14, 439 (1990).

6. D. Bialod, M. Jolion and R. Legoff, *J. Microwave power*, 13, 269 (1978).

7. D.J. Cleland, A.C. Cleland, R. L. Earl and S.J. Byrne, *Int. J. Refrig.*, 9, 220 (1986).

8. A.R. Von Hippel, *Dielectric Materials and Applications*, MIT Press, Boston (1954).

9. J. Wang and T. Schmugge, *IEEE Transactions on geosciences and remote sensing*, 4, 288 (1980).

10. G. Mur, *IEEE Transactions of Electromagnetic Compatibility*, 4, 377 (1981).

11. K.S. Yee, *IEEE Transactions of Antennas Propagation*, AP-14, 302 (1966).

12. S.V. Patankar, *Numerical Heat Transfer and Fluid Flow*, Hemisphere Publishing Corporation, New York (1980).

13. P. Ratanadecho, K. Aoki and M. Akahori, *Drying Technology*, 18 (2001).

14. J. Clemens and C. Saltiel, *Int. J. Heat and Mass Transfer*, 39, 1665 (1996).

15. C. Saltiel, and A. Datta, *Advance Heat Transfer*, 30 1 (1997).

16. R. M. Perkin, *Int. J. Heat and Mass Transfer*, 23, 687 (1980).

17. L.E. Erikkson, *AIAA J.*, 20, 1313 (1982).

Received May 17, 2001

Available online at www.sciencedirect.com
ScienceDirect
ELSEVIER
J. Math. Anal. Appl. 329 (2007) 145–162
Journal of MATHEMATICAL ANALYSIS AND APPLICATIONS
www.elsevier.com/locate/jmaa

Explicit solutions for a two-phase unidimensional Lamé–Clapeyron–Stefan problem with source terms in both phases

A.C. Briozzo [a], M.F. Natale [a], D.A. Tarzia [a,b,*]

[a] *Departamento de Matemática, F.C.E., Universidad Austral, Paraguay 1950, S2000FZF Rosario, Argentina*
[b] *CONICET, Argentina*

Received 26 December 2005

Available online 20 July 2006

Submitted by P. Broadbridge

Abstract

A two-phase Stefan problem with heat source terms of a general similarity type in both liquid and solid phases for a semi-infinite phase-change material is studied. We assume the initial temperature is a negative constant and we consider two different boundary conditions at the fixed face $x = 0$, a constant temperature or a heat flux of the form $-q_0/\sqrt{t}$ $(q_0 > 0)$. The internal heat source functions are given by $g_j(x,t) = \frac{\rho l}{t}\beta_j(\frac{x}{2a_j\sqrt{t}})$ ($j = 1$ solid phase; $j = 2$ liquid phase) where $\beta_j = \beta_j(\eta)$ are functions with appropriate regularity properties, ρ is the mass density, l is the fusion latent heat by unit of mass, a_j^2 is the diffusion coefficient, x is the spatial variable and t is the temporal variable. We obtain for both problems explicit solutions with a restriction for data only for the second boundary conditions on $x = 0$. Moreover, the equivalence of the two free boundary problems is also proved. We generalize the solution obtained in [J.L. Menaldi, D.A. Tarzia, Generalized Lamé–Clapeyron solution for a one-phase source Stefan problem, Comput. Appl. Math. 12 (2) (1993) 123–142] for the one-phase Stefan problem. Finally, a particular case where β_j $(j = 1, 2)$ are of exponential type given by $\beta_j(x) = \exp(-(x + d_j)^2)$ with x and $d_j \in \mathbb{R}$ is also studied in details for both boundary temperature conditions at $x = 0$. This type of heat source terms is important through the use of microwave energy following [E.P. Scott, An analytical solution and sensitivity study of sublimation–dehydration within a porous medium with volumetric heating, J. Heat Transfer 116 (1994) 686–693]. We obtain a unique solution of the similarity type for any data when a temperature

* Corresponding author.
E-mail addresses: adriana.briozzo@fce.austral.edu.ar (A.C. Briozzo), maria.natale@fce.austral.edu.ar (M.F. Natale), domingo.tarzia@fce.austral.edu.ar (D.A. Tarzia).

0022-247X/$ – see front matter
doi:10.1016/j.jmaa.2006.05.083

boundary condition at the fixed face $x = 0$ is considered; a similar result is obtained for a heat flux condition imposed on $x = 0$ if an inequality for parameter q_0 is satisfied.

Keywords: Stefan problem; Free boundary problem; Lamé–Clapeyron solution; Neumann solution; Phase-change process; Fusion; Sublimation–dehydration process; Heat source; Similarity solution

1. Introduction

Following Scott [20], sublimation–dehydration or freeze–drying, is used as a method for removing moisture from biological materials, such as food. Some of the advantages of sublimation–dehydration over evaporative drying are that the structural integrity of the material is maintained and product degradation is minimized (Ang et al. [1], Rosenberg, Bögl [19]). The major disadvantage of the freeze–drying process is that it is generally slow, and consequently, the process is economically unfeasible for certain materials. One of the means of alleviating this problem is through the use of microwave energy.

Several mathematical models have been proposed to describe the freeze–drying process without microwave heating (Fey, Boles [10], Lin [13]). Only a few studies have also included a microwave heat source in the model (Ang et al. [1]). Phase-change problems appear frequently in industrial processes; a large bibliography on the subject was given recently in Tarzia [22].

In Menaldi, Tarzia [14] the one-phase Lamé–Clapeyron–Stefan problem [12] with internal heat sources of general similarity type was studied and a generalized Lamé–Clapeyron explicit solution was obtained. Moreover, necessary and sufficient conditions were given in order to characterize the source term which provides a unique solution.

In Bouillet, Tarzia [5], the self-similar solutions $\theta(x,t) = \theta(\eta) = \theta(x/\sqrt{t})$ of the problem

$$\begin{aligned} &E(\theta)_t - A(\theta)_{xx} = \frac{1}{t} B(\eta), \quad \eta > 0, \\ &\theta(x,t) = C > 0, \quad t > 0, \\ &E\big(\theta(x,0)\big) = 0, \quad x > 0, \end{aligned}$$

were studied where E and A are monotone increasing functions, A being continuous, with $E(0) = A(0) = 0$ and $\lambda = E(0^+) > 0$. This equation can describe the conservation of thermal energy in a heat conduction process for a semi-infinite material with a "self-similar" source or sink term of the type $B(x/\sqrt{t})/t$. Moreover, $E(\theta)$ represents an energy per unit volume at level (temperature) θ, $A'(\theta) \geqslant 0$ is the thermal conductivity and $B(\eta)/t$ represents a singular source or sink depending of the sign of the function B. It was obtained for the inverse function $\eta = \eta(\theta)$ an integral equation equivalent to the above problem and it was proven that for certain hypotheses over data there exists at least a solution of the corresponding integral equation following Bouillet [4].

Several applied papers give us the significance of the source terms in the interior of the material which can undergo a change of phase, e.g. Bhattacharya et al. [3], Carslaw, Jaeger [6], Feng [9], Grigor'ev et al. [11], Mercado et al. [15], Ratanadecho et al. [17], Ward [23]. In Scott [20] there is a mathematical model for sublimation–dehydration with volumetric heating of a particular exponential type from which analytical solutions for dimensionless temperature, vapor concentration, and pressure were obtained for two different temperature boundary conditions. It was considered a semi-infinite frozen porous medium with constant thermal properties subject to a sublimation–dehydration process involving a volumetric heat source of the type

$$g(x,t)=\frac{\text{const.}}{t}\exp\bigl(-(x+d)^2\bigr).$$

A sensitivity study was also conducted in which the effects of the material properties inherent in these solutions were analyzed. The mathematical analysis of the analytical solutions is only given from the numerical computation point of view. In one phase is taken d equals to 0 and in the other one d is proportional to the constant λ which characterizes the interface position; this last choice is, for us, a nonadequate choice of a parameter because it depends on the solution itself.

Analytical solutions can provide important insights into the importance of different material properties on the solution, which can aid in the development of improved mathematical models for this process. These solutions provide an important means of evaluating numerical schemes which can later be used with less restrictive assumptions, if necessary, to simulate actual processes. Moreover, it can be used to obtain super and sub solutions for general conditions by using the maximum principle.

In this paper a semi-infinite homogeneous phase-change material initially in solid phase at the uniform temperature $-C<0$, with a volumetric heat source, is considered. A mathematical description for the temperature within the material is given by

$$\frac{\partial T_2}{\partial t}(x,t)=a_2^2\frac{\partial^2 T_2}{\partial x^2}(x,t)+\frac{1}{\rho c_2}g_2(x,t),\quad 0<x<s(t),\ t>0; \tag{1}$$

$$\frac{\partial T_1}{\partial t}(x,t)=a_1^2\frac{\partial^2 T_1}{\partial x^2}(x,t)+\frac{1}{\rho c_1}g_1(x,t),\quad x>s(t),\ t>0; \tag{2}$$

for two given internal source functions (Bouillet, Tarzia [5], Menaldi, Tarzia [14], Scott [20]) given by

$$g_j=g_j(x,t)=\frac{\rho l}{t}\beta_j\left(\frac{x}{2a_j\sqrt{t}}\right),\quad j=1,2, \tag{3}$$

where $\beta_j=\beta_j(\eta)$ are integrable functions in $(0,\epsilon)$ $\forall\epsilon>0$ and $\beta_j(\eta)\exp(\eta^2)$ are integrable functions in $(M,+\infty)$ $\forall M>0$. We assume that $\beta_1(\eta)\geqslant 0$, $\beta_2(\eta)\leqslant 0$ and ρ is the mass density, l is the fusion latent heat per unit of mass, a_j^2 is the diffusion coefficient, c_j is the specified heat per unit of mass and k_j is the thermal conductivity, for $j=1,2$.

The initial temperature and the temperature as $x\to\infty$ are assumed to be constant

$$T_1(x,0)=T_1(+\infty,t)=-C<0,\quad x>0,\ t>0. \tag{4}$$

At $x=0$, two different temperature boundary conditions are considered, the first is a constant temperature condition

$$T_2(0,t)=B>0,\quad t>0, \tag{5}$$

which is studied in Section 2.1, and the second is an assumed heat flux of the form

$$k_2\frac{\partial T_2}{\partial x}(0,t)=\frac{-q_0}{\sqrt{t}},\quad t>0, \tag{6}$$

which is studied in Section 3.

We remark that $-q_0/\sqrt{t}$ denotes the prescribed heat flux on the boundary $x=0$ which is of the type imposed in Tarzia [21] where it was proven that the heat flux condition (6) on the fixed face $x = 0$ is equivalent to the constant temperature boundary condition (5) for the two phase Stefan problem for a semi-infinite material with constant thermal coefficient in both phases without source terms. This kind of heat flux condition was also considered in several papers, e.g. Barber [2], Coelho Pinheiro [7], Polyanin, Dil'man [16], Rogers [18].

The phase-change interface condition is determined from an energy balance at the free boundary $x = s(t)$:

$$k_1 \frac{\partial T_1}{\partial x}\big(s(t), t\big) - k_2 \frac{\partial T_2}{\partial x}\big(s(t), t\big) = \rho l \dot{s}(t), \quad t > 0, \tag{7}$$

where the temperature conditions at the interface are assumed to be constant:

$$T_1\big(s(t), t\big) = T_2\big(s(t), t\big) = 0, \quad t > 0. \tag{8}$$

Moreover, the initial position of the free boundary is

$$s(0) = 0. \tag{9}$$

In Section 2.1 we obtain an explicit solution for the problem (1)–(5), (7)–(9), when the general type of sources given by (3) verifies appropriate properties, and in Section 2.2 we give monotonicity properties of the solution. Both results are obtained for any data and thermal coefficients (particularly for all β's source terms). We remark that when we consider the particular case $C = 0$ and $\beta_1 = 0$ we obtain the solutions given in Menaldi, Tarzia [14] for the one-phase case.

In Section 3 we solve the same free boundary problem but with the heat flux condition of the type $-\frac{q_0}{\sqrt{t}}$ ($q_0 > 0$) prescribed on the fixed face $x = 0$, and we obtain an explicit solution to this problem if the coefficient q_0 satisfies an appropriate particular inequality given by (46). This result is new for the analytical solution. Furthermore, if we take $\beta_1 = \beta_2 = 0$ we get the inequality (46) which was given in Tarzia [21] for the classical two-phase Stefan problem.

In Section 4 we prove the equivalence of the two free boundary problems: the first one with the Dirichlet constant boundary condition (5) considered in Section 2, and the second one with the Neumann boundary condition (6) considered in Section 3.

In Section 5 we will consider the volumetric heat sources of the type given by expressions (56) proposed by Scott [20] in thermal processes. In this particular case we can explicitly obtain conditions (45) and (46) which guarantees the existence of a unique solution, as a function of the parameters of the two problems, in order to have the corresponding exact similarity solution in both phases. If we take $d_1 = d_2 = 0$ in β's expressions (56) our solution (63) coincides with Scott's solution taking a null vapor mass flow rate.

2. Free boundary problem with temperature boundary condition

2.1. *Solution of the free boundary problem with temperature boundary condition at $x = 0$*

Applying the immobilization domain method (see Crank [8]), we are looking for solutions of the type

$$T_j(x, t) = \theta_j(y), \quad j = 1, 2, \tag{10}$$

where the new independent spatial variable y is defined by

$$y = \frac{x}{s(t)}. \tag{11}$$

Then, the condition (7) is transformed into

$$k_1\theta_1'(1) - k_2\theta_2'(1) = \rho l s(t)\dot{s}(t), \tag{12}$$

and we must have necessarily that $s(t)\dot{s}(t) = \text{const.}$ i.e.,

$$s(t) = 2a_2\lambda\sqrt{t}, \tag{13}$$

where the dimensionless parameter $\lambda > 0$ is unknown.

Next, we define

$$R_j(\eta) = \theta_j\left(\frac{\eta}{\lambda}\right), \quad j = 1, 2,\ \eta = \lambda y, \tag{14}$$

then the problem (1)–(5), (7)–(9) is equivalent to the following one:

$$R_2''(\eta) + 2\eta R_2'(\eta) = -\frac{4l}{c_2}\beta_2(\eta), \quad 0 < \eta < \lambda; \tag{15}$$

$$R_1''(\eta) + 2\frac{a_2^2}{a_1^2}\eta R_1'(\eta) = -\frac{4a_2^2 l}{a_1^2 c_1}\beta_1\left(\frac{a_2}{a_1}\eta\right), \quad \eta > \lambda; \tag{16}$$

$$R_1(\lambda) = R_2(\lambda) = 0; \tag{17}$$

$$k_1R_1'(\lambda) - k_2R_2'(\lambda) = 2\rho l\lambda a_2^2; \tag{18}$$

$$R_1(+\infty) = -C; \tag{19}$$

$$R_2(0) = B. \tag{20}$$

After some elementary computations, from (15), (17) and (20) we obtain

$$R_2(\eta) = B - \big(B + \varphi_2(\lambda)\big)\frac{\operatorname{erf}(\eta)}{\operatorname{erf}(\lambda)} + \varphi_2(\eta), \quad 0 < \eta < \lambda,$$

$$\varphi_2(\eta) = \frac{2l\sqrt{\pi}}{c_2}\int_0^\eta \beta_2(u)\exp\big(u^2\big)\big(\operatorname{erf}(u) - \operatorname{erf}(\eta)\big)\,du \tag{21}$$

and, from (16), (17) and (19), we have

$$R_1(\eta) = -\frac{(C + \varphi_1(+\infty))}{\operatorname{erf}c(\frac{a_2}{a_1}\lambda)}\frac{2}{\sqrt{\pi}}\int_{\frac{a_2}{a_1}\lambda}^{\frac{a_2}{a_1}\eta}\exp\big(-u^2\big)\,du + \varphi_1(\eta), \quad \eta > \lambda,$$

$$\varphi_1(\eta) = \frac{2l\sqrt{\pi}}{c_1}\int_{\frac{a_2}{a_1}\lambda}^{\frac{a_2}{a_1}\eta}\beta_1(u)\exp\big(u^2\big)\left[\operatorname{erf}(u) - \operatorname{erf}\left(\frac{a_2}{a_1}\eta\right)\right]du \tag{22}$$

where λ is the unknown coefficient which must verify the condition (18).

Furthermore, Eq. (18) for λ is equivalent to the following equation

$$f_1(x, \beta_1) = f_2(x, \beta_2), \quad x > 0, \tag{23}$$

where

$$f_1(x,\beta_1) = F_0(x)\, h_1(x,\beta_1), \tag{24}$$

$$f_2(x,\beta_2) = Q\left(\frac{a_2}{a_1}x\right) h_2(x,\beta_2) \tag{25}$$

with

$$Q(x) = \sqrt{\pi}\, x \exp\left(x^2\right)\left(1-\operatorname{erf}(x)\right), \quad x>0, \tag{26}$$

$$F_0(x) = x \operatorname{erf}(x) \exp\left(x^2\right), \quad x>0, \tag{27}$$

$$h_1(x,\beta_1) = \mathrm{Ste}_1 - 2\sqrt{\pi} \int_{\frac{a_2}{a_1}x}^{+\infty} \operatorname{erf} c(u)\beta_1(u) \exp\left(u^2\right) du, \tag{28}$$

$$h_2(x,\beta_2) = \frac{\mathrm{Ste}_2}{\sqrt{\pi}} - F(x,\beta_2), \quad x>0, \tag{29}$$

with

$$F(x,\beta_2) = F_0(x) - 2\int_0^x \operatorname{erf}(u)\beta_2(u)\exp\left(u^2\right) du, \quad x>0, \tag{30}$$

and

$$\mathrm{Ste}_1 = \frac{Cc_1}{l}, \qquad \mathrm{Ste}_2 = \frac{Bc_2}{l} \tag{31}$$

are the Stefan numbers for phases $j=1$ and $j=2$, respectively.

Theorem 1. *Equation* (23) *has a unique solution* $\lambda>0$. *Moreover, the free boundary problem with heat source terms* (1)–(5), (7)–(9) *has an explicit solution given by*

$$\begin{aligned}
T_1(x,t) &= \frac{-(C+\varphi_1(+\infty))}{\operatorname{erf} c(\frac{a_2}{a_1}\lambda)}\left[\operatorname{erf}\left(\frac{x}{2a_1\sqrt{t}}\right) - \operatorname{erf}\left(\frac{a_2}{a_1}\lambda\right)\right] + \varphi_1\left(\frac{x}{2a_2\sqrt{t}}\right), \\
&\quad \textit{for } x>s(t),\ t>0; \\
T_2(x,t) &= \frac{2l\sqrt{\pi}}{c_2}\int_0^{\frac{x}{2a_2\sqrt{t}}} \beta_2(u)\exp\left(u^2\right)\left(\operatorname{erf}(u) - \operatorname{erf}\left(\frac{x}{2a_2\sqrt{t}}\right)\right) du \\
&\quad + B - \left(B+\varphi_2(\lambda)\right)\frac{\operatorname{erf}(\frac{x}{2a_2\sqrt{t}})}{\operatorname{erf}(\lambda)} \quad \textit{for } 0<x<s(t),\ t>0,
\end{aligned} \tag{32}$$

where $\varphi_1(\eta)$ *and* $\varphi_2(\eta)$ *are defined in* (22), (21) *respectively and the free boundary* $s(t)$ *is given by* (13) *where the coefficient* λ *is the unique solution of Eq.* (23).

Proof. Taking into account Appendix A (Lemma A.1) we can prove that Eq. (23) has a unique solution $\lambda>0$. We invert relations (14), (10) and (11) in order to obtain an explicit solution of problem (1)–(5), (7)–(9) with the source terms g_j defined by (3). □

Remark 1. If the initial temperature $C = 0$ and the solid phase source $\beta_1 = 0$ then we have the one-phase Stefan problem with a constant temperature B at the fixed face $x = 0$ which is the problem considered in Menaldi, Tarzia [14]. The solution is given by

$$\begin{cases} T(x,t) = T_2(x,t) = B - \big(B + \varphi_2(\lambda)\big)\dfrac{\operatorname{erf}(\frac{x}{2a_2\sqrt{t}})}{\operatorname{erf}(\lambda)} \\ \qquad + \dfrac{2l\sqrt{\pi}}{c_2}\displaystyle\int_0^{\frac{x}{2a_2\sqrt{t}}} \beta_2(u)\exp\big(u^2\big)\left(\operatorname{erf}(u) - \operatorname{erf}\left(\frac{x}{2a_2\sqrt{t}}\right)\right)du, \\ \quad 0 < x < s(t),\ t > 0; \\ s(t) = 2\lambda a_2\sqrt{t}, \end{cases} \tag{33}$$

where λ is the unique solution of equation $F(x,\beta_2) = \frac{\mathrm{Ste}_2}{\sqrt{\pi}}$, $x > 0$.

Remark 2. In the particular case $\beta_1 = \beta_2 = 0$ we have the classic Neumann solution (see Carslaw, Jaeger [6]).

2.2. *Monotonicity properties*

We denote by $T_{\beta_1\beta_2,1}(x,t)$, $T_{\beta_1\beta_2,2}(x,t)$ and $s_{\beta_1\beta_2}(t)$ (i.e., $\lambda_{\beta_1\beta_2}$) the solution to problem (1)–(5), (7)–(9) for data β_1 and β_2. We will compare this solution with that corresponding to the case $\beta_1 = 0$ and $\beta_1 = \beta_2 = 0$.

We obtain a monotonicity property for the corresponding free-boundaries in Lemma 2 and for temperatures in Theorem 3.

Lemma 2. *If $\beta_1 \geqslant 0$ and $\beta_2 \leqslant 0$ then we have the following monotonicity properties*:

$$\begin{aligned} &\text{(i)} \quad s_{0\beta_2}(t) \leqslant s_{\beta_1\beta_2}(t) \leqslant s_{\beta_1 0}(t), \quad t > 0, \\ &\text{(ii)} \quad s_{0\beta_2}(t) \leqslant s_{00}(t) \leqslant s_{\beta_1 0}(t), \quad t > 0. \end{aligned} \tag{34}$$

Proof. In order to prove (34) it is sufficient to show the same inequality for the coefficient λ, that is,

$$\begin{aligned} &\text{(i)} \quad \lambda_{0\beta_2} \leqslant \lambda_{\beta_1\beta_2} \leqslant \lambda_{\beta_1 0}, \\ &\text{(ii)} \quad \lambda_{0\beta_2} \leqslant \lambda_{00} \leqslant \lambda_{\beta_1 0}. \end{aligned} \tag{35}$$

We can rewrite Eq. (23) for λ by the following

$$G_1(x,\beta_1) = G_2(x,\beta_2) \tag{36}$$

where the real functions G_1 and G_2 are defined by

$$G_1(x,\beta_1) = F_0(x)\left[\mathrm{Ste}_1 + Q\left(\frac{a_2}{a_1}x\right) - 2\sqrt{\pi}\int_{\frac{a_2}{a_1}x}^{+\infty} \operatorname{erf}c(u)\beta_1(u)\exp\big(u^2\big)\,du\right], \tag{37}$$

$$G_2(x,\beta_2) = Q\left(\frac{a_2}{a_1}x\right)\left[\frac{\mathrm{Ste}_2}{\sqrt{\pi}} + 2\int_0^x \operatorname{erf}(u)\beta_2(u)\exp\big(u^2\big)\,du\right]. \tag{38}$$

Taking into account $\beta_1 \geqslant 0$ and $\beta_2 \leqslant 0$ and by comparison of functions G_1 and G_2 we obtain (35)(i), (ii). See Appendix A (Lemma A.2). □

Theorem 3. *The solution to problem* (1)–(5), (7)–(9) *for data* $\beta_1 \geqslant 0$ *and* $\beta_2 \leqslant 0$ *satisfies the following monotonicity properties*:

$$\begin{aligned}
&\text{(i)} && T_{\beta_1\beta_2,2}(x,t) \leqslant T_{\beta_1 0,2}(x,t), \quad 0 \leqslant x \leqslant s_{\beta_1\beta_2}(t),\ t>0,\\
&\text{(ii)} && T_{00,2}(x,t) \leqslant T_{\beta_1 0,2}(x,t), \quad 0 \leqslant x \leqslant s_{00}(t),\ t>0,\\
&\text{(iii)} && T_{0\beta_2,2}(x,t) \leqslant T_{00,2}(x,t), \quad 0 \leqslant x \leqslant s_{0\beta_2}(t),\ t>0,\\
&\text{(iv)} && T_{0\beta_2,1}(x,t) \leqslant T_{00,1}(x,t), \quad x > s_{00}(t),\ t>0,\\
&\text{(v)} && T_{0\beta_2,2}(x,t) \leqslant T_{\beta_1\beta_2,2}(x,t), \quad 0 \leqslant x \leqslant s_{0\beta_2}(t),\ t>0,\\
&\text{(vi)} && T_{0\beta_2,1}(x,t) \leqslant T_{\beta_1\beta_2,1}(x,t), \quad x > s_{\beta_1\beta_2}(t),\ t>0,\\
&\text{(vii)} && T_{00,1}(x,t) \leqslant T_{\beta_1 0,1}(x,t), \quad x > s_{\beta_1 0}(t),\ t>0,\\
&\text{(viii)} && T_{\beta_1\beta_2,1}(x,t) \leqslant T_{\beta_1 0,1}(x,t), \quad x > s_{\beta_1 0}(t),\ t>0.
\end{aligned} \tag{39}$$

Proof. From maximum principle we obtain (39). We will only give the proof of the property (vii).

Let $u(x,t) = T_{\beta_1 0,1}(x,t) - T_{00,1}(x,t)$. Function u satisfies the following conditions:

$$\begin{aligned}
&u_t - a_1^2 u_{xx} = \frac{l}{c_1 t}\beta_1\left(\frac{x}{2a_1\sqrt{t}}\right) \geqslant 0, \quad x > s_{\beta_1 0}(t),\ t>0,\\
&u\big(s_{\beta_1 0}(t),t\big) = -T_{00,1}\big(s_{\beta_1 0}(t),t\big) \geqslant 0, \quad t>0,\\
&u(x,0) = T_{\beta_1 0,1}(x,0) - T_{00,1}(x,0) = -C - (-C) = 0, \quad x > s_{\beta_1 0}(t).
\end{aligned}$$

Then we have $u(x,t) \geqslant 0$ for $x > s_{\beta_1 0}(t)$, $t>0$. □

These monotonicity properties can be interpreted by physical considerations and can be used in order to obtain super and sub explicit solutions for general conditions by using the maximum principle.

3. Solution of the free boundary problem with a heat flux condition on the fixed face $x = 0$

In this section we consider problem (1)–(5), (7)–(9), but condition (5) will be replaced by condition (6) (see Rogers [18], Tarzia [21]). We can define the same transformations (10), (11) and (14) as were done for the previous problem, and we obtain (15)–(19) and

$$R_2'(0) = \frac{-2q_0}{\rho c_2 a_2}. \tag{40}$$

It easy to see that the free boundary must be of the type $s(t) = 2a_2\mu\sqrt{t}$ where μ is a dimensionless constant to be determined. The solution to problem (15)–(19) and (40) is given by

$$R_1(\eta) = -\frac{(C+\varphi_1(+\infty))}{\operatorname{erf}c(\frac{a_2}{a_1}\mu)}\left[\operatorname{erf}\left(\frac{a_2}{a_1}\eta\right) - \operatorname{erf}\left(\frac{a_2}{a_1}\mu\right)\right] + \varphi_3(\eta), \quad \eta > \mu,$$

$$\varphi_3(\eta) = \frac{2l\sqrt{\pi}}{c_1} \int_{\frac{a_2}{a_1}\mu}^{\frac{a_2}{a_1}\eta} \beta_1(u)\exp\left(u^2\right)\left[\operatorname{erf}(u) - \operatorname{erf}\left(\frac{a_2}{a_1}\eta\right)\right] du \tag{41}$$

and

$$R_2(\eta) = \frac{q_0\sqrt{\pi}}{\rho c_2 a_2}\left(\operatorname{erf}(\mu) - \operatorname{erf}(\eta)\right) + \varphi_2(\eta) - \varphi_2(\mu), \quad 0 < \eta < \mu, \tag{42}$$

where φ_2 was defined in (21) and the unknown μ must satisfy the following equation

$$W(x, \beta_1) = V(x, \beta_2), \quad x > 0, \tag{43}$$

where

$$W(x, \beta_1) = \frac{x\exp(x^2)}{Q(\frac{a_2}{a_1}x)}\left[\mathrm{Ste}_1 - 2\sqrt{\pi}\int_{\frac{a_2}{a_1}x}^{+\infty} \operatorname{erf}c(u)\beta_1(u)\exp\left(u^2\right) du\right]$$

and

$$V(x, \beta_2) = \frac{q_0}{\rho l a_2} - x\exp\left(x^2\right) + 2\int_0^x \beta_2(u)\exp\left(u^2\right) du. \tag{44}$$

Theorem 4.

(a) *If condition*

$$\int_0^{+\infty} \operatorname{erf}c(u)\beta_1(u)\exp\left(u^2\right) du \leqslant \frac{\mathrm{Ste}_1}{2\sqrt{\pi}} \tag{45}$$

holds then Eq. (43) *has a unique solution* $\mu > 0$ *if and only if* q_0 *satisfies the following inequality*:

$$q_0 \geqslant 2a_1\rho l\left[\frac{\mathrm{Ste}_1}{2\sqrt{\pi}} - \int_0^{+\infty} \operatorname{erf}c(u)\beta_1(u)\exp\left(u^2\right) du\right]. \tag{46}$$

(b) *If*

$$\int_0^{+\infty} \operatorname{erf}c(u)\beta_1(u)\exp\left(u^2\right) du > \frac{\mathrm{Ste}_1}{2\sqrt{\pi}} \tag{47}$$

holds, then Eq. (43) *has at least a solution* $\mu > 0\ \forall q_0 > 0$.

(c) *Under the hypothesis assumed for* β_i $(i = 1, 2)$ *given in the Introduction, the free boundary problem with sources term* (1)–(4), (6)–(9) *has an explicit solution given by*

$$T_1(x, t) = \frac{-(C + \varphi_3(+\infty))}{\operatorname{erf}c(\frac{a_2}{a_1}\mu)}\left[\operatorname{erf}\left(\frac{x}{2a_1\sqrt{t}}\right) - \operatorname{erf}\left(\frac{a_2}{a_1}\mu\right)\right] + \varphi_3\left(\frac{x}{2a_2\sqrt{t}}\right)$$
$$\text{for } x > s(t),\ t > 0, \tag{48}$$

$$T_2(x,t) = \frac{q_0\sqrt{\pi}}{\rho c_2 a_2}\left[\operatorname{erf}(\mu) - \operatorname{erf}\left(\frac{x}{2a_2\sqrt{t}}\right)\right] + \varphi_2\left(\frac{x}{2a_2\sqrt{t}}\right) - \varphi_2(\mu)$$
$$\text{for } 0 < x < s(t),\ t > 0, \tag{49}$$

where φ_3 *and* φ_2 *are defined in* (41) *and* (21) *respectively, the free boundary is given by*

$$s(t) = 2a_2\mu\sqrt{t},$$

and μ *is the unique solution given in* (a) *or* (b).

Proof. To prove (a) and (b) we use the definitions of the functions W and V, and Lemma A.2 (see Appendix A).

We invert relations (14), (10) and (11) in order to obtain (48)–(49). □

Remark 3. In the particular case $\beta_1 \equiv 0$ and $\beta_2 \leqslant 0$ we have that

$$\exists!\mu > 0 \quad \text{solution of Eq. (43)} \quad \Longleftrightarrow \quad q_0 > \frac{Ck_1}{a_1\sqrt{\pi}}$$

which was the result obtained by Tarzia [21].

Remark 4. Taking into account Lemma A.2 (Appendix A) we can prove the same monotonicity properties given in Section 2.2.

4. Equivalence of the two free boundary problems

We consider the solution $T_2(x,t)$ of problem (1)–(4), (6)–(9) given by (49). We compute $T_2(0,t)$ and we have

$$\begin{aligned} T_2(0,t) &= \frac{q_0\sqrt{\pi}}{\rho c_2 a_2}\operatorname{erf}(\mu) - \varphi_2(\mu) \\ &= \frac{q_0\sqrt{\pi}}{\rho c_2 a_2}\operatorname{erf}(\mu) - \frac{2l\sqrt{\pi}}{c_2}\int_0^{\mu} \beta_2(z)\exp(z^2)\big(\operatorname{erf}(z) - \operatorname{erf}(\mu)\big)\,dz \\ &= B_0(\mu) \end{aligned} \tag{50}$$

which is constant in time.

If we replace B by $B_0(\mu)$ in condition (5) and we solve problem (1)–(5), (7)–(9) we obtain the similarity solutions

$$T_1^*(x,t) = \frac{-(C + \varphi_1(+\infty))}{\operatorname{erf} c(\frac{a_2}{a_1}\lambda)}\left[\operatorname{erf}\left(\frac{x}{2a_1\sqrt{t}}\right) - \operatorname{erf}\left(\frac{a_2}{a_1}\lambda\right)\right] + \varphi_1\left(\frac{x}{2a_2\sqrt{t}}\right),$$
$$\text{for } x > s(t),\ t > 0,$$

$$\begin{aligned} T_2^*(x,t) &= B_0(\mu) - \big(B_0(\mu) + \varphi_2(\lambda)\big)\frac{\operatorname{erf}(\frac{x}{2a_2\sqrt{t}})}{\operatorname{erf}(\lambda)} \\ &\quad + \frac{2l\sqrt{\pi}}{c_2}\int_0^{\frac{x}{2a_2\sqrt{t}}} \beta_2(u)\exp(u^2)\left(\operatorname{erf}(u) - \operatorname{erf}\left(\frac{x}{2a_2\sqrt{t}}\right)\right)du, \end{aligned}$$
$$\text{for } 0 < x < s(t),\ t > 0,$$

where $\varphi_1(\eta)$ and $\varphi_2(\eta)$ are defined in (22), (21) respectively and $s(t) = 2\lambda a_2\sqrt{t}$ is the free boundary. The coefficient λ must be the solution of the following equation:

$$f_1(x,\beta_1) = Q\left(\frac{a_2}{a_1}x\right)\left[\frac{\mathrm{Ste}_2^*}{\sqrt{\pi}} - F(x,\beta_2)\right], \quad x > 0,\ \mathrm{Ste}_2^* = \frac{B_0(\mu)c_2}{l}. \tag{51}$$

We remark that Eq. (51) is Eq. (23) where Ste_2 has been replaced by Ste_2^*.

Theorem 5. *Under the hypotheses* (45) *and* (46) *the solution μ of Eq.* (43) *is also solution of Eq.* (51)*, i.e., $\mu = \lambda$.*

Proof. We have:

$$\begin{aligned}
&\mu \text{ is a solution of Eq. (51)}\\
\iff\quad & f_1(\mu,\beta_1) = Q\left(\frac{a_2}{a_1}\mu\right)\left[\frac{B_0(\mu)c_2}{l\sqrt{\pi}} - F(\mu,\beta_2)\right]\\
\iff\quad & F_0(\mu)\left(\mathrm{Ste}_1 - 2\sqrt{\pi}\int_{\frac{a_2}{a_1}\mu}^{+\infty} \operatorname{erf}c(z)\beta_1(z)\exp\left(z^2\right)dz\right)\\
&\qquad = Q\left(\frac{a_2}{a_1}\mu\right)\operatorname{erf}(\mu)\left(\frac{q_0}{\rho l a_2} + 2\int_0^{\mu}\beta_2(z)\exp\left(z^2\right)dz - \mu\exp\left(\mu^2\right)\right)\\
\iff\quad & W(\mu,\beta_1) = V(\mu,\beta_2)\\
\iff\quad & \mu \text{ is a solution of Eq. (43), i.e., } \mu = \lambda. \qquad \square
\end{aligned}$$

Corollary 6. *The coefficient λ a solution of Eq.* (23) *satisfies the following inequality*:

$$\frac{B + \varphi_2(\lambda)}{\operatorname{erf}(\lambda)} \geqslant \frac{l a_1}{c_2 a_2}\left[\mathrm{Ste}_1 - 2\sqrt{\pi}\int_0^{+\infty} \operatorname{erf}c(z)\beta_1(z)\exp\left(z^2\right)dz\right]. \tag{52}$$

Inequality (52) is a generalization of the inequality for the coefficient which characterizes the free boundary $s(t)$ of the Neumann solution for the particular case $\beta_1 = \beta_2 = 0$ obtained in Tarzia [21], given by

$$\operatorname{erf}(\lambda) < \frac{B a_2 c_2}{C a_1 c_1} = \frac{B}{C}\sqrt{\frac{c_2 k_2}{c_1 k_1}}. \tag{53}$$

5. Study of a particular case

We study the important particular case which has been considered in Scott [20] for sublimation–dehydration with volumetric heating since it is of interest in microwave energy. Taking into account the g's internal source functions given in [20] and definition (3) we can choose in our computation the following expressions for β_i's function:

$$\beta_1(x/2a_1\sqrt{t}) = \exp\left(-(x/2a_1\sqrt{t} + d_1)^2\right), \tag{54}$$

$$\beta_2(x/2a_2\sqrt{t}) = -\exp\left(-(x/2a_2\sqrt{t} + d_2)^2\right), \quad d_1, d_2 \in \mathbb{R}. \tag{55}$$

From (11) and (14) we can take from now on

$$\beta_1(\eta)=\exp\bigl(-(\eta+d_1)^2\bigr),\qquad \beta_2(\eta)=-\exp\bigl(-(\eta+d_2)^2\bigr),\quad d_1,d_2\in\mathbb{R}. \tag{56}$$

The functions φ_1, φ_2 and φ_3 defined by (22), (21) and (41) respectively, are given by

$$\begin{aligned}\varphi_1(\eta)={}&\frac{l\sqrt{\pi}}{c_1d_1}\exp\bigl(-d_1^2\bigr)\biggl[\exp\biggl(-2\frac{a_2}{a_1}\lambda d_1\biggr)\biggl(\operatorname{erf}\biggl(\frac{a_2}{a_1}\lambda\biggr)-\operatorname{erf}\biggl(\frac{a_2}{a_1}\eta\biggr)\biggr)\\&+\exp\bigl(d_1^2\bigr)\biggl(\operatorname{erf}\biggl(\frac{a_2}{a_1}\eta+d_1\biggr)-\operatorname{erf}\biggl(\frac{a_2}{a_1}\lambda+d_1\biggr)\biggr)\biggr],\quad \text{if } d_1\neq 0,\end{aligned} \tag{57}$$

$$\begin{aligned}\varphi_1(\eta)={}&\frac{2l\sqrt{\pi}}{c_1}\biggl[\frac{a_2}{a_1}\lambda\biggl(\operatorname{erf}\biggl(\frac{a_2}{a_1}\eta\biggr)-\operatorname{erf}\biggl(\frac{a_2}{a_1}\lambda\biggr)\biggr)\\&+\frac{1}{\sqrt{\pi}}\biggl(\exp\biggl(-\biggl(\frac{a_2}{a_1}\eta\biggr)^2\biggr)-\exp\biggl(-\biggl(\frac{a_2}{a_1}\lambda\biggr)^2\biggr)\biggr)\biggr],\quad \text{if } d_1=0,\end{aligned} \tag{58}$$

$$\varphi_2(\eta)=\frac{-l\sqrt{\pi}}{c_2d_2}\bigl[\operatorname{erf}(\eta+d_2)-\operatorname{erf}(d_2)-\operatorname{erf}(\eta)\exp\bigl(-d_2^2\bigr)\bigr],\quad \text{if } d_2\neq 0, \tag{59}$$

$$\varphi_2(\eta)=\frac{2l}{c_2}\bigl[1-\exp\bigl(-\eta^2\bigr)\bigr],\quad \text{if } d_2=0, \tag{60}$$

$$\begin{aligned}\varphi_3(\eta)={}&\frac{l\sqrt{\pi}}{c_1d_1}\exp\bigl(-d_1^2\bigr)\biggl[\exp\biggl(-2\frac{a_2}{a_1}\mu d_1\biggr)\biggl(\operatorname{erf}\biggl(\frac{a_2}{a_1}\mu\biggr)-\operatorname{erf}\biggl(\frac{a_2}{a_1}\eta\biggr)\biggr)\\&+\exp\bigl(d_1^2\bigr)\biggl(\operatorname{erf}\biggl(\frac{a_2}{a_1}\eta+d_1\biggr)-\operatorname{erf}\biggl(\frac{a_2}{a_1}\mu+d_1\biggr)\biggr)\biggr],\quad \text{if } d_1\neq 0,\end{aligned} \tag{61}$$

and

$$\begin{aligned}\varphi_3(\eta)={}&\frac{2l\sqrt{\pi}}{c_1}\biggl[\frac{a_2}{a_1}\mu\biggl(\operatorname{erf}\biggl(\frac{a_2}{a_1}\eta\biggr)-\operatorname{erf}\biggl(\frac{a_2}{a_1}\mu\biggr)\biggr)\\&+\frac{1}{\sqrt{\pi}}\biggl(\exp\biggl(-\biggl(\frac{a_2}{a_1}\eta\biggr)^2\biggr)-\exp\biggl(-\biggl(\frac{a_2}{a_1}\mu\biggr)^2\biggr)\biggr)\biggr],\quad \text{if } d_1=0.\end{aligned} \tag{62}$$

Theorem 7. *The explicit solution to the free boundary problem with sources term* (1)–(5)*,* (7)–(9) *is given by*

$$\begin{aligned}&T_1(x,t)=\frac{-(C+\varphi_1(+\infty))}{\operatorname{erf}c(\frac{a_2}{a_1}\lambda)}\biggl[\operatorname{erf}\biggl(\frac{x}{2a_1\sqrt{t}}\biggr)-\operatorname{erf}\biggl(\frac{a_2}{a_1}\lambda\biggr)\biggr]+\varphi_1\biggl(\frac{x}{2a_2\sqrt{t}}\biggr),\\&\quad \textit{for } x>s(t),\ t>0;\\&T_2(x,t)=\varphi_2\biggl(\frac{x}{2a_2\sqrt{t}}\biggr)+B-\bigl(B+\varphi_2(\lambda)\bigr)\frac{\operatorname{erf}(\frac{x}{2a_2\sqrt{t}})}{\operatorname{erf}(\lambda)},\\&\quad \textit{for } 0<x<s(t),\ t>0,\end{aligned} \tag{63}$$

where φ_1 and φ_2 are given by (57)–(60)*, and*

$$s(t)=2\lambda a_2\sqrt{t} \tag{64}$$

is the free boundary with λ the unique solution of Eq. (23)*.*

Proof. Taking into account expressions (57)–(60) we obtain the explicit expressions (63) for the temperatures T_1 and T_2. $\square$

Theorem 8.

(a) *Inequality* (45) *is equivalent to*

$$\mathrm{Ste}_1 \geqslant 2, \quad \textit{for } d_1 \geqslant 0, \qquad \mathrm{Ste}_1 \geqslant 2\sqrt{\pi}\,P(d_1), \quad \textit{for } d_1 < 0, \tag{65}$$

where

$$P(x) = \frac{\exp(-x^2) - \operatorname{erf} c(x)}{2x}. \tag{66}$$

(b) *Inequality* (46) *is equivalent to*

$$q_0 \geqslant a_1 \rho l \left[\frac{\mathrm{Ste}_1}{\sqrt{\pi}} - \frac{1}{d_1}\bigl(\exp\bigl(-d_1^2\bigr) - \operatorname{erf} c(d_1)\bigr)\right] \quad \textit{if } d_1 \neq 0, \tag{67}$$

$$q_0 \geqslant \frac{a_1 \rho l}{\sqrt{\pi}}[\mathrm{Ste}_1 - 2] \quad \textit{if } d_1 = 0. \tag{68}$$

(c) *Inequality* (52) *is equivalent to*

$$\frac{B - \frac{l\sqrt{\pi}}{c_2 d_2}(\operatorname{erf}(\lambda + d_2) - \operatorname{erf}(d_2) - \operatorname{erf}(\lambda)\exp(-d_2^2))}{\operatorname{erf}(\lambda)} \geqslant \frac{l a_1}{c_2 a_2}\left[\mathrm{Ste}_1 - \frac{\sqrt{\pi}}{d_1}\bigl(\exp\bigl(-d_1^2\bigr) - \operatorname{erf} c(d_1)\bigr)\right] \quad \textit{if } d_1 \neq 0, \tag{69}$$

and

$$\frac{B - \frac{2l}{c_2}[1 - \exp(-\lambda^2)]}{\operatorname{erf}(\lambda)} \geqslant \frac{l a_1}{c_2 a_2}[\mathrm{Ste}_1 - 2] \quad \textit{if } d_1 = 0. \tag{70}$$

(d) *The free boundary problem with sources term* (1)–(4), (6)–(9) *has an explicit solution given by*

$$T_1(x,t) = \frac{-(C + \varphi_3(+\infty))}{\operatorname{erf} c(\frac{a_2}{a_1}\mu)}\left[\operatorname{erf}\left(\frac{x}{2a_1\sqrt{t}}\right) - \operatorname{erf}\left(\frac{a_2}{a_1}\mu\right)\right] + \varphi_3\left(\frac{x}{2a_2\sqrt{t}}\right) \quad \textit{for } x > s(t),\ t > 0; \tag{71}$$

$$T_2(x,t) = \frac{q_0\sqrt{\pi}}{\rho c_2 a_2}\left[\operatorname{erf}(\mu) - \operatorname{erf}\left(\frac{x}{2a_2\sqrt{t}}\right)\right] + \varphi_2\left(\frac{x}{2a_2\sqrt{t}}\right) - \varphi_2(\mu) \quad \textit{for } 0 < x < s(t),\ t > 0, \tag{72}$$

where φ_3 and φ_2 are defined in (61)–(62) *and* (59)–(60) *respectively, the free boundary is given by*

$$s(t) = 2a_2\mu\sqrt{t}, \tag{73}$$

and μ is the unique solution of Eq. (43).

Proof. (a) We have

$$\int_0^{+\infty} \operatorname{erf} c(u)\beta_1(u)\exp\bigl(u^2\bigr)\,du = \begin{cases} P(d_1) = \frac{\exp(-d_1^2) - \operatorname{erf} c(d_1)}{2d_1}, & \text{if } d_1 \neq 0, \\ \frac{1}{\sqrt{\pi}}, & \text{if } d_1 = 0, \end{cases} \tag{74}$$

where the function $P(x)$ satisfies the following properties:

$$P(0)=\frac{1}{\sqrt{\pi}},\qquad P(+\infty)=0,\qquad P(-\infty)=0,\qquad P(x)>0\quad \forall x.$$

Then we obtain that condition (45) is equivalent to

$$2\leqslant \mathrm{Ste}_1,\quad \text{if } d_1=0 \quad \text{or}\quad 2\sqrt{\pi}P(d_1)\leqslant \mathrm{Ste}_1,\quad \text{if } d_1\neq 0.$$

(b) To obtain (67) we replace expression (74) in (46).

(c) If we replace $\varphi_2(\lambda)$ for expressions (59) or (60) in (52) we obtain (69) or (70) respectively.

(d) Taking into account expressions (59)–(62) we obtain explicit expressions (71) and (72) for the temperatures T_1 and T_2. □

Remark 5. If we take $d_1=d_2=0$ in (56) solution (63) was given by Scott [20] by taking

$$T_d(x,t)=\frac{T_s-T_v}{B}T_2(x,t)+T_v\quad \text{and}\quad T_f(x,t)=\frac{T_v-T_i}{C}T_1(x,t)+T_v$$

where T_s, T_v and T_d were defined in Scott [20].

6. Conclusions

As regards the two-phase Stefan problem with general source terms of a similarity type in both liquid and solid phases for a semi-infinite phase-change material we have arrived at the following conclusions:

(1) An explicit solution for a constant temperature condition $B>0$ at the fixed face $x=0$ for any data has been obtained.
(2) An explicit solution for an assumed heat flux of the form $-\frac{q_0}{\sqrt{t}}$ ($q_0>0$) has been obtained for data verifying restrictions (45) and (46).
(3) The equivalence of the two previous free boundary problems has also been proved and an inequality (52) for the coefficient λ which characterizes the phase change position is obtained.
(4) An explicit solution for the particular case (56) where functions β_j $(j=1,2)$ are of an exponential type which are of interest in microwave energy is obtained for any temperature boundary condition $B>0$.
(5) An explicit solution for the particular case (56) is obtained when a heat flux condition of the type (6) is imposed on $x=0$; this kind of solution there exists when the parameter q_0 satisfies the inequalities (67) and (68); this is new with respect to Scott [20].

Acknowledgments

This paper has been partially sponsored by the projects "Free Boundary Problems for the Heat-Diffusion Equation" from CONICET-UA, Rosario (Argentina), "Partial Differential Equations and Numerical Optimization with Applications" from Fundación Antorchas (Argentina), and ANPCYT PICT #03-11165 from Agencia (Argentina).

Appendix A. Mathematical properties of some useful functions

Lemma A.1.

(A) *Functions $Q(x)$, $F_0(x)$ and $F(x,\beta_2)$ satisfy the following properties*:

(i) $Q(0)=0, \quad Q(+\infty)=1, \quad Q'(x)>0,\ \forall x>0, \quad Q'(0)=\sqrt{\pi}.$

(ii) $F_0(0)=0, \quad F_0(+\infty)=+\infty, \quad F_0'(x)>0,\ \forall x>0.$

$$\text{(iii)} \quad F(0,\beta_2)=0, \quad F(+\infty,\beta_2)=+\infty, \quad \frac{\partial F}{\partial x}(x,\beta_2)>0,\ \forall x>0. \tag{A.1}$$

(B) *Functions* $h_j(x,\beta_j)$ $(j=1,2)$ *satisfy the following properties*:

(i) $h_1(0^+,\beta_1)=\mathrm{Ste}_1-2\sqrt{\pi}\int_0^{+\infty}\operatorname{erf}c(u)\beta_1(u)\exp(u^2)\,du;$

(ii) $h_1(+\infty,\beta_1)=\mathrm{Ste}_1;$

(iii) $\frac{\partial h_1}{\partial x}(x,\beta_1)=2\sqrt{\pi}\frac{a_2}{a_1}\operatorname{erf}c\left(\frac{a_2}{a_1}x\right)\exp\left(\frac{a_2}{a_1}x\right)^2\beta_1\left(\frac{a_2}{a_1}x\right)>0, \quad \forall x>0;$

(iv) *if*

$$\int_0^{+\infty}\operatorname{erf}c(u)\beta_1(u)\exp(u^2)\,du\leqslant\frac{\mathrm{Ste}_1}{2\sqrt{\pi}} \tag{A.2}$$

then $h_1(x,\beta_1)>0,\ \forall x>0;$

(v) *if*

$$\int_0^{+\infty}\operatorname{erf}c(u)\beta_1(u)\exp(u^2)\,du>\frac{\mathrm{Ste}_1}{2\sqrt{\pi}} \tag{A.3}$$

then there exists a unique $\xi_1>0$*, such that* $h_1(\xi_1,\beta_1)=0$ *and* $h_1(x,\beta_1)$ *is negative in* $(0,\xi_1)$*, is positive in* $(\xi_1,+\infty)$*;*

(vi) $h_2(0^+,\beta_2)=\frac{\mathrm{Ste}_2}{\sqrt{\pi}};$

(vii) $h_2(+\infty,\beta_2)=-\infty;$

(viii) $\frac{\partial h_2}{\partial x}(x,\beta_2)=-\left\{\frac{2x}{\sqrt{\pi}}+\exp(x^2)\operatorname{erf}(x)\left[1+2x^2-2\beta_2(x)\right]\right\}<0;$

(ix) *there exist a unique* $\xi_2>0$ *such that* $h_2(\xi_2,\beta_2)=0$.

(C) (a) *Function* $f_1(x,\beta_1)$*, satisfies the following properties*:

(i) $f_1(0^+,\beta_1)=0;$

(ii) $f_1(+\infty,\beta_1)=+\infty;$

(iii) *if condition* (A.2) *is verified then* $f_1(x,\beta_1)>0\ \forall x>0$*,*

$$\frac{\partial f_1}{\partial x}(x,\beta_1)>0 \quad \textit{and} \quad \frac{\partial f_1}{\partial x}(0^+,\beta_1)=0^+;$$

(iv) *if condition* (A.3) *is verified then* $f_1(\xi_1,\beta_1)=0$ *and* $f_1(x,\beta_1)$ *is negative in* $(0,\xi_1)$*, and is positive in* $(\xi_1,+\infty)$*; then there exists* $x_1\in(0,\xi_1)$ *such that* $\frac{\partial f_1}{\partial x}(x_1,\beta_1)=0$. *Moreover we have* $\frac{\partial f_1}{\partial x}(x,\beta_1)>0\ \forall x>\xi_1$.

(b) *Function* $f_2(x,\beta_2)$ *satisfies the following properties*:

(i) $f_2(0^+,\beta_2)=0;$

(ii) $f_2(+\infty,\beta_2)=-\infty;$

(iii) $f_2(\xi_2, \beta_2) = 0$;

(iv) $\dfrac{\partial f_2}{\partial x}(x, \beta_2) = \dfrac{a_2}{a_1} Q'\left(\dfrac{a_2}{a_1}x\right) h_2(x, \beta_2) + Q\left(\dfrac{a_2}{a_1}x\right)\dfrac{\partial h_2}{\partial x}(x, \beta_2)$;

(v) $\dfrac{\partial f_2}{\partial x}(0^+, \beta_2) = \dfrac{a_2}{a_1}\mathrm{Ste}_2 > 0$;

(vi) *there exists* $x_2 \in (0, \xi_2)$ *such that* $\frac{\partial f_2}{\partial x}(x_2, \beta_2) = 0$;

(vii) $\frac{\partial f_2}{\partial x}(x, \beta_2) < 0, \ \forall x > \xi_2$.

Proof. (A) The properties for F_0 and Q are easy to check and the function F appears for the one-phase case which was considered in Menaldi, Tarzia [14].

(B) It easily follows from (A) and definitions (28)–(29).

(C) We use the definitions of the corresponding real functions and (A) and (B). We remark that in (a)(iv) we have $f_1(x, \beta_1) < 0 \ \forall x \in (0, \xi_1)$ and in (b)(vi) we have $f_2(x, \beta_2) > 0$ in $(0, \xi_2)$. □

Lemma A.2. *Function G_1 has the following properties*:

(i) $G_1(0, \beta_1) = 0$,
(ii) $G_1(+\infty, \beta_1) = +\infty$,
(iii) *if condition* (A.2) *is verified then* $G_1(x, \beta_1) > 0, \ \forall x > 0$,
(iv) *if condition* (A.3) *is verified then there exists a unique* $\xi > 0$ *such that* $G_1(\xi, \beta_1) = 0$ *and* $G_1(x, \beta_1)$ *is* negative *in* $(0, \xi)$, G_1 *is* positive *in* $(\xi, +\infty)$,
(v) $G_1(0, 0) = 0$,
(vi) $G_1(+\infty, 0) = +\infty$,
(vii) $\dfrac{\partial G_1}{\partial x}(x, 0) > 0, \quad \forall x > 0, \quad$ *and* $\quad \dfrac{\partial G_1}{\partial x}(0, 0) = 0.$

Function G_2 has the following properties:

(i) $G_2(0, \beta_2) = 0$,
(ii) $G_2(0, 0) = 0$,
(iii) $G_2(+\infty, 0) = \frac{\mathrm{Ste}_2}{\sqrt{\pi}}$,
(iv) $G_2(+\infty, \beta_2) = \dfrac{\mathrm{Ste}_2}{\sqrt{\pi}} + 2\displaystyle\int_0^{+\infty} \mathrm{erf}(u)\beta_2(u)\exp\bigl(u^2\bigr)\,du$,
(v) $\frac{\partial G_2}{\partial x}(x, 0) > 0 \ \forall x > 0$,
(vi) $G_2(x, \beta_2) \leqslant G_2(x, 0) \ \forall x \geqslant 0$.

Lemma A.3.

(a) *Function $W(x, \beta_1)$ satisfies the following properties*:

(i) $W(0, \beta_1) = \dfrac{a_1}{a_2\sqrt{\pi}}\left[\mathrm{Ste}_1 - 2\sqrt{\pi}\displaystyle\int_0^{+\infty} \mathrm{erf}\,c(u)\beta_1(u)\exp\bigl(u^2\bigr)\,du\right]$,

(ii) $W(+\infty, \beta_1) = +\infty$,
(iii) $W(x, \beta_1) \leqslant W(x, 0)$, $\forall x > 0$, $\beta_1 > 0$,
(iv) *if condition* (A.2) *is verified then* $W(0, \beta_1) \geqslant 0$ *and*

$$\frac{\partial W}{\partial x}(x, \beta_1) > 0, \quad \forall x > 0,$$

(v) *if condition* (A.3) *is verified then* $W(0, \beta_1) < 0$.

(b) *Function* $V(x, \beta_2)$ *satisfies the following properties*:
(i) $V(0, \beta_2) = \frac{q_0}{\rho l a_2}$,
(ii) $V(+\infty, \beta_2) = -\infty$,
(iii) $\frac{\partial V}{\partial x}(x, \beta_2) < 0$, $\forall x > 0$,
(iv) $V(x, \beta_2) \leqslant V(x, 0)$, $\forall x > 0$, $\beta_2 < 0$.

Proof. In order to prove (a)(iii) we use that $Q'(x)$ is given by $Q'(x) = \frac{Q(x)(1+2x^2)-2x^2}{x}$.
We demonstrate the other properties by elementary computations. $\square$

References

[1] T.K. Ang, J.D. Ford, D.C.T. Pei, Microwave freeze–drying of food: Theoretical investigation, Int. J. Heat Mass Transfer 20 (1977) 517–526.
[2] J.R. Barber, An asymptotic solution for short-time transient heat conduction between two similar contacting bodies, Int. J. Heat Mass Transfer 32 (5) (1989) 943–949.
[3] S. Bhattacharya, S. Nandi, S. DasGupta, S. De, Analytical solution of transient heat transfer with variable source for applications in nuclear reactors, Int. Comm. Heat Mass Transfer 28 (7) (2001) 1005–1013.
[4] J.E. Bouillet, Self-similar solutions, having jumps and intervals of constancy, of a diffusion-heat conduction equation, IMA Preprints #230, Univ. Minnesota, 1986.
[5] J.E. Bouillet, D.A. Tarzia, An integral equation for a Stefan problem with many phases and a singular source, Rev. Un. Mat. Argentina 41 (4) (2000) 1–8.
[6] H.S. Carslaw, J.C. Jaeger, Conduction of Heat in Solids, Oxford Univ. Press, London, 1959.
[7] M.N. Coelho Pinheiro, Liquid phase mass transfer coefficients for bubbles growing in a pressure field: A simplified analysis, Int. Comm. Heat Mass Transfer 27 (1) (2000) 99–108.
[8] J. Crank, Free and Moving Boundary Problems, Clarendon Press, Oxford, 1984.
[9] H. Feng, Analysis of microwave assisted fluidized-bed drying of particulate product with a simplified heat and mass transfer model, Int. Comm. Heat Mass Transfer 29 (8) (2002) 1021–1028.
[10] Y.C. Fey, M.A. Boles, An analytical study of the effect of convection heat transfer on the sublimation of a frozen semi-infinite porous medium, Int. J. Heat Mass Transfer 30 (1987) 771–779.
[11] A.I. Grigor'ev, V.V. Morozov, S.O. Shiryaeva, Formation and dispersion of an electrolyte film on an ice electrode melting as a result of joule heat evolution, Technical Physics 47 (10) (2002) 1237–1245.
[12] G. Lamé, B.P. Clapeyron, Memoire sur la solidification par refroidissement d'un globe liquide, Annales Chimie Physique 47 (1831) 250–256.
[13] S. Lin, An exact solution of the sublimation problem in a porous medium, ASME J. Heat Transfer 103 (1981) 165–168.
[14] J.L. Menaldi, D.A. Tarzia, Generalized Lamé–Clapeyron solution for a one-phase source Stefan problem, Comput. Appl. Math. 12 (2) (1993) 123–142.
[15] G.A. Mercado, B.P. Luce, J. Xin, Modelling thermal front dynamics in microwave heating, IMA J. Appl. Math. 67 (2002) 419–439.
[16] A.D. Polyanin, V.V. Dil'man, The method of the 'carry over' of integral transforms in non-linear mass and heat transfer problems, Int. J. Heat Mass Transfer 33 (1) (1990) 175–181.
[17] P. Ratanadecho, K. Aoki, M. Akahori, A numerical and experimental investigation of the modeling of microwave melting of frozen packed beds using a rectangular wave guide, Int. Comm. Heat Mass Transfer 28 (2001) 751–762.
[18] C. Rogers, Application of a reciprocal transformation to a two-phase Stefan problem, J. Phys. A 18 (1985) 105–109.
[19] U. Rosenberg, W. Bögl, Microwave thawing, drying, and baking in the food industry, Food Technology 41 (6) (1987) 834–838.

[20] E.P. Scott, An analytical solution and sensitivity study of sublimation–dehydration within a porous medium with volumetric heating, J. Heat Transfer 116 (1994) 686–693.
[21] D.A. Tarzia, An inequality for the coefficient σ of the free boundary $s(t) = 2\sigma\sqrt{t}$ of the Neumann solution for the two-phase Stefan problem, Quart. Appl. Math. 39 (1981–1982) 491–497.
[22] D.A. Tarzia, A bibliography on moving – free boundary problems for the heat-diffusion equation. The Stefan and related problems, MAT-Serie A, #2 (2000) (with 5869 titles on the subject, 300 pages). See www.austral.edu.ar/MAT-SerieA/2(2000)/.
[23] M. Ward, Thermal runaway and microwave heating in thin cylindrical domains, IMA J. Appl. Math. 67 (2002) 177–200.

DRYING TECHNOLOGY
Vol. 22, No. 5, pp. 1173–1189, 2004

Qualitative Aspects of Convective and Microwave Drying of Saturated Porous Materials

S. J. Kowalski* and A. Rybicki

Institute of Technology and Chemical Engineering,
Poznan University of Technology, Poland

ABSTRACT

The differences in distribution and temporal evolution of temperature, moisture content, and drying stresses in saturated capillary-porous materials by convective and microwave drying are analyzed. The analysis is based on the mechanistic model of drying taking into account the coupling effects in the heat and mass transfer. The results of numerical simulation allow better understanding of the difference in thermal and mechanical behavior of dried materials to which the energy necessary for drying is supplied volumetrically (microwave drying) or through the material surface (convective drying). The study is carried out on an isotropic cylinder as a model material.

*Correspondence: Professor S. J. Kowalski, Institute of Technology and Chemical Engineering, Poznan University of Technology, pl. Marii Skłodowskiej-Curie 2, 60-965 Poznan, Poland; Fax: (+61) 665 3649; E-mail: Stefan.J.Kowalski@put.poznan.pl.

DOI: 10.1081/DRT-120038586 0737-3937 (Print); 1532-2300 (Online)

Key Words: Thermomechanical model; Microwave drying; Convective drying; Distributions of temperature, moisture content and stresses; Kaolin; Cylindrical sample.

INTRODUCTION

The convective method of drying is used most commonly in industrial technology of drying. In this method, the heat necessary for moisture evaporation is supplied convectively by hot air or superheated steam through the material surface. In such a case, the gradient of temperature is pointed outwards and the heat flux is pointed into the material. So, the thermodiffusional mass flow is in the opposite direction to the diffusional flux of moisture. As a result, the distribution of moisture can achieve a strongly nonlinear mapping, and this may be a reason for the generation of strong shrinkage stresses. Therefore, one should look for another means of heat supply, namely, such a means by which the diffusional and thermodiffusional fluxes of moisture are pointed in the same direction. One of several possible ways is to apply the microwave generation of heat inside the material.

The main aim of this article is to show that heat supplied volumetrically to the dried material causes the diffusional and thermodiffusional flow of moisture in the same direction, and thus, more uniform distribution of the moisture content in the material and smaller values of the shrinkage stresses. Our attention is concentrated on the microwave drying, by which the heat is generated volumetrically inside the dried material.

Microwave drying has been studied recently by several authors: Chen et al.,[1] Constant et al.,[2] Feng et al.,[3] Perre and Turner,[7] Ratanadecho et al.,[8–10] Sanga et al.,[12] Turner and Illic,[13] Zhang and Mujumdar,[16] Zielonka et al.,[17] among others. However, little attention has been devoted to the analysis of mechanical effects arising in materials under this kind of drying, and in particular to the drying induced stresses. Generally, one can state that the volumetrically generated heat in dried materials, as it takes place in microwave drying, gives better mechanical quality products than by convective heat supply through the boundary surface, mainly due to substantial reduction of drying induced stresses.

The mechanistic drying theory presented in Kowalski[5] forms the basis for the present analysis. The governing equations for heat and mass transfer, adapted to a cylindrically shaped sample, are solved numerically with the finite element method (Rybicki[11] and Wait and Mitchell[14]).

The temperature, moisture, and stress distributions at different instances for both microwave and convective drying are presented.

GOVERNING EQUATIONS FOR HEAT AND MASS TRANSFER

The general mechanistic drying theory used here for analysis of the mechanical effects in dried materials was developed systematically on the basis of balance equations for mass, momentum, energy, and entropy, as well as on the statements of the conservation laws and the principles of irreversible thermodynamics (Kowalski[5]). Adopting this theory to the present considerations, we made the following assumptions:

– The dried body is assumed to be an isotropic capillary-porous solid of density ρ^s.
– The pores in the body are filled with liquid (l)–vapor (v) mixture of partial mass density $\rho^m = \rho^l + \rho^v \approx \rho^l$, i.e., saturated body.
– The moisture flux inside the material is proportional to the gradient of moisture potential, and that on the boundary surface is proportional to the difference of chemical potentials of vapor at the boundary and far from the boundary. Diffusivity is assumed constant.
– The heat flux includes both conduction and transport of heat by moisture flux.
– The heat and mass transfer includes coupling effects; however, the influence of body volume deformation on heat and mass transfer is neglected.
– The dried material is elastic.
– Gravity forces are neglected.
– The microwave energy absorption term is constructed as the local microwave power multiplied by the water content and an exponentially formulated attenuation term dependent on the distance in microwave propagation and the attenuation factor.
– The boundary value problem is two-dimensional; the analyzed functions depend on coordinates r, z (radius and height of the cylinder), and time t.

The governing equations reduced to solve the axial-symmetry boundary value problem include: the system of equations describing heat and mass transfer, the equations of equilibrium of internal force, and the physical relations.

Let $X = \rho^m/\rho^s$ denotes the ratio of moisture content referred to the mass of a dry body, and $\boldsymbol{W}$ is the mass flux of the moisture. The mass balance for the moisture reads (Kowalski[5])

$$\rho^s \dot{X} = -\mathrm{div}\boldsymbol{W} \tag{1}$$

Based on the above-mentioned reference, we write the following (reduced) form of energy balance

$$\rho^s T\dot{S} = -\mathrm{div}(\boldsymbol{q} \pm s^m T\, \boldsymbol{W}) + \Re \tag{2}$$

where S denotes total entropy referred to the mass of a dry body, $\boldsymbol{q}$ is the heat flux, s^m is the entropy of moisture, T is the temperature of the body, and $\Re$ is the internal source of heat (radiation). This equation points out that the entropy alteration is due to heat flux conducted and heat transported by the mass flux, as well as by the internal heat generation (radiation).

The following mass and heat fluxes resulted from the thermodynamic inequality (see Ref.[5])

$$\boldsymbol{W} = -\Lambda_m \mathrm{grad}\mu, \qquad \Lambda_m \geq 0 \tag{3}$$

$$\boldsymbol{q} = -\Lambda_T \mathrm{grad}T \mp s^m T\, \boldsymbol{W}, \qquad \Lambda_T \geq 0 \tag{4}$$

In these relationships μ is the generalized chemical potential of the moisture, Λ_m is termed the mobility coefficient dependent on the surface tension and viscosity of the moisture, as well as on the permeability and porosity of the dried body, while Λ_T is the effective thermal conductivity, being volume averaged from conductivity coefficients of solid, liquid, and vapor phases. In Eq. (4), the sign "minus" between the conducted and convected heat flux holds when the moisture flux $\boldsymbol{W}$ flows outwards the body.

The generalized chemical potential μ and the entropy S are functions of the body thermodynamic state, defined by the temperature T, volumetric strain ε, and moisture content X. In further considerations, we neglect the influence of the volumetric strain gradient on moisture transport, and the volumetric strain rate on the temperature alteration. So, after substituting mass and heat fluxes of Eqs. (3) and (4) into the balances of mass and energy of Eqs. (1) and (2), we obtain the following system of differential equations describing the heat and mass transfer

$$\rho^s \dot{X} = \Lambda_m (c_T \nabla^2 T + c_X \nabla^2 X) \tag{5}$$

$$\rho^s (c_v \dot{T} + l\dot{X}) = \Lambda_T \nabla^2 T + \Re \quad \text{with} \quad \nabla^2 = \frac{\partial^2}{\partial r^2} + \frac{1}{r}\frac{\partial}{\partial r} + \frac{\partial^2}{\partial z^2} \tag{6}$$

Marcel Dekker, Inc.
270 Madison Avenue, New York, New York 10016

where ∇^2 is the Laplace operator in cylindrical coordinates with axial symmetry, c_T and c_X are the thermodifusional and diffusional coefficients of moisture transport, c_v is the total volume averaged specific heat referred to unit mass of a dry body, and $l = (s^v - s^l)T$ is the latent heat of evaporation, being the difference of vapor and liquid entropy multiplied by temperature.

The internal source of heat $\Re$ is zero for the convective drying. In the case of microwave drying, it expresses the rate of microwave energy absorbed per unit volume, and is constructed as follows

$$\Re = \Re_0 \frac{X}{X_0} \exp[-\alpha(R - r)] \tag{7}$$

where X is the moisture content at time t and radius r, X_0 is the moisture content at time $t = 0$ and radius r, α is the attenuation factor in the direction of microwave propagation distance $(R - r)$, R is the cylinder radius, and $\Re_0$ is the experimentally estimated average microwave power.

Using our 8-modal microwave chamber dryer type WS110 firm PLAZMATRONIKA of maximum microwave power 600 W, we have estimated the average microwave power on the cylindrical kaolin sample using the formula

$$\Re_0 = \frac{2}{R}\left[\alpha_T(T_n - T_a) + l\frac{\Delta m}{A\Delta t}\right] \tag{8}$$

In this formula: α_T denotes the coefficient of convective heat exchange, T_n is the sample surface temperature (adjusted automatically by the microwave dryer), T_a is the temperature of the ambient medium, l is the latent heat of water evaporation, Δm is the loss of a sample weight per time increment Δt, and A is the area of evaporation.

Figure 1 presents the geometry of the sample under consideration. The undersurface of the cylindrically shaped sample is placed on the impermeable plate, whereas the other surfaces are open for moisture release. The sample is assumed to be enough long so that the supply of microwave power takes place mainly through the lateral surface of the cylinder (see Eq. (7)).

The following boundary conditions for mass and heat transfer hold for both convective and microwave drying. These for mass transfer, expressed with the help of moisture potential, are as follows:

$$\frac{\partial\mu}{\partial z}|_{z=0} = 0, \qquad -\Lambda_m \frac{\partial\mu}{\partial z}|_{z=H} = \alpha_m(\mu|_{z=H} - \mu_a) \tag{9a}$$

$$\frac{\partial\mu}{\partial r}|_{r=0} = 0, \qquad -\Lambda_m \frac{\partial\mu}{\partial z}|_{z=R} = \alpha_m(\mu|_{z=R} - \mu_a) \tag{9b}$$

Marcel Dekker, Inc.
270 Madison Avenue, New York, New York 10016

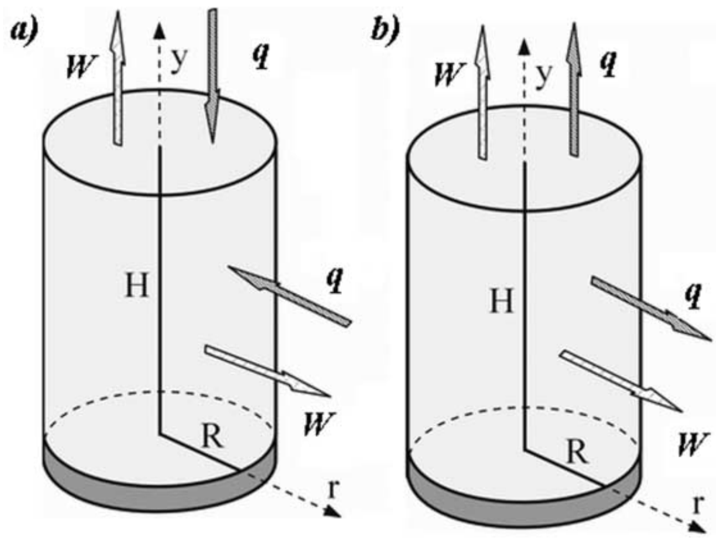

Figure 1. Geometry of the dried sample: (a) convective drying, (b) microwave drying.

where α_m denotes the coefficient of convective mass transfer, and μ_a is the chemical potential of vapor in the ambient medium. The conditions on the left express impermeability (the upper) and symmetry (the lower one), while these on the right, represent the convective exchange of mass.

The boundary conditions for heat transfer are similar in form to these for mass transfer, namely

$$
\begin{aligned}
&-\Lambda_T \frac{\partial T}{\partial z}|_{z=0} = \alpha_T\,(T|_{z=0} - T_a),\\
&\quad -\Lambda_T \frac{\partial T}{\partial z}|_{z=H} = \alpha_T\,(T|_{z=H} - T_a) - l\alpha_m(\mu|_{z=H} - \mu_a)
\end{aligned}
\tag{10a}
$$

$$
\begin{aligned}
&\frac{\partial T}{\partial r}|_{r=0} = 0, -\Lambda_T \frac{\partial T}{\partial z}|_{z=R}\\
&\qquad = \alpha_T(T|_{z=R} - T_a) - l\alpha_m(\mu|_{z=R} - \mu_a)
\end{aligned}
\tag{10b}
$$

where constant value of the coefficient of convective heat exchange α_T is assumed.

The upper condition on the left expresses the convective exchange of heat on the lower moisture-impermeable plate, the lower on the left is the symmetry condition. The conditions on the right describe the convective heat exchange with taking into account the heat escaping with the vapor.

The initial conditions express the values of moisture content and temperature at the beginning of drying, that is

$$X(r,z,t)|_{t=0} = X_0 = \text{const} \quad \text{and} \quad T(r,z,t)|_{t=0} = T_0 = \text{const} \tag{11}$$

The numerical method used for solution of this initial-boundary value problem was the Galerkin discretization method (finite element method) for spatial derivatives, and the finite difference method for time derivatives (see Kowalski and Rybicki,[6] Rybicki,[11] Wait and Mitchell[14]).

NUMERICAL PREDCTION OF TEMPERATURE AND MOISTURE CONTENT

In numerical calculations the gradient of moisture potential inside the material was replaced by the gradients of temperature and moisture content, that is

$$\text{grad}\mu = c_T \text{grad} T + c_X \text{grad} X \tag{12}$$

The moisture potential on the external boundary surface was assumed to be equal to the vapor moisture potential at the boundary, i.e.,

$$\mu|_{r=R} = \mu(p^v|_{r=R}, T|_{r=R}) = \mu(p, x|_{r=R}, T|_{r=R}) \tag{13}$$

where $p^v|_{r=R} = px|_{r=R}$ denotes the vapor partial pressure and $x|_{r=R}$ is the molar vapor content in air at the boundary, and p is the total pressure of air.

Developing the moisture (vapor) potentials in air in Taylor's series one can replace the difference in moisture potentials on the right hand side of boundary conditions (9a) and (9b) by the following expression

$$\alpha_m(\mu|_B - \mu_a) \cong \beta_x(x|_B - x_a) + \beta_T(T|_B - T_a) \tag{14}$$

where β_x and β_T can be termed as the diffusion and thermodiffusion coefficients of vapor in the surrounding air, and $|_B$ means the boundary surface.

All numerical calculations, for both convective and microwave drying, refer to the kaolin cylinder of radius $R = 0.025$ m and height $H = 0.1$ m. The initial moisture content of the cylinder was assumed to be $X_0 = 28\%$ (dry basis state), and the initial temperature $T_0 = 15°C$. The following data of material coefficients suitable for kaolin material were taken for numerical calculus

$$
\begin{aligned}
\Lambda_m &= 6.04 \times 10^{-8} (\mathrm{kg\,s\,m^{-3}}) & \Lambda_T &= 1.7 \times 10^{-3} (\mathrm{W\,m^{-1}\,K^{-1}}) \\
c_X &= 3.06\,(\mathrm{J\,kg^{-1}}) & c_T &= 0.52\,(\mathrm{J\,kg^{-1}\,K^{-1}}) \\
\beta_x &= 9.64 \times 10^{-6} (\mathrm{kg\,m^{-2}\,s}) & \beta_T &= 40\,(\mathrm{kg\,m^2\,s^{-1}\,K^{-1}}) \\
c_v &= 23.3 \times 10^5\,(\mathrm{J\,kg^{-1} K^{-1}}) & l &= 2000\,(\mathrm{kJ\,kg^{-1}}) \\
\rho^s &= 2600\,(\mathrm{kg\,m^{-3}}) & a &= 150\,(\mathrm{m^{-1}}) \\
\alpha_m &= 8.64 \times 10^{-5} (\mathrm{kg\,s\,m^{-4}}) & \Re_0 &= 180\,(\mathrm{W\,m^{-3}})
\end{aligned}
$$

Temperature T_a of air in the drying chamber (convective drying) was fixed at 50°C, and the relative humidity was $\varphi = 10\%$. Under these conditions the wet bulb temperature reached about 35°C. In our microwave chamber dryer, on the other hand, it is possible to fix automatically the temperature of the upper cylinder surface, so it was fixed to be 35°C. The temperature of air in this chamber was c.a. 20°C, and the relative humidity $\varphi = 40\%$.

Figure 2 illustrates the temperature distribution in the cylindrical samples by convective drying and by microwave drying.

The plots present the isolines of constant temperatures of given values. Note that the bottom base of the cylinder is placed on a plate impermeable to moisture flow but conductive for heat. The upper base and the lateral surfaces of the cylinder are open, so the heat and mass exchange with the ambient air is possible through these surfaces.

In the case of convective drying, the cylinder is assumed to be continuously heated from the hot ambient air, however, due to evaporation of moisture and escaping of vapor from the upper and lateral surfaces, the greatest temperature occurs in the middle of the cylinder, particularly at its bottom base (Fig. 2a). The calculations refer to the stable drying conditions, so that the distribution of temperature is also stable, although nonuniformly distributed through the cylinder, due to heating from below through the impermeable for moisture plate.

A quite different distribution of temperature was obtained for microwave drying of the cylinder. In this case the heat was generated inside the material, proportionally to the local amount of moisture. The propagation of microwaves was assumed to proceed in radial direction only and with exponential attenuation term increasing with a distance. It is obvious that the temperature of the ambient air in microwave drying is lower than the temperature of the drying object.

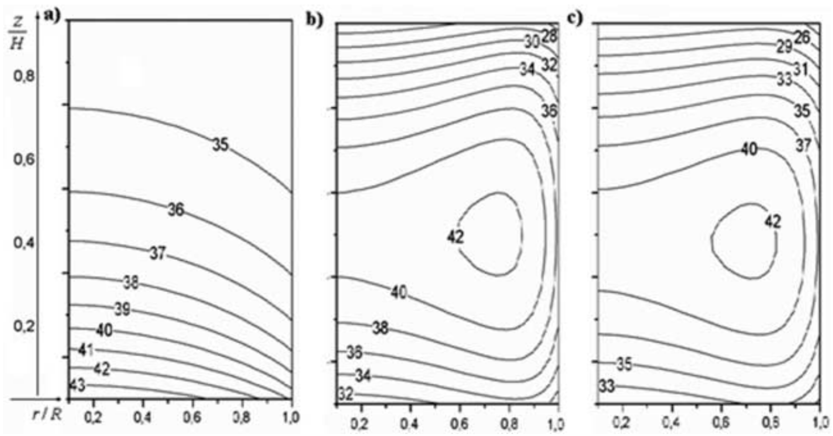

Figure 2. Distribution of temperature in the cylindrical samples: (a) 60-min convective drying, (b) 60-min microwave drying, (c) 180-min microwave drying.

Note that the escape of heat through the upper and the lateral surfaces of the cylinder during microwave drying is doubled, namely, due to convection and due to transport with vapor. Because there is no vapor escape through the bottom base of the cylinder, the temperature at this base is greater than at the upper one. Due to attenuation of microwaves with distance and proportionality of the heat generation to the magnitude of local moisture content, the highest temperature appears not in the center of the cylinder $r = 0$, but is in some other cross-section $0 < r < R$. Similarly, because of asymmetry of cylinder cooling on its upper and bottom surfaces, the highest temperature is not in the middle of the cylinder height $z = H/2$, but in some other plane $0 < z < H/2$.

Figure 3 presents the moisture content distribution in the cylinder during convective drying after 60, 120, and 180 min of a drying time.

This figure illustrates clearly how the dry zone moves towards the interior of the cylinder in the course of drying. The driest area is located at the upper corner of the cylinder, and the least dry area somewhere in the middle of the cylinder. The upper surface is open for the moisture exchange, similar as the lateral one. On the other hand, the bottom surface is closed to moisture transfer, but it is warmer than the other surfaces (see Fig. 2a). Therefore, the removal of moisture in lateral direction is greater than in other places, and the moisture content at this surface is a bit lower than in a slightly higher cross-section of the cylinder (see Fig. 3c).

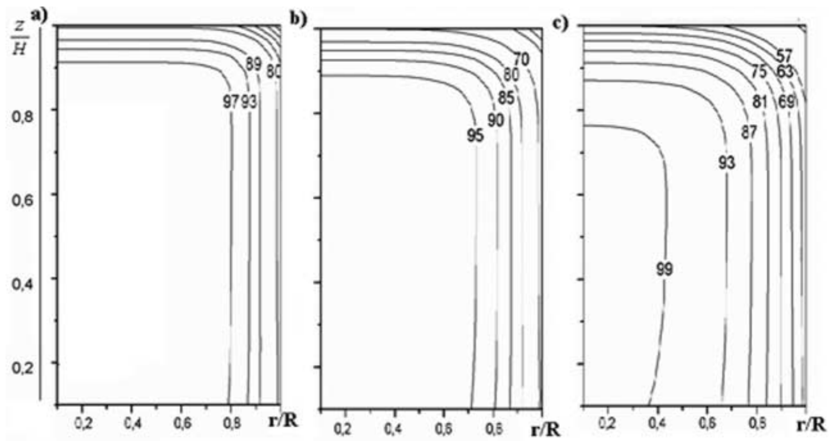

Figure 3. Distribution of moisture content (in % of initial moisture) in the cylindrical sample by convective drying: (a) 60 min, (b) 120 min, (c) 180 min.

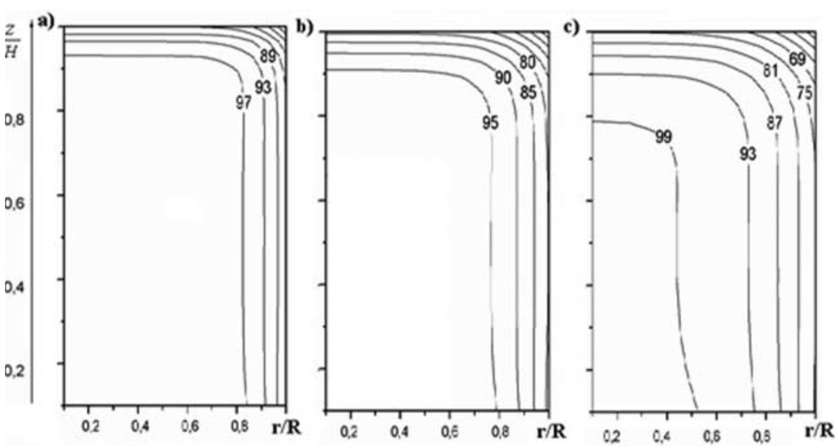

Figure 4. Distribution of moisture content (in % of initial moisture) in the cylindrical sample by microwave drying: (a) 60 min, (b) 120 min, (c) 180 min.

Figure 4 presents the distribution of moisture content distribution in the cylinder by microwave drying after 60, 120, and 180 min of a drying time.

The distribution of moisture in this kind of drying is quite similar to that by convective drying, however, is more uniform. This is evidenced by the fact that the isolines are less dense than in convective drying. Another difference is visible at the bottom of the cylinder. In this place the moisture removal is the slowest by microwave drying. This was not the case of convective drying. Besides, the drying rate is greater in microwave than in convective drying.

DRYING INDUCED STRESSES

Having determined the distributions of temperature and moisture content, one can calculate the distribution of stresses. The stresses have to satisfy the equilibrium equations, which in the axial symmetry take the form

$$\frac{\partial \sigma_{rr}}{\partial r} + \frac{\partial \sigma_{rz}}{\partial z} + \frac{\sigma_{rr} - \sigma_{\varphi\varphi}}{r} = 0 \tag{15a}$$

$$\frac{\partial \sigma_{rz}}{\partial r} + \frac{\sigma_{rz}}{r} + \frac{\partial \sigma_{zz}}{\partial z} = 0 \tag{15b}$$

The stresses are related to the strains as follows:

$$\sigma_{rr} = 2M\varepsilon_{rr} + A\varepsilon - 3K\varepsilon^{(TX)} \tag{16a}$$

$$\sigma_{\varphi\varphi} = 2M\varepsilon_{\varphi\varphi} + A\varepsilon - 3K\varepsilon^{(TX)} \tag{16b}$$

$$\sigma_{zz} = 2M\varepsilon_{zz} + A\varepsilon - 3K\varepsilon^{(TX)} \tag{16c}$$

$$\sigma_{zr} = 2M\varepsilon_{zr} \tag{16d}$$

where M and A are the coefficients equivalent to Lame constants in the theory of elasticity, $3K = 2M + 3A$, and

$$\varepsilon^{(TX)} = \kappa^{(T)}(T - T_0) + \kappa^{(X)}(X - X_0) \tag{17}$$

denotes the thermal-moist strain, with $\kappa^{(T)}$ and $\kappa^{(X)}$ being the coefficients of thermal and moist expansion (or shrinkage).

The geometrical relations for axial symmetry are:

$$\varepsilon_{rr} = \frac{\partial u_r}{\partial r}, \quad \varepsilon_{\varphi\varphi} = \frac{u_r}{r}, \quad \varepsilon_{zz} = \frac{\partial u_z}{\partial z}, \quad \varepsilon_{rz} = \frac{1}{2}\left(\frac{\partial u_r}{\partial z} + \frac{\partial u_z}{\partial r}\right) \tag{18}$$

with

$$\varepsilon = \varepsilon_{rr} + \varepsilon_{\varphi\varphi} + \varepsilon_{zz} = \frac{1}{r}\frac{\partial}{\partial r}(r u_r) + \frac{\partial u_z}{\partial z} = 0 \tag{19}$$

Marcel Dekker, Inc.
270 Madison Avenue, New York, New York 10016

being the volumetric strain, and u_r, u_z denote the displacements in radial and axial directions, respectively.

Substituting the physical relations from Eq. (16a) to Eq. (16b) into the equations of force equilibrium (15a) and (15b), we obtain the system of two coupled equations for determination of displacements u_r and u_z

$$M\nabla^2 u_r + \frac{\partial}{\partial r}\left[(M+A)\varepsilon - 3K\varepsilon^{(TX)}\right] = M\frac{u_r}{r^2} \tag{20a}$$

$$M\nabla^2 u_z + \frac{\partial}{\partial z}\left[(M+A)\varepsilon - 3K\varepsilon^{(TX)}\right] = 0 \tag{20b}$$

where ∇^2 denotes the Laplace operator in cylindrical coordinates (see Eq. (6)).

In order to solve this system of equations explicitly, the following boundary conditions are assumed:

- Zero-valued stresses at the free surfaces of the cylinder, that is

$$\sigma_{rr}|_{r=R} = 0, \qquad \sigma_{zz}|_{z=H} = 0 \tag{21a}$$

- Zero-valued displacements at the bottom and in the center of the cylinder, that is

$$u_r|_{r=0} = 0, \qquad u_z|_{z=0} = 0 \tag{21b}$$

The stresses arise when the temperature and/or moisture content are distributed nonuniformly. We have assumed uniform distribution of temperature and moisture content at the beginning of a drying process, and this means the stress-free initial state of the cylinder.

The finite element procedure of Galerkin type was applied to numerical calculus of displacements, strains, and stresses. In our considerations we are interested mostly in comparison of stresses generated by convective and microwave drying. This issue will be illustrated on the circumferential stresses $\sigma_{\varphi\varphi}$.

Figure 5 visualizes the stress distribution in the longitudinal plane (r, z) of the cylinder. The lines perform the circumferential stresses of the same value (stress-isolines).

It is seen from this figure that stresses are tensional at the surfaces where the removal of moisture takes place and the shrinkage of dried material occurs. As the cylinder as a whole has to be in equilibrium, the tensional stresses have to be balanced by the compressive stresses in the core of the cylinder. The neutral (zero-valued) line separates the areas of

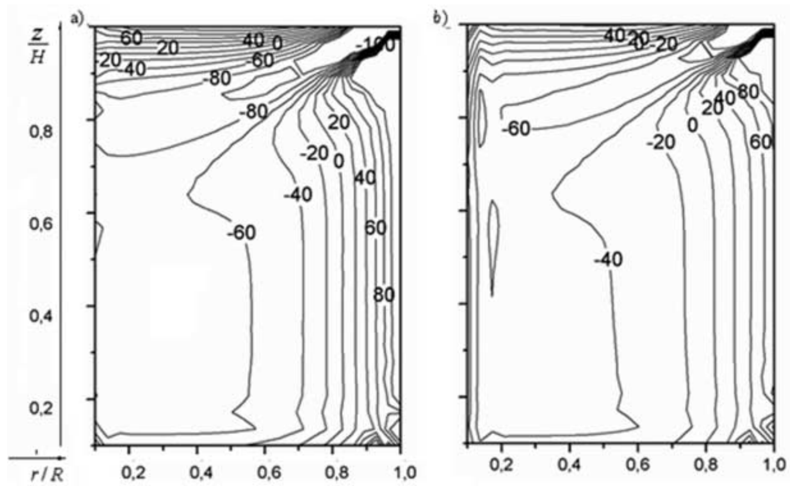

Figure 5. Isolines of circumferential stresses in the longitudinal section of the cylinder sample at 120 min drying time: (a) convective drying, (b) microwave drying.

tensional and compressive stresses. The most complicated and of greatest values state of stress appears in the upper corner of the cylinder. The material placed in this corner is tensed simultaneously in r (radial) and z (longitudinal) directions. It is obvious that a destruction of the material will proceed in this place first.

Mapping of the stress distribution is quite similar in the cylinders dried convectively and by microwaves. However, microwave drying generates weaker stresses. This is clearly visible in Fig. 6, where distribution of stresses along the cylinder radius in the middle height of the cylinder ($z = H/2$) at 120 min drying time is presented.

The fact that microwave drying generates smaller value stresses is even more visible in Fig. 7, where the evolution of circumferential stresses in time at the cylinder surface ($r = R$) and in its center ($r = 0$) for $z = H/2$ is presented.

The weaker stresses in microwave drying follow mainly from more uniform distribution of the moisture content (see Figs. 3 and 4). Now, we can conclude that the volumetrically supplied heat in microwave drying causes the diffusional and thermodiffusional fluxes of moisture to flow in the same direction, and this results in more uniform distribution of moisture content and smaller value stresses. This is not the case of

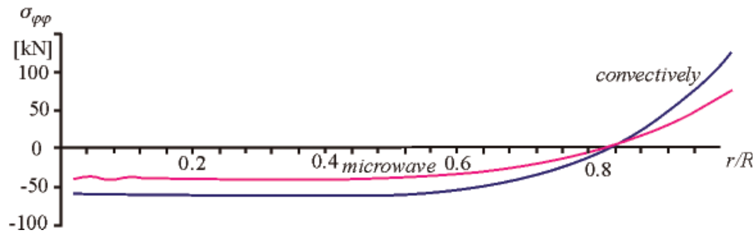

Figure 6. Distribution of circumferential stresses along cylinder radius for $z = H/2$ at 120 min drying time. *(View this art in color at www.dekker.com.)*

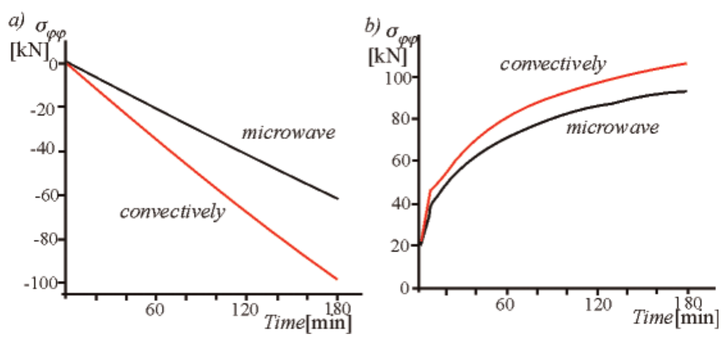

Figure 7. Evolution of circumferential stresses in time for $z = H/2$: (a) for $r = 0$, (b) for $r = R$. *(View this art in color at www.dekker.com.)*

convective drying, where the diffusional and thermodiffusional fluxes have opposite directions.

FINAL REMARKS

The main goal of this article was to demonstrate that the volumetrically supplied heat to the dried material results in more uniform distribution of the moisture content during drying, and thus also in smaller value drying-induced stresses. By convective drying, particularly when the drying proceeds in high temperatures and small relative humidity of the drying medium, the thermodiffusional flux of moisture blockades the outflow of moisture due to diffusion, mainly at the boundary, and this causes strongly nonuniform distribution of the moisture content than in microwave drying. Therefore, the convective drying generates larger stresses (Hasatani et al.,[4] Kowalski and Rybicki,[6] Zagrouba et al.[15]).

When the weaker stresses are generated during drying a better quality dry product is obtained from the mechanical standpoint. In this context, microwave drying has the predominance over the convective drying.

NOMENCLATURE

Symbols

A	Area of evaporation (m^2)
A	Bulk elasticity constant (MPa)
c_T	Thermodiffusion coefficient (m^2/K s^2)
c_X	Diffusion coefficient (m^2/s^2)
c_v	Specific heat per unit mass of dry body (J/kg K)
H	Height of the cylinder (m)
K	Volumetric modulus of elasticity (MPa)
l	Latent heat of evaporation (J/kg)
M	Shear elasticity constant (MPa)
$\boldsymbol{q}$	Heat flux (W/m^2)
r	Radial coordinate (m)
R	Radius of the cylinder (m)
S	Total entropy (J/kg K)
s^m	Entropy of moisture (J/kg K)
T	Temperature (K)
t	Time (s)
u_r, u_z	Displacements in radial and axial directions (m)
$\boldsymbol{W}$	Moisture flux (kg/m^2 s)
X	Moisture content (dry basis) (L)
x	Molar vapor content in air (L)
z	Axial coordinate (m)

Greek Letters

α	Attenuation factor (L/m)
α_m	Coefficient of the convective mass exchange (kg s/m^4)
α_T	Coefficient of the convective heat exchange (W/m^2 K)
β_T	Coefficient of thermodiffusion (kg/m^2 K s^2)
β_x	Coefficient of diffusion (kg/m^2 s^2)
ε_{ij}	Strain tensor (L)
$\kappa^{(T)}$	Coefficient thermal expansion (L/K)
$\kappa^{(X)}$	Coefficient moist expansion (L)

Λ_m Mobility coefficient (kg s/m^3)
Λ_T Effective thermal conductivity (W/m K)
μ Moisture potential (J/kg)
Internal source of heat (W/m^3)
σ_{ij} Stress tensor (MPa)

ACKNOWLEDGMENT

This work was carried out as a part of the research project No 7 T09C 035 21 sponsored by the Polish State Committee for Scientific Research.

REFERENCES

1. Chen, G.; Wang, W.; Mujumdar, A.S. Theoretical study of microwave heating patterns and batch fluidized bed drying of porous material. Chemical Engineering Science **2001**, *19* (1), 167–183.
2. Constant, T.; Moyne, C.; Perre, P. Drying with internal heat generation: theoretical aspects in application to microwave heating. AIChE Journal **1996**, *42* (2), 359–368.
3. Feng, H.; Tang, J.; Cavalieri, R.P.; Plumb, O.A. Heat and mass transport in microwave drying of porous materials in a spouted bed. AIChE Journal **2001**, *47* (7), 1499–1512.
4. Hasatani, M.; Itaya, Y.; Hayakawa, K. Fundamental study on shrinkage of formed clay during drying. Drying Technology **1992**, *10* (4), 1013–1036.
5. Kowalski, S.J. *Thermomechanics of Drying Processes*; Springer-Verlag, Berlin Heidelberg: New York, 2003.
6. Kowalski, S.J.; Rybicki, A. Drying stress formation induced by inhomogeneous moisture and temperature distribution. Transport in Porous Media **1996**, *24*, 239–248.
7. Perre, P.; Turner, W. Microwave drying of softwood in an oversized waveguide. AIChE Journal **1997**, *43* (10), 2579–2595.
8. Ratanadecho, P.; Aoki, K.; Akahori, M. Experimental and numerical study of microwave drying in unsaturated porous material. Int. Comm. Heat Mass Transfer **2001**, *28* (5), 605–616.
9. Ratanadecho, P.; Aoki, K.; Akahori, M. A numerical and experimental investigation of the modelling of microwave melting and frozen packed beds using a rectangular wave guide. Int. Comm. Heat Mass Transfer **2001**, *28* (6), 751–762.

10. Ratanadecho, P.; Aoki, K.; Akahori, M. Influence of irradiation time, particle sizes and initial moisture content during microwave drying of multi-layered capillary porous materials. J. Heat Transfer **2002**, *124* (2), 1–11.
11. Rybicki, A. Determination of drying induced stresses in a prismatic bar. Eng. Transactions **1993**, *41* (2), 139–156.
12. Sanga, E.C.M.; Mujumdar, A.S.; Raghavan, G.S.V. Simulation of convection-microwave drying for shrinkage material. Chemical Engineering and Processing **2002**, *41*, 487–499.
13. Turner, W.; Illic, M. Combined microwave and convective drying of a porous material. Drying Technology **1991**, *9* (5), 1209–1269.
14. Wait, R.; Mitchell, A.R. *Finite Elements Analysis and Applications*; Wiley: New York, 1986.
15. Zagrouba, F.; Mihoubi, D.; Bellagi, A. Drying of clay. II, Rheological modelisation and simulation of physical phenomena. Drying Technology **2002**, *20* (10), 1895–1917.
16. Zhang, D.; Mujumdar, A.S. Deformation and stress analysis of porous capillary bodies during intermittent volumetric thermal drying. Drying Technology **1992**, *10* (2), 421–443.
17. Zielonka, P.; Gierlik, E.; Matejak, M.; Dolowy, K. The comparison of experimental and theoretical temperature distribution during microwave wood heating. Holtz als Roh- und Werkstoff **1997**, *55*, 395–398.

Available online at www.sciencedirect.com
ScienceDirect
J. Math. Anal. Appl. 329 (2007) 145–162
Journal of MATHEMATICAL ANALYSIS AND APPLICATIONS
www.elsevier.com/locate/jmaa

Explicit solutions for a two-phase unidimensional Lamé–Clapeyron–Stefan problem with source terms in both phases

A.C. Briozzo [a], M.F. Natale [a], D.A. Tarzia [a,b,*]

[a] Departamento de Matemática, F.C.E., Universidad Austral, Paraguay 1950, S2000FZF Rosario, Argentina
[b] CONICET, Argentina

Received 26 December 2005
Available online 20 July 2006
Submitted by P. Broadbridge

Abstract

A two-phase Stefan problem with heat source terms of a general similarity type in both liquid and solid phases for a semi-infinite phase-change material is studied. We assume the initial temperature is a negative constant and we consider two different boundary conditions at the fixed face $x = 0$, a constant temperature or a heat flux of the form $-q_0/\sqrt{t}$ ($q_0 > 0$). The internal heat source functions are given by $g_j(x,t) = \frac{\rho l}{t}\beta_j(\frac{x}{2a_j\sqrt{t}})$ ($j = 1$ solid phase; $j = 2$ liquid phase) where $\beta_j = \beta_j(\eta)$ are functions with appropriate regularity properties, ρ is the mass density, l is the fusion latent heat by unit of mass, a_j^2 is the diffusion coefficient, x is the spatial variable and t is the temporal variable. We obtain for both problems explicit solutions with a restriction for data only for the second boundary conditions on $x = 0$. Moreover, the equivalence of the two free boundary problems is also proved. We generalize the solution obtained in [J.L. Menaldi, D.A. Tarzia, Generalized Lamé–Clapeyron solution for a one-phase source Stefan problem, Comput. Appl. Math. 12 (2) (1993) 123–142] for the one-phase Stefan problem. Finally, a particular case where β_j ($j = 1, 2$) are of exponential type given by $\beta_j(x) = \exp(-(x + d_j)^2)$ with x and $d_j \in \mathbb{R}$ is also studied in details for both boundary temperature conditions at $x = 0$. This type of heat source terms is important through the use of microwave energy following [E.P. Scott, An analytical solution and sensitivity study of sublimation–dehydration within a porous medium with volumetric heating, J. Heat Transfer 116 (1994) 686–693]. We obtain a unique solution of the similarity type for any data when a temperature

* Corresponding author.
E-mail addresses: adriana.briozzo@fce.austral.edu.ar (A.C. Briozzo), maria.natale@fce.austral.edu.ar (M.F. Natale), domingo.tarzia@fce.austral.edu.ar (D.A. Tarzia).

doi:10.1016/j.jmaa.2006.05.083

boundary condition at the fixed face $x = 0$ is considered; a similar result is obtained for a heat flux condition imposed on $x = 0$ if an inequality for parameter q_0 is satisfied.

Keywords: Stefan problem; Free boundary problem; Lamé–Clapeyron solution; Neumann solution; Phase-change process; Fusion; Sublimation–dehydration process; Heat source; Similarity solution

1. Introduction

Following Scott [20], sublimation–dehydration or freeze–drying, is used as a method for removing moisture from biological materials, such as food. Some of the advantages of sublimation–dehydration over evaporative drying are that the structural integrity of the material is maintained and product degradation is minimized (Ang et al. [1], Rosenberg, Bögl [19]). The major disadvantage of the freeze–drying process is that it is generally slow, and consequently, the process is economically unfeasible for certain materials. One of the means of alleviating this problem is through the use of microwave energy.

Several mathematical models have been proposed to describe the freeze–drying process without microwave heating (Fey, Boles [10], Lin [13]). Only a few studies have also included a microwave heat source in the model (Ang et al. [1]). Phase-change problems appear frequently in industrial processes; a large bibliography on the subject was given recently in Tarzia [22].

In Menaldi, Tarzia [14] the one-phase Lamé–Clapeyron–Stefan problem [12] with internal heat sources of general similarity type was studied and a generalized Lamé–Clapeyron explicit solution was obtained. Moreover, necessary and sufficient conditions were given in order to characterize the source term which provides a unique solution.

In Bouillet, Tarzia [5], the self-similar solutions $\theta(x,t) = \theta(\eta) = \theta(x/\sqrt{t})$ of the problem

$$
\begin{aligned}
&E(\theta)_t - A(\theta)_{xx} = \frac{1}{t}B(\eta), \quad \eta > 0,\\
&\theta(x,t) = C > 0, \quad t > 0,\\
&E\big(\theta(x,0)\big) = 0, \quad x > 0,
\end{aligned}
$$

were studied where E and A are monotone increasing functions, A being continuous, with $E(0) = A(0) = 0$ and $\lambda = E(0^+) > 0$. This equation can describe the conservation of thermal energy in a heat conduction process for a semi-infinite material with a "self-similar" source or sink term of the type $B(x/\sqrt{t})/t$. Moreover, $E(\theta)$ represents an energy per unit volume at level (temperature) θ, $A'(\theta) \geqslant 0$ is the thermal conductivity and $B(\eta)/t$ represents a singular source or sink depending of the sign of the function B. It was obtained for the inverse function $\eta = \eta(\theta)$ an integral equation equivalent to the above problem and it was proven that for certain hypotheses over data there exists at least a solution of the corresponding integral equation following Bouillet [4].

Several applied papers give us the significance of the source terms in the interior of the material which can undergo a change of phase, e.g. Bhattacharya et al. [3], Carslaw, Jaeger [6], Feng [9], Grigor'ev et al. [11], Mercado et al. [15], Ratanadecho et al. [17], Ward [23]. In Scott [20] there is a mathematical model for sublimation–dehydration with volumetric heating of a particular exponential type from which analytical solutions for dimensionless temperature, vapor concentration, and pressure were obtained for two different temperature boundary conditions. It was considered a semi-infinite frozen porous medium with constant thermal properties subject to a sublimation–dehydration process involving a volumetric heat source of the type

$$g(x,t)=\frac{\text{const.}}{t}\exp\bigl(-(x+d)^2\bigr).$$

A sensitivity study was also conducted in which the effects of the material properties inherent in these solutions were analyzed. The mathematical analysis of the analytical solutions is only given from the numerical computation point of view. In one phase is taken d equals to 0 and in the other one d is proportional to the constant λ which characterizes the interface position; this last choice is, for us, a nonadequate choice of a parameter because it depends on the solution itself.

Analytical solutions can provide important insights into the importance of different material properties on the solution, which can aid in the development of improved mathematical models for this process. These solutions provide an important means of evaluating numerical schemes which can later be used with less restrictive assumptions, if necessary, to simulate actual processes. Moreover, it can be used to obtain super and sub solutions for general conditions by using the maximum principle.

In this paper a semi-infinite homogeneous phase-change material initially in solid phase at the uniform temperature $-C<0$, with a volumetric heat source, is considered. A mathematical description for the temperature within the material is given by

$$\frac{\partial T_2}{\partial t}(x,t)=a_2^2\frac{\partial^2 T_2}{\partial x^2}(x,t)+\frac{1}{\rho c_2}g_2(x,t),\quad 0<x<s(t),\ t>0; \tag{1}$$

$$\frac{\partial T_1}{\partial t}(x,t)=a_1^2\frac{\partial^2 T_1}{\partial x^2}(x,t)+\frac{1}{\rho c_1}g_1(x,t),\quad x>s(t),\ t>0; \tag{2}$$

for two given internal source functions (Bouillet, Tarzia [5], Menaldi, Tarzia [14], Scott [20]) given by

$$g_j=g_j(x,t)=\frac{\rho l}{t}\beta_j\left(\frac{x}{2a_j\sqrt{t}}\right),\quad j=1,2, \tag{3}$$

where $\beta_j=\beta_j(\eta)$ are integrable functions in $(0,\epsilon)$ $\forall\epsilon>0$ and $\beta_j(\eta)\exp(\eta^2)$ are integrable functions in $(M,+\infty)$ $\forall M>0$. We assume that $\beta_1(\eta)\geqslant 0$, $\beta_2(\eta)\leqslant 0$ and ρ is the mass density, l is the fusion latent heat per unit of mass, a_j^2 is the diffusion coefficient, c_j is the specified heat per unit of mass and k_j is the thermal conductivity, for $j=1,2$.

The initial temperature and the temperature as $x\to\infty$ are assumed to be constant

$$T_1(x,0)=T_1(+\infty,t)=-C<0,\quad x>0,\ t>0. \tag{4}$$

At $x=0$, two different temperature boundary conditions are considered, the first is a constant temperature condition

$$T_2(0,t)=B>0,\quad t>0, \tag{5}$$

which is studied in Section 2.1, and the second is an assumed heat flux of the form

$$k_2\frac{\partial T_2}{\partial x}(0,t)=\frac{-q_0}{\sqrt{t}},\quad t>0, \tag{6}$$

which is studied in Section 3.

We remark that $-q_0/\sqrt{t}$ denotes the prescribed heat flux on the boundary $x=0$ which is of the type imposed in Tarzia [21] where it was proven that the heat flux condition (6) on the fixed face $x = 0$ is equivalent to the constant temperature boundary condition (5) for the two phase Stefan problem for a semi-infinite material with constant thermal coefficient in both phases without source terms. This kind of heat flux condition was also considered in several papers, e.g. Barber [2], Coelho Pinheiro [7], Polyanin, Dil'man [16], Rogers [18].

The phase-change interface condition is determined from an energy balance at the free boundary $x = s(t)$:

$$k_1 \frac{\partial T_1}{\partial x}\big(s(t), t\big) - k_2 \frac{\partial T_2}{\partial x}\big(s(t), t\big) = \rho l \dot{s}(t), \quad t > 0, \tag{7}$$

where the temperature conditions at the interface are assumed to be constant:

$$T_1\big(s(t), t\big) = T_2\big(s(t), t\big) = 0, \quad t > 0. \tag{8}$$

Moreover, the initial position of the free boundary is

$$s(0) = 0. \tag{9}$$

In Section 2.1 we obtain an explicit solution for the problem (1)–(5), (7)–(9), when the general type of sources given by (3) verifies appropriate properties, and in Section 2.2 we give monotonicity properties of the solution. Both results are obtained for any data and thermal coefficients (particularly for all β's source terms). We remark that when we consider the particular case $C = 0$ and $\beta_1 = 0$ we obtain the solutions given in Menaldi, Tarzia [14] for the one-phase case.

In Section 3 we solve the same free boundary problem but with the heat flux condition of the type $-\frac{q_0}{\sqrt{t}}$ ($q_0 > 0$) prescribed on the fixed face $x = 0$, and we obtain an explicit solution to this problem if the coefficient q_0 satisfies an appropriate particular inequality given by (46). This result is new for the analytical solution. Furthermore, if we take $\beta_1 = \beta_2 = 0$ we get the inequality (46) which was given in Tarzia [21] for the classical two-phase Stefan problem.

In Section 4 we prove the equivalence of the two free boundary problems: the first one with the Dirichlet constant boundary condition (5) considered in Section 2, and the second one with the Neumann boundary condition (6) considered in Section 3.

In Section 5 we will consider the volumetric heat sources of the type given by expressions (56) proposed by Scott [20] in thermal processes. In this particular case we can explicitly obtain conditions (45) and (46) which guarantees the existence of a unique solution, as a function of the parameters of the two problems, in order to have the corresponding exact similarity solution in both phases. If we take $d_1 = d_2 = 0$ in β's expressions (56) our solution (63) coincides with Scott's solution taking a null vapor mass flow rate.

2. Free boundary problem with temperature boundary condition

2.1. *Solution of the free boundary problem with temperature boundary condition at $x = 0$*

Applying the immobilization domain method (see Crank [8]), we are looking for solutions of the type

$$T_j(x, t) = \theta_j(y), \quad j = 1, 2, \tag{10}$$

where the new independent spatial variable y is defined by

$$y = \frac{x}{s(t)}. \tag{11}$$

Then, the condition (7) is transformed into

$$k_1\theta_1'(1) - k_2\theta_2'(1) = \rho l s(t)\dot{s}(t), \tag{12}$$

and we must have necessarily that $s(t)\dot{s}(t) = \text{const.}$ i.e.,

$$s(t) = 2a_2\lambda\sqrt{t}, \tag{13}$$

where the dimensionless parameter $\lambda > 0$ is unknown.

Next, we define

$$R_j(\eta) = \theta_j\left(\frac{\eta}{\lambda}\right), \quad j = 1, 2, \ \eta = \lambda y, \tag{14}$$

then the problem (1)–(5), (7)–(9) is equivalent to the following one:

$$R_2''(\eta) + 2\eta R_2'(\eta) = -\frac{4l}{c_2}\beta_2(\eta), \quad 0 < \eta < \lambda; \tag{15}$$

$$R_1''(\eta) + 2\frac{a_2^2}{a_1^2}\eta R_1'(\eta) = -\frac{4a_2^2 l}{a_1^2 c_1}\beta_1\left(\frac{a_2}{a_1}\eta\right), \quad \eta > \lambda; \tag{16}$$

$$R_1(\lambda) = R_2(\lambda) = 0; \tag{17}$$

$$k_1 R_1'(\lambda) - k_2 R_2'(\lambda) = 2\rho l\lambda a_2^2; \tag{18}$$

$$R_1(+\infty) = -C; \tag{19}$$

$$R_2(0) = B. \tag{20}$$

After some elementary computations, from (15), (17) and (20) we obtain

$$R_2(\eta) = B - \big(B + \varphi_2(\lambda)\big)\frac{\operatorname{erf}(\eta)}{\operatorname{erf}(\lambda)} + \varphi_2(\eta), \quad 0 < \eta < \lambda,$$

$$\varphi_2(\eta) = \frac{2l\sqrt{\pi}}{c_2}\int_0^\eta \beta_2(u)\exp\big(u^2\big)\big(\operatorname{erf}(u) - \operatorname{erf}(\eta)\big)\,du \tag{21}$$

and, from (16), (17) and (19), we have

$$R_1(\eta) = -\frac{(C + \varphi_1(+\infty))}{\operatorname{erf}c(\frac{a_2}{a_1}\lambda)}\frac{2}{\sqrt{\pi}}\int_{\frac{a_2}{a_1}\lambda}^{\frac{a_2}{a_1}\eta} \exp\big(-u^2\big)\,du + \varphi_1(\eta), \quad \eta > \lambda,$$

$$\varphi_1(\eta) = \frac{2l\sqrt{\pi}}{c_1}\int_{\frac{a_2}{a_1}\lambda}^{\frac{a_2}{a_1}\eta} \beta_1(u)\exp\big(u^2\big)\left[\operatorname{erf}(u) - \operatorname{erf}\left(\frac{a_2}{a_1}\eta\right)\right]du \tag{22}$$

where λ is the unknown coefficient which must verify the condition (18).

Furthermore, Eq. (18) for λ is equivalent to the following equation

$$f_1(x, \beta_1) = f_2(x, \beta_2), \quad x > 0, \tag{23}$$

where

$$f_1(x,\beta_1) = F_0(x)\, h_1(x,\beta_1), \tag{24}$$

$$f_2(x,\beta_2) = Q\left(\frac{a_2}{a_1}x\right) h_2(x,\beta_2) \tag{25}$$

with

$$Q(x) = \sqrt{\pi}\, x \exp\left(x^2\right)\left(1 - \operatorname{erf}(x)\right), \quad x > 0, \tag{26}$$

$$F_0(x) = x \operatorname{erf}(x) \exp\left(x^2\right), \quad x > 0, \tag{27}$$

$$h_1(x,\beta_1) = \mathrm{Ste}_1 - 2\sqrt{\pi} \int_{\frac{a_2}{a_1}x}^{+\infty} \operatorname{erf} c(u) \beta_1(u) \exp\left(u^2\right) du, \tag{28}$$

$$h_2(x,\beta_2) = \frac{\mathrm{Ste}_2}{\sqrt{\pi}} - F(x,\beta_2), \quad x > 0, \tag{29}$$

with

$$F(x,\beta_2) = F_0(x) - 2\int_0^x \operatorname{erf}(u) \beta_2(u) \exp\left(u^2\right) du, \quad x > 0, \tag{30}$$

and

$$\mathrm{Ste}_1 = \frac{Cc_1}{l}, \qquad \mathrm{Ste}_2 = \frac{Bc_2}{l} \tag{31}$$

are the Stefan numbers for phases $j = 1$ and $j = 2$, respectively.

Theorem 1. *Equation* (23) *has a unique solution* $\lambda > 0$. *Moreover, the free boundary problem with heat source terms* (1)–(5), (7)–(9) *has an explicit solution given by*

$$\begin{aligned}
T_1(x,t) &= \frac{-(C + \varphi_1(+\infty))}{\operatorname{erf} c(\frac{a_2}{a_1}\lambda)} \left[\operatorname{erf}\left(\frac{x}{2a_1\sqrt{t}}\right) - \operatorname{erf}\left(\frac{a_2}{a_1}\lambda\right)\right] + \varphi_1\left(\frac{x}{2a_2\sqrt{t}}\right), \\
&\quad \textit{for } x > s(t),\ t > 0; \\
T_2(x,t) &= \frac{2l\sqrt{\pi}}{c_2} \int_0^{\frac{x}{2a_2\sqrt{t}}} \beta_2(u) \exp\left(u^2\right)\left(\operatorname{erf}(u) - \operatorname{erf}\left(\frac{x}{2a_2\sqrt{t}}\right)\right) du \\
&\quad + B - \left(B + \varphi_2(\lambda)\right) \frac{\operatorname{erf}(\frac{x}{2a_2\sqrt{t}})}{\operatorname{erf}(\lambda)} \quad \textit{for } 0 < x < s(t),\ t > 0,
\end{aligned} \tag{32}$$

where $\varphi_1(\eta)$ *and* $\varphi_2(\eta)$ *are defined in* (22), (21) *respectively and the free boundary* $s(t)$ *is given by* (13) *where the coefficient* λ *is the unique solution of Eq.* (23).

Proof. Taking into account Appendix A (Lemma A.1) we can prove that Eq. (23) has a unique solution $\lambda > 0$. We invert relations (14), (10) and (11) in order to obtain an explicit solution of problem (1)–(5), (7)–(9) with the source terms g_j defined by (3). $\square$

Remark 1. If the initial temperature $C = 0$ and the solid phase source $\beta_1 = 0$ then we have the one-phase Stefan problem with a constant temperature B at the fixed face $x = 0$ which is the problem considered in Menaldi, Tarzia [14]. The solution is given by

$$\begin{cases} T(x,t) = T_2(x,t) = B - \big(B + \varphi_2(\lambda)\big)\dfrac{\operatorname{erf}(\frac{x}{2a_2\sqrt{t}})}{\operatorname{erf}(\lambda)} \\ \qquad\qquad + \dfrac{2l\sqrt{\pi}}{c_2}\displaystyle\int_0^{\frac{x}{2a_2\sqrt{t}}} \beta_2(u)\exp\big(u^2\big)\left(\operatorname{erf}(u) - \operatorname{erf}\left(\frac{x}{2a_2\sqrt{t}}\right)\right) du, \\ \quad 0 < x < s(t),\ t > 0; \\ s(t) = 2\lambda a_2\sqrt{t}, \end{cases} \tag{33}$$

where λ is the unique solution of equation $F(x,\beta_2) = \frac{\mathrm{Ste}_2}{\sqrt{\pi}}$, $x > 0$.

Remark 2. In the particular case $\beta_1 = \beta_2 = 0$ we have the classic Neumann solution (see Carslaw, Jaeger [6]).

2.2. Monotonicity properties

We denote by $T_{\beta_1\beta_2,1}(x,t)$, $T_{\beta_1\beta_2,2}(x,t)$ and $s_{\beta_1\beta_2}(t)$ (i.e., $\lambda_{\beta_1\beta_2}$) the solution to problem (1)–(5), (7)–(9) for data β_1 and β_2. We will compare this solution with that corresponding to the case $\beta_1 = 0$ and $\beta_1 = \beta_2 = 0$.

We obtain a monotonicity property for the corresponding free-boundaries in Lemma 2 and for temperatures in Theorem 3.

Lemma 2. *If $\beta_1 \geqslant 0$ and $\beta_2 \leqslant 0$ then we have the following monotonicity properties*:

$$\begin{aligned} &\text{(i)} \quad s_{0\beta_2}(t) \leqslant s_{\beta_1\beta_2}(t) \leqslant s_{\beta_1 0}(t), \quad t > 0, \\ &\text{(ii)} \quad s_{0\beta_2}(t) \leqslant s_{00}(t) \leqslant s_{\beta_1 0}(t), \quad t > 0. \end{aligned} \tag{34}$$

Proof. In order to prove (34) it is sufficient to show the same inequality for the coefficient λ, that is,

$$\begin{aligned} &\text{(i)} \quad \lambda_{0\beta_2} \leqslant \lambda_{\beta_1\beta_2} \leqslant \lambda_{\beta_1 0}, \\ &\text{(ii)} \quad \lambda_{0\beta_2} \leqslant \lambda_{00} \leqslant \lambda_{\beta_1 0}. \end{aligned} \tag{35}$$

We can rewrite Eq. (23) for λ by the following

$$G_1(x,\beta_1) = G_2(x,\beta_2) \tag{36}$$

where the real functions G_1 and G_2 are defined by

$$G_1(x,\beta_1) = F_0(x)\left[\mathrm{Ste}_1 + Q\left(\frac{a_2}{a_1}x\right) - 2\sqrt{\pi}\int_{\frac{a_2}{a_1}x}^{+\infty} \operatorname{erf}c(u)\beta_1(u)\exp\big(u^2\big)\,du\right], \tag{37}$$

$$G_2(x,\beta_2) = Q\left(\frac{a_2}{a_1}x\right)\left[\frac{\mathrm{Ste}_2}{\sqrt{\pi}} + 2\int_0^x \operatorname{erf}(u)\beta_2(u)\exp\big(u^2\big)\,du\right]. \tag{38}$$

Taking into account $\beta_1 \geqslant 0$ and $\beta_2 \leqslant 0$ and by comparison of functions G_1 and G_2 we obtain (35)(i), (ii). See Appendix A (Lemma A.2). □

Theorem 3. *The solution to problem* (1)–(5), (7)–(9) *for data* $\beta_1 \geqslant 0$ *and* $\beta_2 \leqslant 0$ *satisfies the following monotonicity properties*:

$$\begin{aligned}
&\text{(i)} && T_{\beta_1\beta_2,2}(x,t) \leqslant T_{\beta_1 0,2}(x,t), \quad 0 \leqslant x \leqslant s_{\beta_1\beta_2}(t),\ t>0,\\
&\text{(ii)} && T_{00,2}(x,t) \leqslant T_{\beta_1 0,2}(x,t), \quad 0 \leqslant x \leqslant s_{00}(t),\ t>0,\\
&\text{(iii)} && T_{0\beta_2,2}(x,t) \leqslant T_{00,2}(x,t), \quad 0 \leqslant x \leqslant s_{0\beta_2}(t),\ t>0,\\
&\text{(iv)} && T_{0\beta_2,1}(x,t) \leqslant T_{00,1}(x,t), \quad x > s_{00}(t),\ t>0,\\
&\text{(v)} && T_{0\beta_2,2}(x,t) \leqslant T_{\beta_1\beta_2,2}(x,t), \quad 0 \leqslant x \leqslant s_{0\beta_2}(t),\ t>0,\\
&\text{(vi)} && T_{0\beta_2,1}(x,t) \leqslant T_{\beta_1\beta_2,1}(x,t), \quad x > s_{\beta_1\beta_2}(t),\ t>0,\\
&\text{(vii)} && T_{00,1}(x,t) \leqslant T_{\beta_1 0,1}(x,t), \quad x > s_{\beta_1 0}(t),\ t>0,\\
&\text{(viii)} && T_{\beta_1\beta_2,1}(x,t) \leqslant T_{\beta_1 0,1}(x,t), \quad x > s_{\beta_1 0}(t),\ t>0.
\end{aligned} \tag{39}$$

Proof. From maximum principle we obtain (39). We will only give the proof of the property (vii).

Let $u(x,t) = T_{\beta_1 0,1}(x,t) - T_{00,1}(x,t)$. Function u satisfies the following conditions:

$$\begin{aligned}
&u_t - a_1^2 u_{xx} = \frac{l}{c_1 t}\beta_1\left(\frac{x}{2a_1\sqrt{t}}\right) \geqslant 0, \quad x > s_{\beta_1 0}(t),\ t>0,\\
&u\big(s_{\beta_1 0}(t),t\big) = -T_{00,1}\big(s_{\beta_1 0}(t),t\big) \geqslant 0, \quad t>0,\\
&u(x,0) = T_{\beta_1 0,1}(x,0) - T_{00,1}(x,0) = -C-(-C) = 0, \quad x > s_{\beta_1 0}(t).
\end{aligned}$$

Then we have $u(x,t) \geqslant 0$ for $x > s_{\beta_1 0}(t)$, $t>0$. □

These monotonicity properties can be interpreted by physical considerations and can be used in order to obtain super and sub explicit solutions for general conditions by using the maximum principle.

3. Solution of the free boundary problem with a heat flux condition on the fixed face $x = 0$

In this section we consider problem (1)–(5), (7)–(9), but condition (5) will be replaced by condition (6) (see Rogers [18], Tarzia [21]). We can define the same transformations (10), (11) and (14) as were done for the previous problem, and we obtain (15)–(19) and

$$R_2'(0) = \frac{-2q_0}{\rho c_2 a_2}. \tag{40}$$

It easy to see that the free boundary must be of the type $s(t) = 2a_2\mu\sqrt{t}$ where μ is a dimensionless constant to be determined. The solution to problem (15)–(19) and (40) is given by

$$R_1(\eta) = -\frac{(C+\varphi_1(+\infty))}{\operatorname{erf}c(\frac{a_2}{a_1}\mu)}\left[\operatorname{erf}\left(\frac{a_2}{a_1}\eta\right) - \operatorname{erf}\left(\frac{a_2}{a_1}\mu\right)\right] + \varphi_3(\eta), \quad \eta > \mu,$$

$$\varphi_3(\eta)=\frac{2l\sqrt{\pi}}{c_1}\int_{\frac{a_2}{a_1}\mu}^{\frac{a_2}{a_1}\eta}\beta_1(u)\exp\left(u^2\right)\left[\operatorname{erf}(u)-\operatorname{erf}\left(\frac{a_2}{a_1}\eta\right)\right]du \tag{41}$$

and

$$R_2(\eta)=\frac{q_0\sqrt{\pi}}{\rho c_2 a_2}\left(\operatorname{erf}(\mu)-\operatorname{erf}(\eta)\right)+\varphi_2(\eta)-\varphi_2(\mu),\quad 0<\eta<\mu, \tag{42}$$

where φ_2 was defined in (21) and the unknown μ must satisfy the following equation

$$W(x,\beta_1)=V(x,\beta_2),\quad x>0, \tag{43}$$

where

$$W(x,\beta_1)=\frac{x\exp(x^2)}{Q(\frac{a_2}{a_1}x)}\left[\mathrm{Ste}_1-2\sqrt{\pi}\int_{\frac{a_2}{a_1}x}^{+\infty}\operatorname{erf}c(u)\beta_1(u)\exp\left(u^2\right)du\right]$$

and

$$V(x,\beta_2)=\frac{q_0}{\rho l a_2}-x\exp\left(x^2\right)+2\int_0^x\beta_2(u)\exp\left(u^2\right)du. \tag{44}$$

Theorem 4.

(a) *If condition*

$$\int_0^{+\infty}\operatorname{erf}c(u)\beta_1(u)\exp\left(u^2\right)du\leqslant\frac{\mathrm{Ste}_1}{2\sqrt{\pi}} \tag{45}$$

holds then Eq. (43) *has a unique solution* $\mu>0$ *if and only if* q_0 *satisfies the following inequality*:

$$q_0\geqslant 2a_1\rho l\left[\frac{\mathrm{Ste}_1}{2\sqrt{\pi}}-\int_0^{+\infty}\operatorname{erf}c(u)\beta_1(u)\exp\left(u^2\right)du\right]. \tag{46}$$

(b) *If*

$$\int_0^{+\infty}\operatorname{erf}c(u)\beta_1(u)\exp\left(u^2\right)du>\frac{\mathrm{Ste}_1}{2\sqrt{\pi}} \tag{47}$$

holds, then Eq. (43) *has at least a solution* $\mu>0\ \forall q_0>0$.

(c) *Under the hypothesis assumed for* β_i $(i=1,2)$ *given in the Introduction, the free boundary problem with sources term* (1)–(4), (6)–(9) *has an explicit solution given by*

$$T_1(x,t)=\frac{-(C+\varphi_3(+\infty))}{\operatorname{erf}c(\frac{a_2}{a_1}\mu)}\left[\operatorname{erf}\left(\frac{x}{2a_1\sqrt{t}}\right)-\operatorname{erf}\left(\frac{a_2}{a_1}\mu\right)\right]+\varphi_3\left(\frac{x}{2a_2\sqrt{t}}\right)$$
$$\text{for } x>s(t),\ t>0, \tag{48}$$

$$T_2(x,t) = \frac{q_0\sqrt{\pi}}{\rho c_2 a_2}\left[\operatorname{erf}(\mu) - \operatorname{erf}\left(\frac{x}{2a_2\sqrt{t}}\right)\right] + \varphi_2\left(\frac{x}{2a_2\sqrt{t}}\right) - \varphi_2(\mu)$$
$$\text{for } 0 < x < s(t),\ t > 0, \tag{49}$$

where φ_3 and φ_2 are defined in (41) *and* (21) *respectively, the free boundary is given by*

$$s(t) = 2a_2\mu\sqrt{t},$$

and μ is the unique solution given in (a) *or* (b).

Proof. To prove (a) and (b) we use the definitions of the functions W and V, and Lemma A.2 (see Appendix A).

We invert relations (14), (10) and (11) in order to obtain (48)–(49). □

Remark 3. In the particular case $\beta_1 \equiv 0$ and $\beta_2 \leqslant 0$ we have that

$$\exists!\mu > 0 \quad \text{solution of Eq. (43)} \quad \Longleftrightarrow \quad q_0 > \frac{Ck_1}{a_1\sqrt{\pi}}$$

which was the result obtained by Tarzia [21].

Remark 4. Taking into account Lemma A.2 (Appendix A) we can prove the same monotonicity properties given in Section 2.2.

4. Equivalence of the two free boundary problems

We consider the solution $T_2(x,t)$ of problem (1)–(4), (6)–(9) given by (49). We compute $T_2(0,t)$ and we have

$$\begin{aligned}
T_2(0,t) &= \frac{q_0\sqrt{\pi}}{\rho c_2 a_2}\operatorname{erf}(\mu) - \varphi_2(\mu) \\
&= \frac{q_0\sqrt{\pi}}{\rho c_2 a_2}\operatorname{erf}(\mu) - \frac{2l\sqrt{\pi}}{c_2}\int_0^\mu \beta_2(z)\exp(z^2)\bigl(\operatorname{erf}(z) - \operatorname{erf}(\mu)\bigr)\,dz \\
&= B_0(\mu)
\end{aligned} \tag{50}$$

which is constant in time.

If we replace B by $B_0(\mu)$ in condition (5) and we solve problem (1)–(5), (7)–(9) we obtain the similarity solutions

$$T_1^*(x,t) = \frac{-(C + \varphi_1(+\infty))}{\operatorname{erf}c(\frac{a_2}{a_1}\lambda)}\left[\operatorname{erf}\left(\frac{x}{2a_1\sqrt{t}}\right) - \operatorname{erf}\left(\frac{a_2}{a_1}\lambda\right)\right] + \varphi_1\left(\frac{x}{2a_2\sqrt{t}}\right),$$
$$\text{for } x > s(t),\ t > 0,$$
$$T_2^*(x,t) = B_0(\mu) - \bigl(B_0(\mu) + \varphi_2(\lambda)\bigr)\frac{\operatorname{erf}(\frac{x}{2a_2\sqrt{t}})}{\operatorname{erf}(\lambda)}$$
$$+ \frac{2l\sqrt{\pi}}{c_2}\int_0^{\frac{x}{2a_2\sqrt{t}}} \beta_2(u)\exp(u^2)\left(\operatorname{erf}(u) - \operatorname{erf}\left(\frac{x}{2a_2\sqrt{t}}\right)\right)du,$$
$$\text{for } 0 < x < s(t),\ t > 0,$$

where $\varphi_1(\eta)$ and $\varphi_2(\eta)$ are defined in (22), (21) respectively and $s(t) = 2\lambda a_2\sqrt{t}$ is the free boundary. The coefficient λ must be the solution of the following equation:

$$f_1(x,\beta_1) = Q\left(\frac{a_2}{a_1}x\right)\left[\frac{\mathrm{Ste}_2^*}{\sqrt{\pi}} - F(x,\beta_2)\right], \quad x > 0,\ \mathrm{Ste}_2^* = \frac{B_0(\mu)c_2}{l}. \tag{51}$$

We remark that Eq. (51) is Eq. (23) where Ste_2 has been replaced by Ste_2^*.

Theorem 5. *Under the hypotheses* (45) *and* (46) *the solution μ of Eq.* (43) *is also solution of Eq.* (51)*, i.e., $\mu = \lambda$.*

Proof. We have:

$$\begin{aligned}
&\mu \text{ is a solution of Eq. (51)}\\
\iff\quad & f_1(\mu,\beta_1) = Q\left(\frac{a_2}{a_1}\mu\right)\left[\frac{B_0(\mu)c_2}{l\sqrt{\pi}} - F(\mu,\beta_2)\right]\\
\iff\quad & F_0(\mu)\left(\mathrm{Ste}_1 - 2\sqrt{\pi}\int_{\frac{a_2}{a_1}\mu}^{+\infty} \operatorname{erf}c(z)\beta_1(z)\exp(z^2)\,dz\right)\\
&\quad = Q\left(\frac{a_2}{a_1}\mu\right)\operatorname{erf}(\mu)\left(\frac{q_0}{\rho l a_2} + 2\int_0^{\mu}\beta_2(z)\exp(z^2)\,dz - \mu\exp(\mu^2)\right)\\
\iff\quad & W(\mu,\beta_1) = V(\mu,\beta_2)\\
\iff\quad & \mu \text{ is a solution of Eq. (43), i.e., } \mu = \lambda. \qquad \square
\end{aligned}$$

Corollary 6. *The coefficient λ a solution of Eq.* (23) *satisfies the following inequality*:

$$\frac{B + \varphi_2(\lambda)}{\operatorname{erf}(\lambda)} \geqslant \frac{l a_1}{c_2 a_2}\left[\mathrm{Ste}_1 - 2\sqrt{\pi}\int_0^{+\infty} \operatorname{erf}c(z)\beta_1(z)\exp(z^2)\,dz\right]. \tag{52}$$

Inequality (52) is a generalization of the inequality for the coefficient which characterizes the free boundary $s(t)$ of the Neumann solution for the particular case $\beta_1 = \beta_2 = 0$ obtained in Tarzia [21], given by

$$\operatorname{erf}(\lambda) < \frac{B a_2 c_2}{C a_1 c_1} = \frac{B}{C}\sqrt{\frac{c_2 k_2}{c_1 k_1}}. \tag{53}$$

5. Study of a particular case

We study the important particular case which has been considered in Scott [20] for sublimation–dehydration with volumetric heating since it is of interest in microwave energy. Taking into account the g's internal source functions given in [20] and definition (3) we can choose in our computation the following expressions for β_i's function:

$$\beta_1(x/2a_1\sqrt{t}) = \exp\left(-(x/2a_1\sqrt{t} + d_1)^2\right), \tag{54}$$

$$\beta_2(x/2a_2\sqrt{t}) = -\exp\left(-(x/2a_2\sqrt{t} + d_2)^2\right), \quad d_1, d_2 \in \mathbb{R}. \tag{55}$$

From (11) and (14) we can take from now on

$$\beta_1(\eta)=\exp\bigl(-(\eta+d_1)^2\bigr),\qquad \beta_2(\eta)=-\exp\bigl(-(\eta+d_2)^2\bigr),\quad d_1,d_2\in\mathbb{R}. \tag{56}$$

The functions φ_1, φ_2 and φ_3 defined by (22), (21) and (41) respectively, are given by

$$\varphi_1(\eta)=\frac{l\sqrt{\pi}}{c_1d_1}\exp\bigl(-d_1^2\bigr)\biggl[\exp\biggl(-2\frac{a_2}{a_1}\lambda d_1\biggr)\biggl(\operatorname{erf}\biggl(\frac{a_2}{a_1}\lambda\biggr)-\operatorname{erf}\biggl(\frac{a_2}{a_1}\eta\biggr)\biggr)$$
$$+\exp\bigl(d_1^2\bigr)\biggl(\operatorname{erf}\biggl(\frac{a_2}{a_1}\eta+d_1\biggr)-\operatorname{erf}\biggl(\frac{a_2}{a_1}\lambda+d_1\biggr)\biggr)\biggr],\quad \text{if } d_1\neq 0, \tag{57}$$

$$\varphi_1(\eta)=\frac{2l\sqrt{\pi}}{c_1}\biggl[\frac{a_2}{a_1}\lambda\biggl(\operatorname{erf}\biggl(\frac{a_2}{a_1}\eta\biggr)-\operatorname{erf}\biggl(\frac{a_2}{a_1}\lambda\biggr)\biggr)$$
$$+\frac{1}{\sqrt{\pi}}\biggl(\exp\biggl(-\biggl(\frac{a_2}{a_1}\eta\biggr)^2\biggr)-\exp\biggl(-\biggl(\frac{a_2}{a_1}\lambda\biggr)^2\biggr)\biggr)\biggr],\quad \text{if } d_1=0, \tag{58}$$

$$\varphi_2(\eta)=\frac{-l\sqrt{\pi}}{c_2d_2}\bigl[\operatorname{erf}(\eta+d_2)-\operatorname{erf}(d_2)-\operatorname{erf}(\eta)\exp\bigl(-d_2^2\bigr)\bigr],\quad \text{if } d_2\neq 0, \tag{59}$$

$$\varphi_2(\eta)=\frac{2l}{c_2}\bigl[1-\exp\bigl(-\eta^2\bigr)\bigr],\quad \text{if } d_2=0, \tag{60}$$

$$\varphi_3(\eta)=\frac{l\sqrt{\pi}}{c_1d_1}\exp\bigl(-d_1^2\bigr)\biggl[\exp\biggl(-2\frac{a_2}{a_1}\mu d_1\biggr)\biggl(\operatorname{erf}\biggl(\frac{a_2}{a_1}\mu\biggr)-\operatorname{erf}\biggl(\frac{a_2}{a_1}\eta\biggr)\biggr)$$
$$+\exp\bigl(d_1^2\bigr)\biggl(\operatorname{erf}\biggl(\frac{a_2}{a_1}\eta+d_1\biggr)-\operatorname{erf}\biggl(\frac{a_2}{a_1}\mu+d_1\biggr)\biggr)\biggr],\quad \text{if } d_1\neq 0, \tag{61}$$

and

$$\varphi_3(\eta)=\frac{2l\sqrt{\pi}}{c_1}\biggl[\frac{a_2}{a_1}\mu\biggl(\operatorname{erf}\biggl(\frac{a_2}{a_1}\eta\biggr)-\operatorname{erf}\biggl(\frac{a_2}{a_1}\mu\biggr)\biggr)$$
$$+\frac{1}{\sqrt{\pi}}\biggl(\exp\biggl(-\biggl(\frac{a_2}{a_1}\eta\biggr)^2\biggr)-\exp\biggl(-\biggl(\frac{a_2}{a_1}\mu\biggr)^2\biggr)\biggr)\biggr],\quad \text{if } d_1=0. \tag{62}$$

Theorem 7. *The explicit solution to the free boundary problem with sources term* (1)–(5), (7)–(9) *is given by*

$$T_1(x,t)=\frac{-(C+\varphi_1(+\infty))}{\operatorname{erf}c(\frac{a_2}{a_1}\lambda)}\biggl[\operatorname{erf}\biggl(\frac{x}{2a_1\sqrt{t}}\biggr)-\operatorname{erf}\biggl(\frac{a_2}{a_1}\lambda\biggr)\biggr]+\varphi_1\biggl(\frac{x}{2a_2\sqrt{t}}\biggr),$$
$$\textit{for } x>s(t),\ t>0;$$
$$T_2(x,t)=\varphi_2\biggl(\frac{x}{2a_2\sqrt{t}}\biggr)+B-\bigl(B+\varphi_2(\lambda)\bigr)\frac{\operatorname{erf}(\frac{x}{2a_2\sqrt{t}})}{\operatorname{erf}(\lambda)},$$
$$\textit{for } 0<x<s(t),\ t>0, \tag{63}$$

where φ_1 and φ_2 are given by (57)–(60)*, and*

$$s(t)=2\lambda a_2\sqrt{t} \tag{64}$$

is the free boundary with λ the unique solution of Eq. (23).

Proof. Taking into account expressions (57)–(60) we obtain the explicit expressions (63) for the temperatures T_1 and T_2. □

Theorem 8.

(a) *Inequality* (45) *is equivalent to*

$$\mathrm{Ste}_1 \geqslant 2, \quad \textit{for } d_1 \geqslant 0, \qquad \mathrm{Ste}_1 \geqslant 2\sqrt{\pi}\,P(d_1), \quad \textit{for } d_1 < 0, \tag{65}$$

where

$$P(x) = \frac{\exp(-x^2) - \operatorname{erf}c(x)}{2x}. \tag{66}$$

(b) *Inequality* (46) *is equivalent to*

$$q_0 \geqslant a_1 \rho l\left[\frac{\mathrm{Ste}_1}{\sqrt{\pi}} - \frac{1}{d_1}\bigl(\exp\bigl(-d_1^2\bigr) - \operatorname{erf}c(d_1)\bigr)\right] \quad \textit{if } d_1 \neq 0, \tag{67}$$

$$q_0 \geqslant \frac{a_1 \rho l}{\sqrt{\pi}}[\mathrm{Ste}_1 - 2] \quad \textit{if } d_1 = 0. \tag{68}$$

(c) *Inequality* (52) *is equivalent to*

$$\frac{B - \frac{l\sqrt{\pi}}{c_2 d_2}(\operatorname{erf}(\lambda + d_2) - \operatorname{erf}(d_2) - \operatorname{erf}(\lambda)\exp(-d_2^2))}{\operatorname{erf}(\lambda)} \geqslant \frac{l a_1}{c_2 a_2}\left[\mathrm{Ste}_1 - \frac{\sqrt{\pi}}{d_1}\bigl(\exp\bigl(-d_1^2\bigr) - \operatorname{erf}c(d_1)\bigr)\right] \quad \textit{if } d_1 \neq 0, \tag{69}$$

and

$$\frac{B - \frac{2l}{c_2}[1 - \exp(-\lambda^2)]}{\operatorname{erf}(\lambda)} \geqslant \frac{l a_1}{c_2 a_2}[\mathrm{Ste}_1 - 2] \quad \textit{if } d_1 = 0. \tag{70}$$

(d) *The free boundary problem with sources term* (1)–(4), (6)–(9) *has an explicit solution given by*

$$T_1(x,t) = \frac{-(C + \varphi_3(+\infty))}{\operatorname{erf}c(\frac{a_2}{a_1}\mu)}\left[\operatorname{erf}\left(\frac{x}{2a_1\sqrt{t}}\right) - \operatorname{erf}\left(\frac{a_2}{a_1}\mu\right)\right] + \varphi_3\left(\frac{x}{2a_2\sqrt{t}}\right) \quad \textit{for } x > s(t),\ t > 0; \tag{71}$$

$$T_2(x,t) = \frac{q_0\sqrt{\pi}}{\rho c_2 a_2}\left[\operatorname{erf}(\mu) - \operatorname{erf}\left(\frac{x}{2a_2\sqrt{t}}\right)\right] + \varphi_2\left(\frac{x}{2a_2\sqrt{t}}\right) - \varphi_2(\mu) \quad \textit{for } 0 < x < s(t),\ t > 0, \tag{72}$$

where φ_3 *and* φ_2 *are defined in* (61)–(62) *and* (59)–(60) *respectively, the free boundary is given by*

$$s(t) = 2a_2\mu\sqrt{t}, \tag{73}$$

and μ *is the unique solution of Eq.* (43).

Proof. (a) We have

$$\int_0^{+\infty} \operatorname{erf}c(u)\beta_1(u)\exp\bigl(u^2\bigr)\,du = \begin{cases} P(d_1) = \frac{\exp(-d_1^2) - \operatorname{erf}c(d_1)}{2d_1}, & \text{if } d_1 \neq 0, \\ \frac{1}{\sqrt{\pi}}, & \text{if } d_1 = 0, \end{cases} \tag{74}$$

where the function $P(x)$ satisfies the following properties:

$$P(0) = \frac{1}{\sqrt{\pi}}, \qquad P(+\infty) = 0, \qquad P(-\infty) = 0, \qquad P(x) > 0 \quad \forall x.$$

Then we obtain that condition (45) is equivalent to

$$2 \leqslant \mathrm{Ste}_1, \quad \text{if } d_1 = 0 \quad \text{or} \quad 2\sqrt{\pi}P(d_1) \leqslant \mathrm{Ste}_1, \quad \text{if } d_1 \neq 0.$$

(b) To obtain (67) we replace expression (74) in (46).

(c) If we replace $\varphi_2(\lambda)$ for expressions (59) or (60) in (52) we obtain (69) or (70) respectively.

(d) Taking into account expressions (59)–(62) we obtain explicit expressions (71) and (72) for the temperatures T_1 and T_2. $\square$

Remark 5. If we take $d_1 = d_2 = 0$ in (56) solution (63) was given by Scott [20] by taking

$$T_d(x,t) = \frac{T_s - T_v}{B} T_2(x,t) + T_v \quad \text{and} \quad T_f(x,t) = \frac{T_v - T_i}{C} T_1(x,t) + T_v$$

where T_s, T_v and T_d were defined in Scott [20].

6. Conclusions

As regards the two-phase Stefan problem with general source terms of a similarity type in both liquid and solid phases for a semi-infinite phase-change material we have arrived at the following conclusions:

(1) An explicit solution for a constant temperature condition $B > 0$ at the fixed face $x = 0$ for any data has been obtained.
(2) An explicit solution for an assumed heat flux of the form $-\frac{q_0}{\sqrt{t}}$ ($q_0 > 0$) has been obtained for data verifying restrictions (45) and (46).
(3) The equivalence of the two previous free boundary problems has also been proved and an inequality (52) for the coefficient λ which characterizes the phase change position is obtained.
(4) An explicit solution for the particular case (56) where functions β_j ($j = 1, 2$) are of an exponential type which are of interest in microwave energy is obtained for any temperature boundary condition $B > 0$.
(5) An explicit solution for the particular case (56) is obtained when a heat flux condition of the type (6) is imposed on $x = 0$; this kind of solution there exists when the parameter q_0 satisfies the inequalities (67) and (68); this is new with respect to Scott [20].

Acknowledgments

This paper has been partially sponsored by the projects "Free Boundary Problems for the Heat-Diffusion Equation" from CONICET-UA, Rosario (Argentina), "Partial Differential Equations and Numerical Optimization with Applications" from Fundación Antorchas (Argentina), and ANPCYT PICT #03-11165 from Agencia (Argentina).

Appendix A. Mathematical properties of some useful functions

Lemma A.1.

(A) *Functions $Q(x)$, $F_0(x)$ and $F(x, \beta_2)$ satisfy the following properties*:

(i) $Q(0)=0,\quad Q(+\infty)=1,\quad Q'(x)>0,\ \forall x>0,\quad Q'(0)=\sqrt{\pi}.$

(ii) $F_0(0)=0,\quad F_0(+\infty)=+\infty,\quad F_0'(x)>0,\ \forall x>0.$

(iii) $F(0,\beta_2)=0,\quad F(+\infty,\beta_2)=+\infty,\quad \dfrac{\partial F}{\partial x}(x,\beta_2)>0,\ \forall x>0.$ (A.1)

(B) *Functions $h_j(x,\beta_j)$ $(j=1,2)$ satisfy the following properties*:

(i) $h_1(0^+,\beta_1)=\mathrm{Ste}_1-2\sqrt{\pi}\displaystyle\int_0^{+\infty}\operatorname{erf}c(u)\beta_1(u)\exp(u^2)\,du;$

(ii) $h_1(+\infty,\beta_1)=\mathrm{Ste}_1;$

(iii) $\dfrac{\partial h_1}{\partial x}(x,\beta_1)=2\sqrt{\pi}\dfrac{a_2}{a_1}\operatorname{erf}c\left(\dfrac{a_2}{a_1}x\right)\exp\left(\dfrac{a_2}{a_1}x\right)^2\beta_1\left(\dfrac{a_2}{a_1}x\right)>0,\quad \forall x>0;$

(iv) *if*

$$\int_0^{+\infty}\operatorname{erf}c(u)\beta_1(u)\exp(u^2)\,du\leqslant\frac{\mathrm{Ste}_1}{2\sqrt{\pi}} \tag{A.2}$$

then $h_1(x,\beta_1)>0,\ \forall x>0;$

(v) *if*

$$\int_0^{+\infty}\operatorname{erf}c(u)\beta_1(u)\exp(u^2)\,du>\frac{\mathrm{Ste}_1}{2\sqrt{\pi}} \tag{A.3}$$

then there exists a unique $\xi_1>0$*, such that* $h_1(\xi_1,\beta_1)=0$ *and* $h_1(x,\beta_1)$ *is negative in* $(0,\xi_1)$*, is positive in* $(\xi_1,+\infty)$*;*

(vi) $h_2(0^+,\beta_2)=\dfrac{\mathrm{Ste}_2}{\sqrt{\pi}};$

(vii) $h_2(+\infty,\beta_2)=-\infty;$

(viii) $\dfrac{\partial h_2}{\partial x}(x,\beta_2)=-\left\{\dfrac{2x}{\sqrt{\pi}}+\exp(x^2)\operatorname{erf}(x)\left[1+2x^2-2\beta_2(x)\right]\right\}<0;$

(ix) *there exist a unique* $\xi_2>0$ *such that* $h_2(\xi_2,\beta_2)=0.$

(C) (a) *Function* $f_1(x,\beta_1)$*, satisfies the following properties*:

(i) $f_1(0^+,\beta_1)=0;$

(ii) $f_1(+\infty,\beta_1)=+\infty;$

(iii) *if condition* (A.2) *is verified then* $f_1(x,\beta_1)>0\ \forall x>0,$

$$\frac{\partial f_1}{\partial x}(x,\beta_1)>0\quad \textit{and}\quad \frac{\partial f_1}{\partial x}(0^+,\beta_1)=0^+;$$

(iv) *if condition* (A.3) *is verified then* $f_1(\xi_1,\beta_1)=0$ *and* $f_1(x,\beta_1)$ *is negative in* $(0,\xi_1)$*, and is positive in* $(\xi_1,+\infty)$*; then there exists* $x_1\in(0,\xi_1)$ *such that* $\frac{\partial f_1}{\partial x}(x_1,\beta_1)=0.$ *Moreover we have* $\frac{\partial f_1}{\partial x}(x,\beta_1)>0\ \forall x>\xi_1.$

(b) *Function* $f_2(x,\beta_2)$ *satisfies the following properties*:

(i) $f_2(0^+,\beta_2)=0;$

(ii) $f_2(+\infty,\beta_2)=-\infty;$

(iii) $f_2(\xi_2, \beta_2) = 0$;

(iv) $\dfrac{\partial f_2}{\partial x}(x, \beta_2) = \dfrac{a_2}{a_1} Q'\left(\dfrac{a_2}{a_1}x\right) h_2(x, \beta_2) + Q\left(\dfrac{a_2}{a_1}x\right)\dfrac{\partial h_2}{\partial x}(x, \beta_2)$;

(v) $\dfrac{\partial f_2}{\partial x}(0^+, \beta_2) = \dfrac{a_2}{a_1}\mathrm{Ste}_2 > 0$;

(vi) *there exists* $x_2 \in (0, \xi_2)$ *such that* $\frac{\partial f_2}{\partial x}(x_2, \beta_2) = 0$;

(vii) $\frac{\partial f_2}{\partial x}(x, \beta_2) < 0,\ \forall x > \xi_2$.

Proof. (A) The properties for F_0 and Q are easy to check and the function F appears for the one-phase case which was considered in Menaldi, Tarzia [14].

(B) It easily follows from (A) and definitions (28)–(29).

(C) We use the definitions of the corresponding real functions and (A) and (B). We remark that in (a)(iv) we have $f_1(x, \beta_1) < 0\ \forall x \in (0, \xi_1)$ and in (b)(vi) we have $f_2(x, \beta_2) > 0$ in $(0, \xi_2)$. $\square$

Lemma A.2. *Function G_1 has the following properties*:

(i) $G_1(0, \beta_1) = 0$,
(ii) $G_1(+\infty, \beta_1) = +\infty$,
(iii) *if condition* (A.2) *is verified then* $G_1(x, \beta_1) > 0,\ \forall x > 0$,
(iv) *if condition* (A.3) *is verified then there exists a unique* $\xi > 0$ *such that* $G_1(\xi, \beta_1) = 0$ *and* $G_1(x, \beta_1)$ *is* negative *in* $(0, \xi)$, G_1 *is* positive *in* $(\xi, +\infty)$,
(v) $G_1(0, 0) = 0$,
(vi) $G_1(+\infty, 0) = +\infty$,
(vii) $\dfrac{\partial G_1}{\partial x}(x, 0) > 0,\quad \forall x > 0,\quad$ *and* $\quad \dfrac{\partial G_1}{\partial x}(0, 0) = 0$.

Function G_2 has the following properties:

(i) $G_2(0, \beta_2) = 0$,
(ii) $G_2(0, 0) = 0$,
(iii) $G_2(+\infty, 0) = \frac{\mathrm{Ste}_2}{\sqrt{\pi}}$,

(iv) $G_2(+\infty, \beta_2) = \dfrac{\mathrm{Ste}_2}{\sqrt{\pi}} + 2\displaystyle\int_0^{+\infty} \mathrm{erf}(u)\beta_2(u)\exp\left(u^2\right) du$,

(v) $\frac{\partial G_2}{\partial x}(x, 0) > 0\ \forall x > 0$,
(vi) $G_2(x, \beta_2) \leqslant G_2(x, 0)\ \forall x \geqslant 0$.

Lemma A.3.

(a) *Function $W(x, \beta_1)$ satisfies the following properties*:

(i) $W(0, \beta_1) = \dfrac{a_1}{a_2\sqrt{\pi}}\left[\mathrm{Ste}_1 - 2\sqrt{\pi}\displaystyle\int_0^{+\infty} \mathrm{erf}\,c(u)\beta_1(u)\exp\left(u^2\right) du\right]$,

(ii) $W(+\infty, \beta_1) = +\infty$,
(iii) $W(x, \beta_1) \leqslant W(x, 0),\ \forall x > 0,\ \beta_1 > 0$,
(iv) *if condition* (A.2) *is verified then* $W(0, \beta_1) \geqslant 0$ *and*

$$\frac{\partial W}{\partial x}(x, \beta_1) > 0, \quad \forall x > 0,$$

(v) *if condition* (A.3) *is verified then* $W(0, \beta_1) < 0$.

(b) *Function* $V(x, \beta_2)$ *satisfies the following properties*:
(i) $V(0, \beta_2) = \frac{q_0}{\rho l a_2}$,
(ii) $V(+\infty, \beta_2) = -\infty$,
(iii) $\frac{\partial V}{\partial x}(x, \beta_2) < 0,\ \forall x > 0$,
(iv) $V(x, \beta_2) \leqslant V(x, 0),\ \forall x > 0,\ \beta_2 < 0$.

Proof. In order to prove (a)(iii) we use that $Q'(x)$ is given by $Q'(x) = \frac{Q(x)(1+2x^2)-2x^2}{x}$.
We demonstrate the other properties by elementary computations. □

References

[1] T.K. Ang, J.D. Ford, D.C.T. Pei, Microwave freeze–drying of food: Theoretical investigation, Int. J. Heat Mass Transfer 20 (1977) 517–526.
[2] J.R. Barber, An asymptotic solution for short-time transient heat conduction between two similar contacting bodies, Int. J. Heat Mass Transfer 32 (5) (1989) 943–949.
[3] S. Bhattacharya, S. Nandi, S. DasGupta, S. De, Analytical solution of transient heat transfer with variable source for applications in nuclear reactors, Int. Comm. Heat Mass Transfer 28 (7) (2001) 1005–1013.
[4] J.E. Bouillet, Self-similar solutions, having jumps and intervals of constancy, of a diffusion-heat conduction equation, IMA Preprints #230, Univ. Minnesota, 1986.
[5] J.E. Bouillet, D.A. Tarzia, An integral equation for a Stefan problem with many phases and a singular source, Rev. Un. Mat. Argentina 41 (4) (2000) 1–8.
[6] H.S. Carslaw, J.C. Jaeger, Conduction of Heat in Solids, Oxford Univ. Press, London, 1959.
[7] M.N. Coelho Pinheiro, Liquid phase mass transfer coefficients for bubbles growing in a pressure field: A simplified analysis, Int. Comm. Heat Mass Transfer 27 (1) (2000) 99–108.
[8] J. Crank, Free and Moving Boundary Problems, Clarendon Press, Oxford, 1984.
[9] H. Feng, Analysis of microwave assisted fluidized-bed drying of particulate product with a simplified heat and mass transfer model, Int. Comm. Heat Mass Transfer 29 (8) (2002) 1021–1028.
[10] Y.C. Fey, M.A. Boles, An analytical study of the effect of convection heat transfer on the sublimation of a frozen semi-infinite porous medium, Int. J. Heat Mass Transfer 30 (1987) 771–779.
[11] A.I. Grigor'ev, V.V. Morozov, S.O. Shiryaeva, Formation and dispersion of an electrolyte film on an ice electrode melting as a result of joule heat evolution, Technical Physics 47 (10) (2002) 1237–1245.
[12] G. Lamé, B.P. Clapeyron, Memoire sur la solidification par refroidissement d'un globe liquide, Annales Chimie Physique 47 (1831) 250–256.
[13] S. Lin, An exact solution of the sublimation problem in a porous medium, ASME J. Heat Transfer 103 (1981) 165–168.
[14] J.L. Menaldi, D.A. Tarzia, Generalized Lamé–Clapeyron solution for a one-phase source Stefan problem, Comput. Appl. Math. 12 (2) (1993) 123–142.
[15] G.A. Mercado, B.P. Luce, J. Xin, Modelling thermal front dynamics in microwave heating, IMA J. Appl. Math. 67 (2002) 419–439.
[16] A.D. Polyanin, V.V. Dil'man, The method of the 'carry over' of integral transforms in non-linear mass and heat transfer problems, Int. J. Heat Mass Transfer 33 (1) (1990) 175–181.
[17] P. Ratanadecho, K. Aoki, M. Akahori, A numerical and experimental investigation of the modeling of microwave melting of frozen packed beds using a rectangular wave guide, Int. Comm. Heat Mass Transfer 28 (2001) 751–762.
[18] C. Rogers, Application of a reciprocal transformation to a two-phase Stefan problem, J. Phys. A 18 (1985) 105–109.
[19] U. Rosenberg, W. Bögl, Microwave thawing, drying, and baking in the food industry, Food Technology 41 (6) (1987) 834–838.

[20] E.P. Scott, An analytical solution and sensitivity study of sublimation–dehydration within a porous medium with volumetric heating, J. Heat Transfer 116 (1994) 686–693.
[21] D.A. Tarzia, An inequality for the coefficient σ of the free boundary $s(t) = 2\sigma\sqrt{t}$ of the Neumann solution for the two-phase Stefan problem, Quart. Appl. Math. 39 (1981–1982) 491–497.
[22] D.A. Tarzia, A bibliography on moving – free boundary problems for the heat-diffusion equation. The Stefan and related problems, MAT-Serie A, #2 (2000) (with 5869 titles on the subject, 300 pages). See www.austral.edu.ar/MAT-SerieA/2(2000)/.
[23] M. Ward, Thermal runaway and microwave heating in thin cylindrical domains, IMA J. Appl. Math. 67 (2002) 177–200.

DRYING TECHNOLOGY
Vol. 22, No. 5, pp. 1173–1189, 2004

Qualitative Aspects of Convective and Microwave Drying of Saturated Porous Materials

S. J. Kowalski* **and A. Rybicki**

Institute of Technology and Chemical Engineering,
Poznan University of Technology, Poland

ABSTRACT

The differences in distribution and temporal evolution of temperature, moisture content, and drying stresses in saturated capillary-porous materials by convective and microwave drying are analyzed. The analysis is based on the mechanistic model of drying taking into account the coupling effects in the heat and mass transfer. The results of numerical simulation allow better understanding of the difference in thermal and mechanical behavior of dried materials to which the energy necessary for drying is supplied volumetrically (microwave drying) or through the material surface (convective drying). The study is carried out on an isotropic cylinder as a model material.

*Correspondence: Professor S. J. Kowalski, Institute of Technology and Chemical Engineering, Poznan University of Technology, pl. Marii Skłodowskiej-Curie 2, 60-965 Poznan, Poland; Fax: (+61) 665 3649; E-mail: Stefan.J.Kowalski@put.poznan.pl.

DOI: 10.1081/DRT-120038586 0737-3937 (Print); 1532-2300 (Online)

Key Words: Thermomechanical model; Microwave drying; Convective drying; Distributions of temperature, moisture content and stresses; Kaolin; Cylindrical sample.

INTRODUCTION

The convective method of drying is used most commonly in industrial technology of drying. In this method, the heat necessary for moisture evaporation is supplied convectively by hot air or superheated steam through the material surface. In such a case, the gradient of temperature is pointed outwards and the heat flux is pointed into the material. So, the thermodiffusional mass flow is in the opposite direction to the diffusional flux of moisture. As a result, the distribution of moisture can achieve a strongly nonlinear mapping, and this may be a reason for the generation of strong shrinkage stresses. Therefore, one should look for another means of heat supply, namely, such a means by which the diffusional and thermodiffusional fluxes of moisture are pointed in the same direction. One of several possible ways is to apply the microwave generation of heat inside the material.

The main aim of this article is to show that heat supplied volumetrically to the dried material causes the diffusional and thermodiffusional flow of moisture in the same direction, and thus, more uniform distribution of the moisture content in the material and smaller values of the shrinkage stresses. Our attention is concentrated on the microwave drying, by which the heat is generated volumetrically inside the dried material.

Microwave drying has been studied recently by several authors: Chen et al.,[1] Constant et al.,[2] Feng et al.,[3] Perre and Turner,[7] Ratanadecho et al.,[8–10] Sanga et al.,[12] Turner and Illic,[13] Zhang and Mujumdar,[16] Zielonka et al.,[17] among others. However, little attention has been devoted to the analysis of mechanical effects arising in materials under this kind of drying, and in particular to the drying induced stresses. Generally, one can state that the volumetrically generated heat in dried materials, as it takes place in microwave drying, gives better mechanical quality products than by convective heat supply through the boundary surface, mainly due to substantial reduction of drying induced stresses.

The mechanistic drying theory presented in Kowalski[5] forms the basis for the present analysis. The governing equations for heat and mass transfer, adapted to a cylindrically shaped sample, are solved numerically with the finite element method (Rybicki[11] and Wait and Mitchell[14]).

The temperature, moisture, and stress distributions at different instances for both microwave and convective drying are presented.

GOVERNING EQUATIONS FOR HEAT AND MASS TRANSFER

The general mechanistic drying theory used here for analysis of the mechanical effects in dried materials was developed systematically on the basis of balance equations for mass, momentum, energy, and entropy, as well as on the statements of the conservation laws and the principles of irreversible thermodynamics (Kowalski[5]). Adopting this theory to the present considerations, we made the following assumptions:

- The dried body is assumed to be an isotropic capillary-porous solid of density ρ^s.
- The pores in the body are filled with liquid (l)–vapor (v) mixture of partial mass density $\rho^m = \rho^l + \rho^v \approx \rho^l$, i.e., saturated body.
- The moisture flux inside the material is proportional to the gradient of moisture potential, and that on the boundary surface is proportional to the difference of chemical potentials of vapor at the boundary and far from the boundary. Diffusivity is assumed constant.
- The heat flux includes both conduction and transport of heat by moisture flux.
- The heat and mass transfer includes coupling effects; however, the influence of body volume deformation on heat and mass transfer is neglected.
- The dried material is elastic.
- Gravity forces are neglected.
- The microwave energy absorption term is constructed as the local microwave power multiplied by the water content and an exponentially formulated attenuation term dependent on the distance in microwave propagation and the attenuation factor.
- The boundary value problem is two-dimensional; the analyzed functions depend on coordinates r, z (radius and height of the cylinder), and time t.

The governing equations reduced to solve the axial-symmetry boundary value problem include: the system of equations describing heat and mass transfer, the equations of equilibrium of internal force, and the physical relations.

Let $X = \rho^m/\rho^s$ denotes the ratio of moisture content referred to the mass of a dry body, and $\boldsymbol{W}$ is the mass flux of the moisture. The mass balance for the moisture reads (Kowalski[5])

$$\rho^s \dot{X} = -\mathrm{div}\boldsymbol{W} \tag{1}$$

Based on the above-mentioned reference, we write the following (reduced) form of energy balance

$$\rho^s T\dot{S} = -\mathrm{div}(\boldsymbol{q} \pm s^m T\, \boldsymbol{W}) + \Re \tag{2}$$

where S denotes total entropy referred to the mass of a dry body, $\boldsymbol{q}$ is the heat flux, s^m is the entropy of moisture, T is the temperature of the body, and $\Re$ is the internal source of heat (radiation). This equation points out that the entropy alteration is due to heat flux conducted and heat transported by the mass flux, as well as by the internal heat generation (radiation).

The following mass and heat fluxes resulted from the thermodynamic inequality (see Ref.[5])

$$\boldsymbol{W} = -\Lambda_m \mathrm{grad}\mu, \qquad \Lambda_m \geq 0 \tag{3}$$

$$\boldsymbol{q} = -\Lambda_T \mathrm{grad}T \mp s^m T\, \boldsymbol{W}, \qquad \Lambda_T \geq 0 \tag{4}$$

In these relationships μ is the generalized chemical potential of the moisture, Λ_m is termed the mobility coefficient dependent on the surface tension and viscosity of the moisture, as well as on the permeability and porosity of the dried body, while Λ_T is the effective thermal conductivity, being volume averaged from conductivity coefficients of solid, liquid, and vapor phases. In Eq. (4), the sign "minus" between the conducted and convected heat flux holds when the moisture flux $\boldsymbol{W}$ flows outwards the body.

The generalized chemical potential μ and the entropy S are functions of the body thermodynamic state, defined by the temperature T, volumetric strain ε, and moisture content X. In further considerations, we neglect the influence of the volumetric strain gradient on moisture transport, and the volumetric strain rate on the temperature alteration. So, after substituting mass and heat fluxes of Eqs. (3) and (4) into the balances of mass and energy of Eqs. (1) and (2), we obtain the following system of differential equations describing the heat and mass transfer

$$\rho^s \dot{X} = \Lambda_m (c_T \nabla^2 T + c_X \nabla^2 X) \tag{5}$$

$$\rho^s (c_v \dot{T} + l\dot{X}) = \Lambda_T \nabla^2 T + \Re \quad \text{with} \quad \nabla^2 = \frac{\partial^2}{\partial r^2} + \frac{1}{r}\frac{\partial}{\partial r} + \frac{\partial^2}{\partial z^2} \tag{6}$$

where ∇^2 is the Laplace operator in cylindrical coordinates with axial symmetry, c_T and c_X are the thermodifusional and diffusional coefficients of moisture transport, c_v is the total volume averaged specific heat referred to unit mass of a dry body, and $l=(s^v-s^l)T$ is the latent heat of evaporation, being the difference of vapor and liquid entropy multiplied by temperature.

The internal source of heat $\Re$ is zero for the convective drying. In the case of microwave drying, it expresses the rate of microwave energy absorbed per unit volume, and is constructed as follows

$$\Re = \Re_0 \frac{X}{X_0} \exp[-\alpha(R-r)] \tag{7}$$

where X is the moisture content at time t and radius r, X_0 is the moisture content at time $t=0$ and radius r, α is the attenuation factor in the direction of microwave propagation distance $(R-r)$, R is the cylinder radius, and $\Re_0$ is the experimentally estimated average microwave power.

Using our 8-modal microwave chamber dryer type WS110 firm PLAZMATRONIKA of maximum microwave power 600 W, we have estimated the average microwave power on the cylindrical kaolin sample using the formula

$$\Re_0 = \frac{2}{R}\left[\alpha_T(T_n - T_a) + l\frac{\Delta m}{A\Delta t}\right] \tag{8}$$

In this formula: α_T denotes the coefficient of convective heat exchange, T_n is the sample surface temperature (adjusted automatically by the microwave dryer), T_a is the temperature of the ambient medium, l is the latent heat of water evaporation, Δm is the loss of a sample weight per time increment Δt, and A is the area of evaporation.

Figure 1 presents the geometry of the sample under consideration. The undersurface of the cylindrically shaped sample is placed on the impermeable plate, whereas the other surfaces are open for moisture release. The sample is assumed to be enough long so that the supply of microwave power takes place mainly through the lateral surface of the cylinder (see Eq. (7)).

The following boundary conditions for mass and heat transfer hold for both convective and microwave drying. These for mass transfer, expressed with the help of moisture potential, are as follows:

$$\frac{\partial\mu}{\partial z}|_{z=0} = 0, \qquad -\Lambda_m\frac{\partial\mu}{\partial z}|_{z=H} = \alpha_m(\mu|_{z=H} - \mu_a) \tag{9a}$$

$$\frac{\partial\mu}{\partial r}|_{r=0} = 0, \qquad -\Lambda_m\frac{\partial\mu}{\partial z}|_{z=R} = \alpha_m(\mu|_{z=R} - \mu_a) \tag{9b}$$

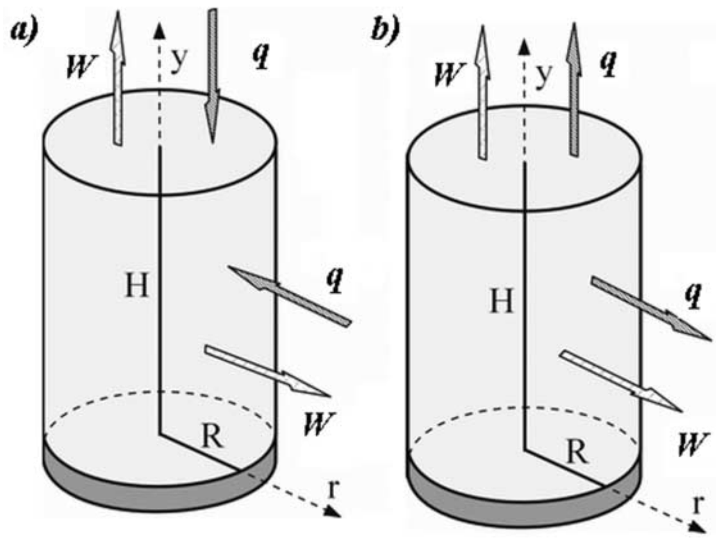

Figure 1. Geometry of the dried sample: (a) convective drying, (b) microwave drying.

where α_m denotes the coefficient of convective mass transfer, and μ_a is the chemical potential of vapor in the ambient medium. The conditions on the left express impermeability (the upper) and symmetry (the lower one), while these on the right, represent the convective exchange of mass.

The boundary conditions for heat transfer are similar in form to these for mass transfer, namely

$$- \Lambda_T \frac{\partial T}{\partial z}|_{z=0} = \alpha_T (T|_{z=0} - T_a),$$
$$- \Lambda_T \frac{\partial T}{\partial z}|_{z=H} = \alpha_T (T|_{z=H} - T_a) - l\alpha_m(\mu|_{z=H} - \mu_a) \tag{10a}$$

$$\frac{\partial T}{\partial r}|_{r=0} = 0, - \Lambda_T \frac{\partial T}{\partial z}|_{z=R}$$
$$= \alpha_T(T|_{z=R} - T_a) - l\alpha_m(\mu|_{z=R} - \mu_a) \tag{10b}$$

where constant value of the coefficient of convective heat exchange α_T is assumed.

The upper condition on the left expresses the convective exchange of heat on the lower moisture-impermeable plate, the lower on the left is the symmetry condition. The conditions on the right describe the convective heat exchange with taking into account the heat escaping with the vapor.

The initial conditions express the values of moisture content and temperature at the beginning of drying, that is

$$X(r,z,t)|_{t=0} = X_0 = \text{const} \quad \text{and} \quad T(r,z,t)|_{t=0} = T_0 = \text{const} \tag{11}$$

The numerical method used for solution of this initial-boundary value problem was the Galerkin discretization method (finite element method) for spatial derivatives, and the finite difference method for time derivatives (see Kowalski and Rybicki,[6] Rybicki,[11] Wait and Mitchell[14]).

NUMERICAL PREDCTION OF TEMPERATURE AND MOISTURE CONTENT

In numerical calculations the gradient of moisture potential inside the material was replaced by the gradients of temperature and moisture content, that is

$$\text{grad}\mu = c_T \text{grad} T + c_X \text{grad} X \tag{12}$$

The moisture potential on the external boundary surface was assumed to be equal to the vapor moisture potential at the boundary, i.e.,

$$\mu|_{r=R} = \mu(p^v|_{r=R}, T|_{r=R}) = \mu(p, x|_{r=R}, T|_{r=R}) \tag{13}$$

where $p^v|_{r=R} = px|_{r=R}$ denotes the vapor partial pressure and $x|_{r=R}$ is the molar vapor content in air at the boundary, and p is the total pressure of air.

Developing the moisture (vapor) potentials in air in Taylor's series one can replace the difference in moisture potentials on the right hand side of boundary conditions (9a) and (9b) by the following expression

$$\alpha_m(\mu|_B - \mu_a) \cong \beta_x(x|_B - x_a) + \beta_T(T|_B - T_a) \tag{14}$$

where β_x and β_T can be termed as the diffusion and thermodiffusion coefficients of vapor in the surrounding air, and $|_B$ means the boundary surface.

All numerical calculations, for both convective and microwave drying, refer to the kaolin cylinder of radius $R = 0.025$ m and height $H = 0.1$ m. The initial moisture content of the cylinder was assumed to be $X_0 = 28\%$ (dry basis state), and the initial temperature $T_0 = 15°C$. The following data of material coefficients suitable for kaolin material were taken for numerical calculus

$$
\begin{aligned}
\Lambda_m &= 6.04\times10^{-8}(\mathrm{kg\,s\,m^{-3}}) & \Lambda_T &= 1.7\times10^{-3}(\mathrm{W\,m^{-1}\,K^{-1}})\\
c_X &= 3.06\,(\mathrm{J\,kg^{-1}}) & c_T &= 0.52\,(\mathrm{J\,kg^{-1}\,K^{-1}})\\
\beta_x &= 9.64\times10^{-6}(\mathrm{kg\,m^{-2}\,s}) & \beta_T &= 40\,(\mathrm{kg\,m^2\,s^{-1}\,K^{-1}})\\
c_v &= 23.3\times10^5\,(\mathrm{J\,kg^{-1}K^{-1}}) & l &= 2000\,(\mathrm{kJ\,kg^{-1}})\\
\rho^s &= 2600\,(\mathrm{kg\,m^{-3}}) & a &= 150\,(\mathrm{m^{-1}})\\
\alpha_m &= 8.64\times10^{-5}(\mathrm{kg\,s\,m^{-4}}) & \Re_0 &= 180\,(\mathrm{W\,m^{-3}})
\end{aligned}
$$

Temperature T_a of air in the drying chamber (convective drying) was fixed at 50°C, and the relative humidity was $\varphi = 10\%$. Under these conditions the wet bulb temperature reached about 35°C. In our microwave chamber dryer, on the other hand, it is possible to fix automatically the temperature of the upper cylinder surface, so it was fixed to be 35°C. The temperature of air in this chamber was c.a. 20°C, and the relative humidity $\varphi = 40\%$.

Figure 2 illustrates the temperature distribution in the cylindrical samples by convective drying and by microwave drying.

The plots present the isolines of constant temperatures of given values. Note that the bottom base of the cylinder is placed on a plate impermeable to moisture flow but conductive for heat. The upper base and the lateral surfaces of the cylinder are open, so the heat and mass exchange with the ambient air is possible through these surfaces.

In the case of convective drying, the cylinder is assumed to be continuously heated from the hot ambient air, however, due to evaporation of moisture and escaping of vapor from the upper and lateral surfaces, the greatest temperature occurs in the middle of the cylinder, particularly at its bottom base (Fig. 2a). The calculations refer to the stable drying conditions, so that the distribution of temperature is also stable, although nonuniformly distributed through the cylinder, due to heating from below through the impermeable for moisture plate.

A quite different distribution of temperature was obtained for microwave drying of the cylinder. In this case the heat was generated inside the material, proportionally to the local amount of moisture. The propagation of microwaves was assumed to proceed in radial direction only and with exponential attenuation term increasing with a distance. It is obvious that the temperature of the ambient air in microwave drying is lower than the temperature of the drying object.

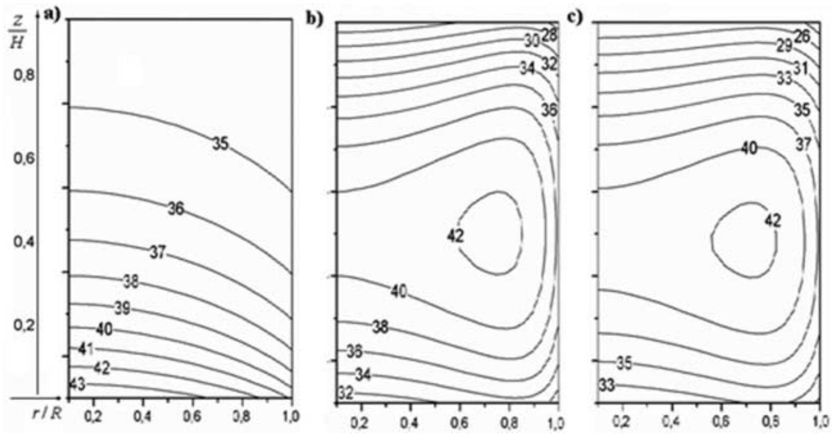

Figure 2. Distribution of temperature in the cylindrical samples: (a) 60-min convective drying, (b) 60-min microwave drying, (c) 180-min microwave drying.

Note that the escape of heat through the upper and the lateral surfaces of the cylinder during microwave drying is doubled, namely, due to convection and due to transport with vapor. Because there is no vapor escape through the bottom base of the cylinder, the temperature at this base is greater than at the upper one. Due to attenuation of microwaves with distance and proportionality of the heat generation to the magnitude of local moisture content, the highest temperature appears not in the center of the cylinder $r=0$, but is in some other cross-section $0<r<R$. Similarly, because of asymmetry of cylinder cooling on its upper and bottom surfaces, the highest temperature is not in the middle of the cylinder height $z=H/2$, but in some other plane $0<z<H/2$.

Figure 3 presents the moisture content distribution in the cylinder during convective drying after 60, 120, and 180 min of a drying time.

This figure illustrates clearly how the dry zone moves towards the interior of the cylinder in the course of drying. The driest area is located at the upper corner of the cylinder, and the least dry area somewhere in the middle of the cylinder. The upper surface is open for the moisture exchange, similar as the lateral one. On the other hand, the bottom surface is closed to moisture transfer, but it is warmer than the other surfaces (see Fig. 2a). Therefore, the removal of moisture in lateral direction is greater than in other places, and the moisture content at this surface is a bit lower than in a slightly higher cross-section of the cylinder (see Fig. 3c).

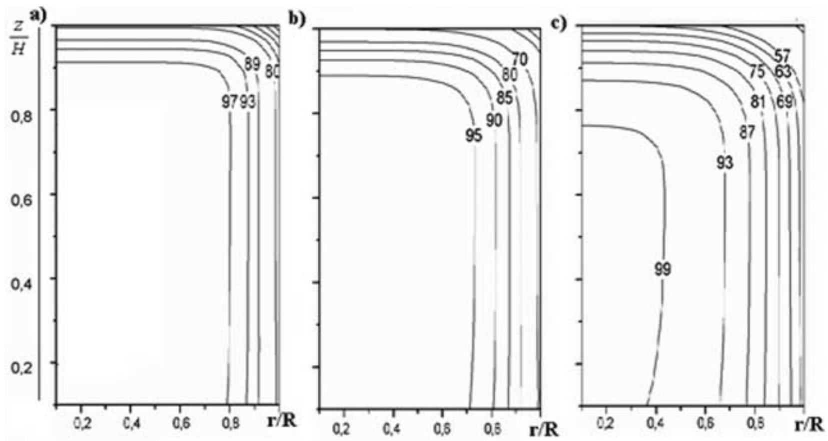

Figure 3. Distribution of moisture content (in % of initial moisture) in the cylindrical sample by convective drying: (a) 60 min, (b) 120 min, (c) 180 min.

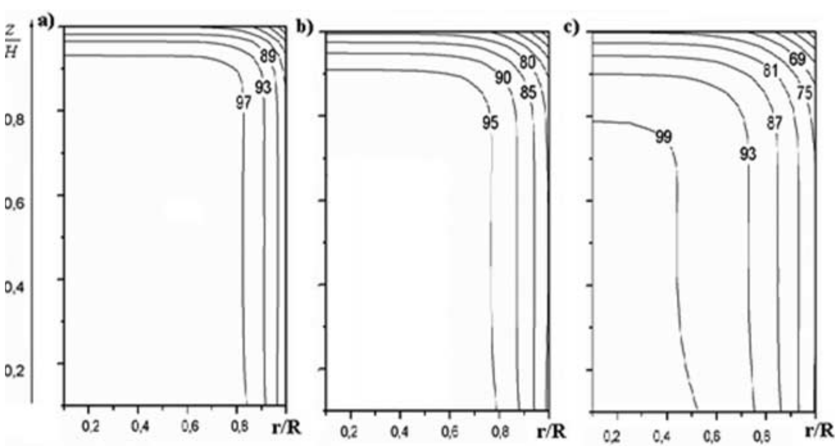

Figure 4. Distribution of moisture content (in % of initial moisture) in the cylindrical sample by microwave drying: (a) 60 min, (b) 120 min, (c) 180 min.

Figure 4 presents the distribution of moisture content distribution in the cylinder by microwave drying after 60, 120, and 180 min of a drying time.

The distribution of moisture in this kind of drying is quite similar to that by convective drying, however, is more uniform. This is evidenced by the fact that the isolines are less dense than in convective drying. Another difference is visible at the bottom of the cylinder. In this place the moisture removal is the slowest by microwave drying. This was not the case of convective drying. Besides, the drying rate is greater in microwave than in convective drying.

DRYING INDUCED STRESSES

Having determined the distributions of temperature and moisture content, one can calculate the distribution of stresses. The stresses have to satisfy the equilibrium equations, which in the axial symmetry take the form

$$\frac{\partial\sigma_{rr}}{\partial r}+\frac{\partial\sigma_{rz}}{\partial z}+\frac{\sigma_{rr}-\sigma_{\varphi\varphi}}{r}=0 \tag{15a}$$

$$\frac{\partial\sigma_{rz}}{\partial r}+\frac{\sigma_{rz}}{r}+\frac{\partial\sigma_{zz}}{\partial z}=0 \tag{15b}$$

The stresses are related to the strains as follows:

$$\sigma_{rr}=2M\varepsilon_{rr}+A\varepsilon-3K\varepsilon^{(TX)} \tag{16a}$$

$$\sigma_{\varphi\varphi}=2M\varepsilon_{\varphi\varphi}+A\varepsilon-3K\varepsilon^{(TX)} \tag{16b}$$

$$\sigma_{zz}=2M\varepsilon_{zz}+A\varepsilon-3K\varepsilon^{(TX)} \tag{16c}$$

$$\sigma_{zr}=2M\varepsilon_{zr} \tag{16d}$$

where M and A are the coefficients equivalent to Lame constants in the theory of elasticity, $3K=2M+3A$, and

$$\varepsilon^{(TX)}=\kappa^{(T)}(T-T_0)+\kappa^{(X)}(X-X_0) \tag{17}$$

denotes the thermal-moist strain, with $\kappa^{(T)}$ and $\kappa^{(X)}$ being the coefficients of thermal and moist expansion (or shrinkage).

The geometrical relations for axial symmetry are:

$$\varepsilon_{rr}=\frac{\partial u_r}{\partial r},\quad \varepsilon_{\varphi\varphi}=\frac{u_r}{r},\quad \varepsilon_{zz}=\frac{\partial u_z}{\partial z},\quad \varepsilon_{rz}=\frac{1}{2}\left(\frac{\partial u_r}{\partial z}+\frac{\partial u_z}{\partial r}\right) \tag{18}$$

with

$$\varepsilon=\varepsilon_{rr}+\varepsilon_{\varphi\varphi}+\varepsilon_{zz}=\frac{1}{r}\frac{\partial}{\partial r}(ru_r)+\frac{\partial u_z}{\partial z}=0 \tag{19}$$

being the volumetric strain, and u_r, u_z denote the displacements in radial and axial directions, respectively.

Substituting the physical relations from Eq. (16a) to Eq. (16b) into the equations of force equilibrium (15a) and (15b), we obtain the system of two coupled equations for determination of displacements u_r and u_z

$$M\nabla^2 u_r + \frac{\partial}{\partial r}\left[(M+A)\varepsilon - 3K\varepsilon^{(TX)}\right] = M\frac{u_r}{r^2} \tag{20a}$$

$$M\nabla^2 u_z + \frac{\partial}{\partial z}\left[(M+A)\varepsilon - 3K\varepsilon^{(TX)}\right] = 0 \tag{20b}$$

where ∇^2 denotes the Laplace operator in cylindrical coordinates (see Eq. (6)).

In order to solve this system of equations explicitly, the following boundary conditions are assumed:

– Zero-valued stresses at the free surfaces of the cylinder, that is

$$\sigma_{rr}|_{r=R} = 0, \qquad \sigma_{zz}|_{z=H} = 0 \tag{21a}$$

– Zero-valued displacements at the bottom and in the center of the cylinder, that is

$$u_r|_{r=0} = 0, \qquad u_z|_{z=0} = 0 \tag{21b}$$

The stresses arise when the temperature and/or moisture content are distributed nonuniformly. We have assumed uniform distribution of temperature and moisture content at the beginning of a drying process, and this means the stress-free initial state of the cylinder.

The finite element procedure of Galerkin type was applied to numerical calculus of displacements, strains, and stresses. In our considerations we are interested mostly in comparison of stresses generated by convective and microwave drying. This issue will be illustrated on the circumferential stresses $\sigma_{\varphi\varphi}$.

Figure 5 visualizes the stress distribution in the longitudinal plane (r, z) of the cylinder. The lines perform the circumferential stresses of the same value (stress-isolines).

It is seen from this figure that stresses are tensional at the surfaces where the removal of moisture takes place and the shrinkage of dried material occurs. As the cylinder as a whole has to be in equilibrium, the tensional stresses have to be balanced by the compressive stresses in the core of the cylinder. The neutral (zero-valued) line separates the areas of

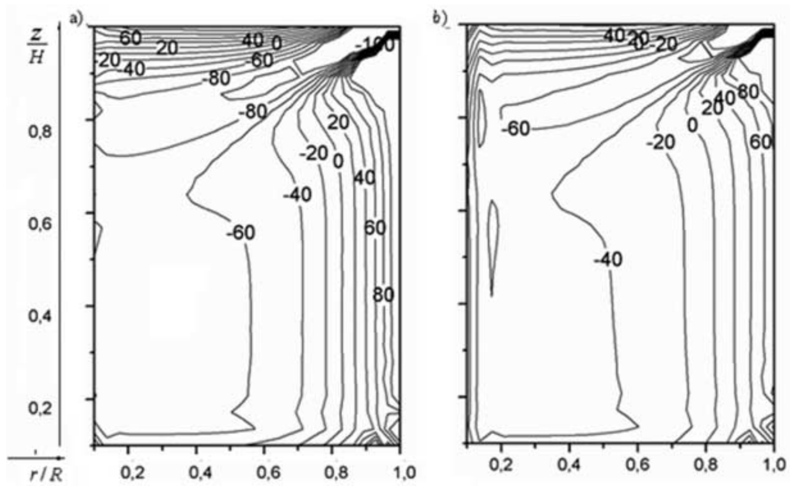

Figure 5. Isolines of circumferential stresses in the longitudinal section of the cylinder sample at 120 min drying time: (a) convective drying, (b) microwave drying.

tensional and compressive stresses. The most complicated and of greatest values state of stress appears in the upper corner of the cylinder. The material placed in this corner is tensed simultaneously in r (radial) and z (longitudinal) directions. It is obvious that a destruction of the material will proceed in this place first.

Mapping of the stress distribution is quite similar in the cylinders dried convectively and by microwaves. However, microwave drying generates weaker stresses. This is clearly visible in Fig. 6, where distribution of stresses along the cylinder radius in the middle height of the cylinder ($z = H/2$) at 120 min drying time is presented.

The fact that microwave drying generates smaller value stresses is even more visible in Fig. 7, where the evolution of circumferential stresses in time at the cylinder surface ($r = R$) and in its center ($r = 0$) for $z = H/2$ is presented.

The weaker stresses in microwave drying follow mainly from more uniform distribution of the moisture content (see Figs. 3 and 4). Now, we can conclude that the volumetrically supplied heat in microwave drying causes the diffusional and thermodiffusional fluxes of moisture to flow in the same direction, and this results in more uniform distribution of moisture content and smaller value stresses. This is not the case of

Marcel Dekker, Inc.
270 Madison Avenue, New York, New York 10016

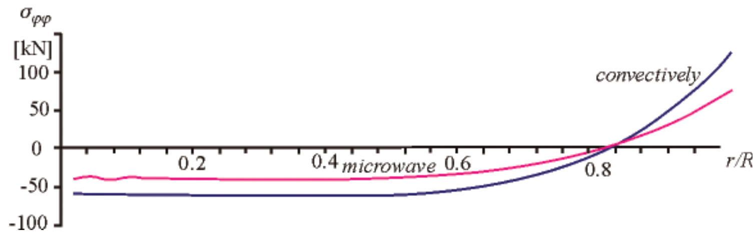

Figure 6. Distribution of circumferential stresses along cylinder radius for $z = H/2$ at 120 min drying time. *(View this art in color at www.dekker.com.)*

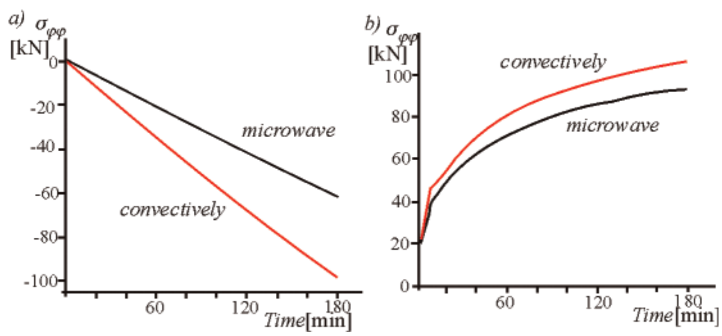

Figure 7. Evolution of circumferential stresses in time for $z = H/2$: (a) for $r = 0$, (b) for $r = R$. *(View this art in color at www.dekker.com.)*

convective drying, where the diffusional and thermodiffusional fluxes have opposite directions.

FINAL REMARKS

The main goal of this article was to demonstrate that the volumetrically supplied heat to the dried material results in more uniform distribution of the moisture content during drying, and thus also in smaller value drying-induced stresses. By convective drying, particularly when the drying proceeds in high temperatures and small relative humidity of the drying medium, the thermodiffusional flux of moisture blockades the outflow of moisture due to diffusion, mainly at the boundary, and this causes strongly nonuniform distribution of the moisture content than in microwave drying. Therefore, the convective drying generates larger stresses (Hasatani et al.,[4] Kowalski and Rybicki,[6] Zagrouba et al.[15]).

When the weaker stresses are generated during drying a better quality dry product is obtained from the mechanical standpoint. In this context, microwave drying has the predominance over the convective drying.

NOMENCLATURE

Symbols

A	Area of evaporation (m^2)
A	Bulk elasticity constant (MPa)
c_T	Thermodiffusion coefficient ($m^2/K\,s^2$)
c_X	Diffusion coefficient (m^2/s^2)
c_v	Specific heat per unit mass of dry body (J/kg K)
H	Height of the cylinder (m)
K	Volumetric modulus of elasticity (MPa)
l	Latent heat of evaporation (J/kg)
M	Shear elasticity constant (MPa)
$\boldsymbol{q}$	Heat flux (W/m^2)
r	Radial coordinate (m)
R	Radius of the cylinder (m)
S	Total entropy (J/kg K)
s^m	Entropy of moisture (J/kg K)
T	Temperature (K)
t	Time (s)
u_r, u_z	Displacements in radial and axial directions (m)
$\boldsymbol{W}$	Moisture flux ($kg/m^2\,s$)
X	Moisture content (dry basis) (L)
x	Molar vapor content in air (L)
z	Axial coordinate (m)

Greek Letters

α	Attenuation factor (L/m)
α_m	Coefficient of the convective mass exchange ($kg\,s/m^4$)
α_T	Coefficient of the convective heat exchange ($W/m^2\,K$)
β_T	Coefficient of thermodiffusion ($kg/m^2\,K\,s^2$)
β_x	Coefficient of diffusion ($kg/m^2\,s^2$)
ε_{ij}	Strain tensor (L)
$\kappa^{(T)}$	Coefficient thermal expansion (L/K)
$\kappa^{(X)}$	Coefficient moist expansion (L)

Marcel Dekker, Inc.
270 Madison Avenue, New York, New York 10016

Λ_m Mobility coefficient (kg s/m^3)
Λ_T Effective thermal conductivity (W/m K)
μ Moisture potential (J/kg)
Internal source of heat (W/m^3)
σ_{ij} Stress tensor (MPa)

ACKNOWLEDGMENT

This work was carried out as a part of the research project No 7 T09C 035 21 sponsored by the Polish State Committee for Scientific Research.

REFERENCES

1. Chen, G.; Wang, W.; Mujumdar, A.S. Theoretical study of microwave heating patterns and batch fluidized bed drying of porous material. Chemical Engineering Science **2001**, *19* (1), 167–183.
2. Constant, T.; Moyne, C.; Perre, P. Drying with internal heat generation: theoretical aspects in application to microwave heating. AIChE Journal **1996**, *42* (2), 359–368.
3. Feng, H.; Tang, J.; Cavalieri, R.P.; Plumb, O.A. Heat and mass transport in microwave drying of porous materials in a spouted bed. AIChE Journal **2001**, *47* (7), 1499–1512.
4. Hasatani, M.; Itaya, Y.; Hayakawa, K. Fundamental study on shrinkage of formed clay during drying. Drying Technology **1992**, *10* (4), 1013–1036.
5. Kowalski, S.J. *Thermomechanics of Drying Processes*; Springer-Verlag, Berlin Heidelberg: New York, 2003.
6. Kowalski, S.J.; Rybicki, A. Drying stress formation induced by inhomogeneous moisture and temperature distribution. Transport in Porous Media **1996**, *24*, 239–248.
7. Perre, P.; Turner, W. Microwave drying of softwood in an oversized waveguide. AIChE Journal **1997**, *43* (10), 2579–2595.
8. Ratanadecho, P.; Aoki, K.; Akahori, M. Experimental and numerical study of microwave drying in unsaturated porous material. Int. Comm. Heat Mass Transfer **2001**, *28* (5), 605–616.
9. Ratanadecho, P.; Aoki, K.; Akahori, M. A numerical and experimental investigation of the modelling of microwave melting and frozen packed beds using a rectangular wave guide. Int. Comm. Heat Mass Transfer **2001**, *28* (6), 751–762.

10. Ratanadecho, P.; Aoki, K.; Akahori, M. Influence of irradiation time, particle sizes and initial moisture content during microwave drying of multi-layered capillary porous materials. J. Heat Transfer **2002**, *124* (2), 1–11.
11. Rybicki, A. Determination of drying induced stresses in a prismatic bar. Eng. Transactions **1993**, *41* (2), 139–156.
12. Sanga, E.C.M.; Mujumdar, A.S.; Raghavan, G.S.V. Simulation of convection-microwave drying for shrinkage material. Chemical Engineering and Processing **2002**, *41*, 487–499.
13. Turner, W.; Illic, M. Combined microwave and convective drying of a porous material. Drying Technology **1991**, *9* (5), 1209–1269.
14. Wait, R.; Mitchell, A.R. *Finite Elements Analysis and Applications*; Wiley: New York, 1986.
15. Zagrouba, F.; Mihoubi, D.; Bellagi, A. Drying of clay. II, Rheological modelisation and simulation of physical phenomena. Drying Technology **2002**, *20* (10), 1895–1917.
16. Zhang, D.; Mujumdar, A.S. Deformation and stress analysis of porous capillary bodies during intermittent volumetric thermal drying. Drying Technology **1992**, *10* (2), 421–443.
17. Zielonka, P.; Gierlik, E.; Matejak, M.; Dolowy, K. The comparison of experimental and theoretical temperature distribution during microwave wood heating. Holtz als Roh- und Werkstoff **1997**, *55*, 395–398.

Doo-ngam, N., Rattanadecho, P., Klinklai, W., Microwave pre-heating of natural rubber using a rectangular wave guide (MODE: TE10), Songklanakarin Journal of Science and Technology 29 (6), pp. 1599-1608, 2007

Basak, T., Analysis of microwave propagation for multilayered material processing: Lambert's law versus exact solution, Industrial and Engineering Chemistry Research 43 (23), pp. 7671-7675, 2004

Ratanadecho, P., Aoki, K., Akahori, M., A numerical and experimental investigation of the modeling of microwave heating for liquid layers using a rectangular wave guide (effects of natural convection and dielectric properties), Applied Mathematical Modelling 26 (3), pp. 449-472, 2002

Ratanadecho, P., Aoki, K., Akahori, M., Experimental validation of a combined electromagnetic and thermal model for a microwave drying of capillary porous materials inside a rectangular wave guide (effects of irradiation time, particle sizes and initial moisture content), Journal of Microwave Power and Electromagnetic Energy 37 (1), pp. 15-40, 2002